NASA CONTRACTOR REPORT 159188
RASA/SRL 14-79-04

NASA-CR-159188
19800008579

# EXPERIMENTAL EVALUATION OF ACTIVE AND PASSIVE MEANS OF ALLEVIATING ROTOR IMPULSIVE NOISE IN DESCENT FLIGHT

D. S. JANAKIRAM

RASA DIVISION
SYSTEMS RESEARCH LABORATORIES, INC
1055 J. CLYDE MORRIS BOULEVARD
NEWPORT NEWS, VIRGINIA 23602

CONTRACT NAS1-15337
NOVEMBER 1979



National Aeronautics and
Space Administration

**Langley Research Center**
Hampton, Virginia 23665
AC 804 827-3966

RASA/SRL 14-79-04

# EXPERIMENTAL EVALUATION OF ACTIVE AND PASSIVE MEANS OF ALLEVIATING ROTOR IMPULSIVE NOISE IN DESCENT FLIGHT

by

D. S. JanakiRam

November 1979

Prepared for

National Aeronautics and Space Administration
Langley Research Center
Hampton, Virginia 23665

by

RASA Division
Systems Research Laboratories, Inc.
1055 J. Clyde Morris Boulevard
Newport News, Virginia 23602

TABLE OF CONTENTS

## SUMMARY

A controlled wind tunnel test program was conducted on a model 2.14 m (7 ft) diameter teetering rotor to determine the effectiveness of blade tips such as the Ogee tip and the TAMI (Tip Air Mass Injection) tip in reducing the impulsive noise due to blade-vortex interaction in descent flight. In addition, a full rectangular tip which has the same span as the Ogee tip and an effective rectangular tip which has the same lifting area as the Ogee tip were also considered. The tests were conducted at two advance ratios (0.125 and 0.14) with various descent rates ranging from steady level flight to about 6 m/sec (20 ft/sec). All tests were conducted at the same rotor thrust (900 N (203 lbs)) and the same rotor rpm (1985 which corresponds to a tip speed of about 248 m/sec (814.3 ft/sec) for the full rectangular and Ogee tip rotors and about 233 m/sec (763 ft/sec) for the effective and TAMI tip rotors). Acoustic data was obtained at three microphone locations. Microphone 1 was located upstream, microphone 2 was located at the scaled fuselage right cabin door (scaling was done on the basis of a full-scale UH-1H helicopter) and microphone 3 was located on the scaled location of the horizontal stabilizer. Acoustic data at microphone 2 was regarded as representative of the cabin noise.

The test results of all of the different rotors (with different blade tips) showed that the peak impulsive noise levels occurred at moderate rates of descent of about 3.5 to 4.5 m/sec (12 to 14 ft/sec). The pressure-time histories at microphones 2 and 3 showed the presence of two distinct blade-vortex interactions occurring at azimuthal locations 70° and 310° respectively. Generally, it was found that at least as far as the data at microphones 1 and 2 is concerned, the Ogee tip was the most effective in reducing the impulsive noise in descent flight. The anticipated benefits of the TAMI tip were not realized. A comparison of spectral levels showed that at the descent rates corresponding to the peak impulsive noise, the spectral levels for the Ogee tip rotor were about 3 to 5 dB less than those for the TAMI tip rotor in the mid-frequency region (1000 to 2500 Hz). Unexpectedly, the acoustic data of the Ogee tip rotor at microphone 2 showed the presence of a strong broad-band noise component which dominated its spectra at lower rates of descent. The full rectangular tip rotor and the effective tip rotor showed similar noise trends, with their noise levels being generally higher than those of the Ogee tip rotor. Despite the slight differences in solidity between rotors with different tips, it could not be concluded that the solidity played a major role in their impulsive noise characteristics. An evaluation of the acoustic spectra of different rotors in terms of dBA versus equivalent full-scale frequency confirmed the

acoustic trends noted above. A comparison of the performance of different rotors showed that for the same tip Mach number and thrust, the Ogee tip rotor absorbed more power than the full rectangular tip rotor, while the TAMI tip rotor absorbed more power than the effective tip rotor.

LIST OF TABLES

LIST OF ILLUSTRATIONS

# INTRODUCTION

Over the past several years, helicopters have gained wider acceptance in both military and commercial areas due to their unique capabilities. However, helicopters did not realize their full potential due to some of the undesirable characteristics associated with them. One such characteristic is the large amount of noise produced by them in some of the most important flight conditions. The impulsive noise (commonly known as blade slap) is one of the most annoying and easily detectable sounds a helicopter can generate and when it occurs it is the dominant source of noise. Impulsive noise can occur during high-speed flight due to the intense compressibility and thickness effects on the advancing blades and during slow-speed partial power descent due to blade-vortex interactions. In the past few years, a large number of research efforts have been conducted in the area of helicopter impulsive noise. The main thrust of these research efforts was to identify the sources of impulsive noise and to find means of alleviating this undesirable noise.

Tangler (Ref 1), in one of the most definitive experimental studies conducted in the area, has sought to identify the sources of impulsive noise and tried to relate the impulsive noise with the aerodynamic events occurring on the blades with the help of Schlieren flow visualization and blade pressure measurements. He has shown that the impulsive noise generated during high-speed flight and partial power descent is mainly due to the local supersonic and transonic velocities and the associated shocks that appear on the advancing blades. He has also identified four advancing and three retreating blade-vortex intersections over a partial power descent range of 0 to 300 m/min (0 to 1000 ft/min). Of these, the advancing blade intersections at 55° and 70° azimuth were found to be the main contributors to that portion of the slap signature attributed to the blade-vortex interaction. It was also shown that the tip region of the blades contributes significantly to the impulsive noise and therefore by suitably modifying the geometric characteristics of the blade tip (such as thickness and shape), the impulsive noise could be reduced. It is well known that blade slap can be substantially reduced by reducing the rotor tip speed. However, this means of reducing blade slap has a practical limit because of the resulting weight and performance penalties.

While impulsive noise due to compressibility and blade thickness effects can result in annoying noise in high-speed forward flight, the impulsive noise caused by blade-vortex interactions during partial power descent into a terminal area can be a more troublesome source to the passengers and the surrounding community. The flight region in which this noise source is of primary

importance, is generally at forward velocities of 20 to 40 m/sec (65 to 130 ft/sec) and at descent rates of 50 to 100 m/min (160 to 325 ft/min). In this flight region, the concentrated tip vortices trailing from the blades intersect the blades and induce strong and rapid pressure fluctuations on the rotating blades. In recent years, several research efforts (both theoretical and experimental) were conducted to understand the blade-vortex interaction mechanism more completely. On the basis of these efforts, the primary parameters associated with the impulsive noise due to blade-vortex interaction have been identified to be the strength of the concentrated tip vortex, the orientation of the tip vortex with respect to the interacting blade and the distance of the concentrated tip vortex from the interacting blade. It was therefore suggested that the impulsive noise due to the blade-vortex interaction could be reduced by suitably modifying the characteristics of the concentrated vortex trailed off the tip of a rotor blade. Analytical studies of the basic aeroacoustic interaction between a blade and vortex have been conducted by Widnall (Ref 2) and others assuming classical attached flow response of the blade to the additional velocity of the vortex. However, due to the complexity of the tip vortex geometry and of the blade's actual response, the success of these predictive techniques in finding means of alleviating this impulsive noise has been very limited. Fortunately, more success has been achieved in the experimental studies conducted to date.

Experimentally, attempts to modify the character of the tip vortex and, therefore, reduce the impulsive noise due to blade-vortex interaction have involved both passive and active devices. Sheiman and Shivers (Ref 3) investigated a number of passive and active devices but found very little beneficial effect of any of the devices on the concentrated tip vortex. Passive approaches using a tip spoiler (Ref 4) or a porous tip (Ref 5) met with varying degrees of success regarding a beneficial modification of the tip vortex. The increase in power requirements to achieve these results by these techniques was prohibitive for helicopter rotors and, therefore, these techniques have not been seriously pursued since then. A partial end plate has been tested and significant tip vortex modifications were noted with only a small increase in power requirements (Ref 6). Another passive method, tip shape modification, has shown promise in reducing the impulsive noise due to blade-vortex interaction. One of the most promising tip configurations has been an Ogee planform. Small-scale smoke studies have shown that this shape would diffuse the rotor blade tip vortex and, therefore, it was suggested that the interaction of the blades with a weaker vortex field would result in reduced impulsive noise. The Ogee tip shape was evaluated by a series of analytical and experimental studies (Refs 7-10). Based on the encouraging results of these studies, NASA has undertaken full-scale testing of this tip shape (Ref 11). These

full-scale tests have shown that the impulsive noise caused by blade-vortex interaction and compressibility was reduced for many of the flight conditions tested. It was found that the blade-vortex interaction noise was reduced by as much as 15 dB with an Ogee tip. The use of an Ogee tip also resulted in moderate performance gains in hover and forward flight for some flight conditions.

A disadvantage with any passive device is that if it draws power from the engine, it will degrade the performance of the aircraft in flight conditions where blade-vortex interaction is not a problem. Therefore, active systems which can be used only during the flight conditions of interest (such as partial power descent) were investigated. One such active system which has shown a lot of promise is the Tip Air Mass Injection (TAMI) system which seeks to modify the characteristics of the tip vortex by injecting an axial stream of air along the axis of the tip vortex as it leaves the blade. This system has been under investigation for more than six years under the sponsorship of the Navy, Army and NASA (Ref 7 and Refs 12-17). These research efforts included both theoretical and experimental investigations and were concerned with the basic aerodynamic characteristics of vortices forming at the tip of a lifting surface and of viscous mixing of linear and swirling flows as well as the application of this basic knowledge to the development of a suitable injection system for the UH-1 series of helicopter blades. The results of nonrotating model investigations conducted in a wind tunnel with a full-scale section of the UH-1 rotor blade have indicated that significant reductions of the peak tangential velocity in the vortex core and a corresponding increase in the size of the vortex core could be realized immediately behind the rotor blade with the use of an airstream exiting at sonic velocity from a nozzle in the tip. These tests have also shown that there is an insignificant effect on the wing profile drag due to the air mass injection. Partial power recovery due to the jet effect of the air mass injection system is a benefit of this type of vortex modification device. The success of the wind tunnel tests prompted testing of a full-scale UH-1 rotor with the TAMI system on the Helicopter Rotor Test Facility (HRTF) (Ref 18) at NASA Langley Research Center. The results of these tests were inconclusive in that the blade-vortex generated impulsive noise could not be obtained on the whirl tower and, thus, the beneficial effects of the vortex modification on the impulsive noise signature could not be obtained. However, smoke visualization tests conducted with this rotor system indicated that considerable change in the tip vortex was obtained. Therefore, a controlled wind tunnel test of the TAMI system under simulated partial power descent flight conditions was conducted (Ref 19) on a 2.14 m (7 ft) diameter teetering rotor to evaluate the beneficial effects, if any, of the TAMI system in reducing the impulsive noise due to blade-vortex interaction. This investigation provided a realistic assessment of the potential of the TAMI

system in reducing the impulsive noise during blade-vortex interaction in descending low-speed flight. It was concluded that the noise output from the model due to blade-vortex interaction could be reduced by as much as 8 dBA using the TAMI system. It was also shown that the blade-vortex interactions occur at the same azimuthal locations on the advancing blade regardless of advance ratio or thrust coefficient. However, it must be noted that the tip speeds considered in these TAMI tests were of the order of 152 m/sec (500 ft/sec). At higher tip speeds, the success of the TAMI system in reducing the blade-vortex interaction may not be as high.

As discussed above, both the passive approach using Ogee planform and the active approach using TAMI system have shown great promise in reducing the impulsive noise due to blade-vortex interaction in low-speed descent. Since TAMI results were obtained during a controlled wind tunnel test with a model rotor and the Ogee tip tests were conducted in flight with the rotor systems not having the same solidity, it is difficult to make a one-to-one comparison of the benefits achievable from the two different approaches. In order to obtain such a comparison, a controlled wind tunnel test program was conducted.

In the following pages, a description of the test program conducted and an analysis of the data obtained during the tests are presented.

## TECHNICAL DISCUSSION

The basic objective of this effort is to conduct an evaluation of the relative effectiveness of the TAMI and Ogee tips in reducing the impulsive noise in descending flight. To achieve this objective, a wind tunnel test program using the two-bladed teetering rotor system previously constructed for the TAMI tests (Ref 19) was conducted. A set of interchangeable tip sections which can be attached to the ends of the rotor blades and which include an Ogee and TAMI tip were used.

It was believed that some of the advantages claimed for the Ogee tip, such as the movement of the blade slap area to higher descent rates and reduced compressibility noise, can be traced to the reduced effective radius of the Ogee tip blade. On the basis of results reported in References 7 and 10, it was determined that the spanwise center of lift and drag of an Ogee tip were the same as those of a rectangular tip having the same effective area as that of the lifting surface of the Ogee tip. The "effective lifting" tip of the Ogee tip configuration was defined as the span at which the rectangular tip planform has the same area as that of Ogee tip. It was believed that the effective tip vortex of the Ogee section is formed more inboard compared to that of a blade with a rectangular tip with the same radius as the Ogee tip blade. It was, therefore, hypothesized that the tip vortex from an Ogee tip blade will intersect the blade at a more inboard station and because of the lower rotational speed of this station less severe impulsive noise will result. To test this hypothesis, two other rectangular tips, one with the same radius as the Ogee tip and the other with the same area as the Ogee tip were also tested. The details of the model and equipment used, the test procedure and a discussion of the results obtained are given below.

### Description of the Model and Test Equipment

The basic rotor test model that was used in the wind tunnel tests is shown in Figure 1. This was designed, constructed and utilized by RASA (Ref 19) under NASA Contract NAS1-14129. The rotor is a two-bladed teetering rotor whose collective pitch can be remotely controlled. Lateral cyclic is obtained by means of rotor shaft tilt which is also remotely controlled. The rotor is powered by a 100 hp motor supplied by the University of Maryland. The rotor blades were made out of an aluminum D-spar with balsa wood core and a fiberglass skin. The blades had a NACA 0015 airfoil section. The blades had no twist and had a constant chord of 10.67 cm (4.2 in). In the case of TAMI tip, the air was supplied through an aluminum pipe inside each blade. The tip sections (see Fig 2) which included an Ogee tip, a TAMI tip, an

effective rectangular tip (which has the same lifting area as that of the Ogee tip) and a full rectangular tip (which has the same span as that of the Ogee tip) were fabricated out of basswood and were attached to the blades with axial screws and contoured aluminum cuffs. The Ogee tip had a constant thickness ratio airfoil section (NACA 0015) along its span except very near the end of the tip where it had an elliptical section. The nozzle in each TAMI tip was designed to provide an exit velocity of about 427 m/sec (1400 ft/sec) at a stagnation pressure of about $6.5 \times 10^5$ N/m$^2$ (94.7 lbf/in$^2$) and a stagnation temperature of 288°K (519°R). For the TAMI system to be effective, it is necessary to inject air into the core of the tip vortex along its axis. Preliminary tests conducted with the TAMI tip showed that it was not very effective in reducing the impulsive noise due to blade-vortex interaction. It was believed that this was attributed to a less than ideal location of the air mass injection nozzle in the TAMI tip.

To clearly establish the position of the tip vortex exit point, and, therefore, the proper location of the nozzle on the TAMI tip, an experiment was conducted in the Anechoic Flow Facility at the NASA Langley Research Center. One of the TAMI rotor blades was installed in the Anechoic Flow Facility vertical jet at a forward sweep of about 10° and an angle of attack of about 10°. A flow speed of 30.5 m/sec (100 ft/sec) was used and the tip vortex formed at the tip was visualized with the help of a neutral buoyancy helium/soap bubble generator and a high intensity light source. The tip vortex was then photographed in two planes against an inscribed grid pattern to determine its location relative to the blade tip. Based on these results, the TAMI tip was redesigned with the nozzle axis located at about 0.97 cm (.38 in) from the end of the tip and canted about 7° upward from the chord line. The TAMI tip was then fabricated as an integral unit with the blade using a magnesium nozzle assembly imbedded in a foam core-fiberglass skin construction.

As was done in an earlier series of TAMI tests (Ref 19), three microphones were used to record the acoustic signal from the rotor. Figure 3 shows the relative location of microphones with respect to the rotor. Microphone 1 was located upstream, microphone 2 was located at the scaled fuselage right cabin door location and microphone 3 was located at the scaled location of the horizontal stabilizer. The scaling was done on the basis of a full-scale UH-1H helicopter. It is to be noted that microphones 2 and 3 were attached to the rotor support structure and moved with the rotor shaft as it was tilted.

## Wind Tunnel Tests

Determination of Test Conditions: - As was noted earlier, the basic purpose of the wind tunnel tests was to conduct a comparative evaluation of the effectiveness of different tips in reducing the impulsive noise of helicopters due to blade-vortex interaction

in descent flight. To have a more practical bearing, it was decided to conduct the tests at the same tip speed and thrust coefficient which were used in the recent flight tests of UH-1H helicopter (Ref 11). The rotor rpm was selected such that the blades with the Ogee and full rectangular tips had the same tip speed (248 m/sec (814.3 ft/sec)) as that of full-scale UH-1H helicopter rotor. The model rotor with effective and TAMI tips were run at the same rpm as that used with the other two tips. Also, the rotors with all the different tips were tested such that they developed the same thrust of about 900 N (200 lbs). This value was selected so that model and full-scale rotors with Ogee and full rectangular tips have the same thrust coefficient of about .00266 (corresponds to the lower nominal gross weight of UH-1H).

In steady level flight, the weight of the aircraft does not contribute to any propulsive force. However, in descending flight, depending on the angle of descent, a component of the weight of the aircraft will act in the direction of motion and, therefore, has to be taken into account in the simulation of descent flight in the wind tunnel. For steady-state level flight simulation of the model rotor in the wind tunnel, the lift balance reading must equal the simulated weight of the model and the drag balance reading must equal the negative of scaled fuselage drag. To simulate the fuselage drag, an equivalent flatplate drag area of 0.093 $m^2$ (1 sq ft) was assumed. In descent flight, the fuselage drag of the aircraft is effectively reduced (see Ref 19) by w sin $\phi$ where w is the simulated helicopter weight and $\phi$ is the angle of descent. The necessary drag balance readings for various rates of descent were determined prior to the tests. The actual drag readings used to trim the rotor in the wind tunnel were the calculated values corrected for the system drag tares obtained without the rotor attached.

Based on the blade slap footprints (Ref 11) obtained in full-scale flight tests of UH-1H, three advance ratios ($\mu$ = 0.125, 0.14 and 0.165) were chosen for wind tunnel tests. However, in the range of rates of descent considered, not much blade-vortex interaction was observed at an advance ratio of 0.165. Therefore, all the wind tunnel tests were conducted at advance ratios of 0.125 and 0.140. Tables 1 and 2 give the model geometric parameters and the test conditions used in the simulated wind tunnel tests, respectively.

Test Procedure: - The wind tunnel tests were conducted in the University of Maryland 2.36 x 3.35 m (7.75 x 11 ft) subsonic wind tunnel. The test section of the tunnel was lined with 5.1 cm (2 in) thick acoustic foam to minimize the acoustic reflections off the tunnel walls. Figure 4 shows the rotor in the tunnel test section.

The rotor support structure without the rotor was first installed in the tunnel test section and at the tunnel velocities of interest the system drag tares were taken. Then the rotor was installed with the chosen blade tip. The tunnel was brought up to speed and the required lift and drag balance readings, corrected for the system tares, of a given flight condition were obtained by adjusting the collective pitch and shaft tilt. When the required flight condition was obtained, the performance and acoustic data were taken. The performance data consisted of the balance readings and the power input to the drive motor. The analog signals from the three microphones (the pressure-time histories) along with the two per rev rpm blip were recorded on an FM tape recorder. On-line spectrum analysis of the microphone signals was carried out and analyzed to evaluate the fidelity and characteristics of the acoustic signals in order to properly conduct a realistic test program in terms of not overlooking important and unexpected results. The above procedure was repeated at each of the chosen flight conditions. At each advance ratio, the data was obtained at several rates of descent starting from steady level flight and going up to about 6.1 m/sec (20 ft/sec) in steps of 0.61 m/sec (2 ft/sec). It was clear from the data obtained that the chosen range of rates of descent included the flight conditions at which maximum blade slap occurred.

In the case of the TAMI tip, in the range of rates of descent at which blade vortex interaction was evident, air was injected from the nozzles in the tip at a stagnation pressure of about $6.5 \times 10^5$ N/m$^2$ (94.7 lbf/in$^2$). Also, at this stagnation pressure, the air mass flow rate as well as the reaction force on the stationary blade as the air exits the nozzle was measured.

The data stored on tape was subsequently fed to analyzers and narrow-band spectrum and 1/3 octave-band data were obtained. Also, polaroid photographs as well as strip chart traces of pressure-time history signals were obtained. In the following section, the results obtained in the wind tunnel tests will be discussed.

## Discussion of Results

As was discussed earlier, the acoustic data which consisted of pressure-time history and narrow-band and 1/3 octave-band spectral plots, was obtained at three different microphone locations. Most of the discussion herein will be concerned with the data obtained at microphone 2 whose location corresponds to the full-scale helicopter right cabin door location. It is believed that this acoustic data will be representative of the near-field rotor noise outside of the cabin of the full-scale helicopter and, therefore, will be of utmost significance as regards passenger annoyance. In addition, acoustic data at microphones 1 and 3 will also be discussed whenever this data shows significantly different trends.

At all test conditions considered, the spectral data has shown that the signal levels are at least 15 to 20 dB above the tunnel background noise in the frequency range of interest (0-5 KHz). It is to be noted that the pressure-time histories presented in this report were not calibrated and therefore they will be considered only on a qualitative basis.

Steady Level Flight: - Figures 5a through 5c show the narrow-band acoustic spectra (in the range of 0-5 KHz) and corresponding pressure-time histories obtained at microphone location 2 for the rotors with three different blade tips (Ogee, effective and full rectangular tips, respectively) operating in steady level flight at an advance ratio of 0.14. These spectra show rotational noise peaks at the first few harmonics of blade passage frequency. These peaks are due to the steady loads acting on the rotor blades and since the total load developed by each rotor is approximately the same, the levels of the rotational noise peaks are approximately the same regardless of the blade tip used. A closer examination of the pressure-time histories shows the presence of impulsive noise in the case of the full rectangular tip rotor (Fig 5c) and a high level of broad-band noise in the case of an Ogee tip rotor (Fig 5a). The acoustic spectrum of the full rectangular tip rotor (Fig 5c) shows the presence of distinct harmonic peaks in the frequency range 1000-1500 Hz characteristic of impulsive noise due to blade vortex interaction. The impulsive noise is relatively weaker in the case of an effective tip rotor (Fig 5b). A comparison of the spectra of the three (3) rotors shows that for frequencies beyond 1500 Hz, the spectral levels of the Ogee tip rotor are about 8 to 15 dB higher than those of the other two (2) rotors. These higher levels of broad-band noise could be due to the increased turbulent flow at the Ogee tip which in turn could have been triggered by the metal cuff used to hold the tip, as well as the different load distribution near the Ogee tip. However, this does not fully explain the absence of such a strong turbulent flow over the other two (2) tips since they were also attached by a metal cuff.

Figures 6a through 6c show the acoustic spectra and the pressure-time histories of the three rotors obtained at microphone location 1 in steady level flight at an advance ratio of 0.14. These figures clearly show a stronger impulsive noise than that observed at microphone 2. These figures also show that the full rectangular tip rotor had the highest level of impulsive noise followed by the effective tip rotor and the Ogee tip rotor. The spectra at microphone 1 also showed a larger number of distinct peaks compared to those at microphone 2. Microphone 1 was located upstream of the rotor and slightly below the plane of the rotor (see Fig 3). The increased levels of impulsive noise observed at microphone 1 could be due to the directivity of the noise originating on the advancing blades of the rotor. Unlike the acoustic

data at microphone 2, the acoustic data of the Ogee tip rotor (see Fig 6a) at microphone 1 did not show any dominant broad-band noise and the spectral levels for this rotor at higher frequencies (>2500 Hz) were only 3 to 5 dB higher than those of the other two rotors.

The impulsive noise observed in steady level flight was very much similar to that which is usually observed due to discrete blade-vortex interaction in descent flight. This could be due to the small amount of upwash caused by the tunnel walls and, therefore, the simulated steady level flight condition may in fact correspond to a low descent velocity flight. The stronger impulsive noise observed in the case of full rectangular tip rotor could be due to a more outboard discrete blade-vortex interaction compared to the effective tip rotor. The weaker impulsive noise observed in the case of Ogee tip rotor is most likely due to a more diffuse tip vortex and therefore a less intense blade-vortex interaction. In addition to the discrete blade-vortex interaction, some of the impulsive noise observed in steady level flight could also have been generated by the induced effects of turbulent wake as well as the strong compressibility effects on the advancing blades. The acoustic data at microphone 3 (located on the retreating side) did not show any impulsive noise which indicated that most of the impulsive noise, at least in steady level flight, was generated on the advancing blades of the rotors. Also, the data at microphone 3 did not show any dominant broad-band noise in the case of the Ogee tip rotor. The trends observed at advance ratio of 0.125 were similar to those discussed above for the advance ratio of 0.14. The TAMI tip was not tested in steady level flight. It is believed, however, that the acoustic trends with TAMI tip would be similar to those observed for the effective tip rotor in steady level flight.

Descent Flight: - In the simulated descent flight conditions in the wind tunnel, as expected, all rotors produced impulsive noise, characteristic of blade-vortex interaction. The blade-vortex interaction and the resulting impulsive noise was noted by the presence of impulsive pressure peaks in the pressure-time histories as well as the presence of a large number of discrete peaks at the blade passage frequencies in the acoustic spectra of the noise signatures. The acoustic spectra in the descent flight conditions also showed the characteristic spectral humping (Ref 19) in the mid-frequency range (800-2500 Hz) which is related to the concentrated vortex energy in the wake interacting with the rotor. However, rotors with different blade tips showed different levels of blade-vortex interaction noise at the same descent velocities. Figures 7 through 10 show the acoustic spectra and pressure-time histories of rotors with different tips at microphone 2 and at the advance ratio of 0.14.

Figure 7a shows the narrow-band spectrum of the full rectangular tip rotor at a rate of descent 0.61 m/sec (2 ft/sec). As can be seen from Figure 7a, the impulsive noise is clearly present, though it is not very strong. However, as the descent rate is increased, the impulsive noise increased, reaching its peak level around a rate of descent of about 4.27 m/sec (14 ft/sec). Figure 7b (see the inset) clearly shows the presence of 2 per rev positive impulsive peaks characteristic of a discrete blade-vortex interaction. The trace at the bottom of the pressure-time history corresponds to 2 per rev electronic blip triggered by each blade as it crosses the $\psi = 0°$ azimuthal position (i.e., downstream position of the blades). The impulsive peaks of the pressure-time history of Figure 7b suggest that the blade-vortex intersection occurred in the second quadrant around $\psi = 107°$. However, on taking into account the lag between the time at which blade-vortex intersection occurred and the time at which the impulsive pressure peak was picked up by microphone 2, it was determined that the blade-vortex intersection occurred in the first quadrant around $\psi = 70°$. This conforms with the experimental observation made by Tangler (Ref 1). In addition, the narrow-band spectrum of the noise signature as shown in Figure 7b, contains a large number of distinct spectral peaks across its entire frequency range. These peaks reach high levels (of the order of 110 dB) in the mid-frequency region (1000-2000 Hz) typical of a discrete blade-vortex interaction. Figure 7c shows the 1/3 octave band spectrum of the same noise signature (shown in Fig 7b) and it clearly shows the presence of spectral humping in the mid-frequency region (1000-4000 Hz). As the rate of descent was increased further, the blade-vortex interaction became weaker. Figure 7d shows the acoustic spectrum and the pressure-time history of the full rectangular tip rotor at a rate of descent of 6.10 m/sec (20 ft/sec, 1200 fpm). The impulsive spike in the pressure-time history is shorter and less sharp than that at 4.27 m/sec (14 ft/sec), though it occurred around the same azimuthal location. The spectral levels in the mid-frequency region (1000-2000 Hz) drop by about 5 to 9 dB from the peak levels obtained at 4.27 m/sec (14 ft/sec). However, these levels are still about 10 to 15 dB higher than those obtained at the descent rate of 0.61 m/sec (2 ft/sec) (Fig 7a). This trend conforms to the "slap pattern" observed in full-scale flight tests (Ref 19). According to this pattern, the impulsive noise at the descent rate of 0.61 m/sec (2 ft/sec) corresponds to the "continuous slap" and the impulsive noise observed at 4.27 m/sec (14 ft/sec) and 6.10 m/sec (20 ft/sec) corresponds to the "maximum slap" and "intermittent slap", respectively. It is to be noted that no data was obtained for descent rates beyond 6.10 m/sec (20 ft/sec). However, it is believed that as the descent rate is increased beyond 6.10 m/sec (20 ft/sec) the impulsive noise due to blade-vortex interaction becomes weaker and disappears ultimately at very high descent rates (of the order of 9.15 m/sec (30 ft/sec)). It can also be seen that the spectral

levels of the first few rotational noise peaks do not change significantly with the descent rate. This is due to the fact that these rotational noise peaks are due to the steady loads developed by the rotor which remain the same since the rotor thrust was kept constant for all descent rates considered.

Figures 8a through 8d give the acoustic spectra and pressure-time histories of the Ogee tip rotor. Unlike the full rectangular tip rotor considered above, the Ogee tip rotor did not show any significant impulsive noise characteristic of blade-vortex interaction until higher descent rates are reached. Figure 8a shows the narrow-band spectrum at a descent rate of 3.05 m/sec (10 ft/sec). The impulsive noise due to a relatively weaker blade-vortex interaction can be seen by the presence of spectral peaks in the frequency range 800-1500 Hz (see Fig 8a). It is to be noted that such a weak blade-vortex interaction was observed at a relatively lower descent rate of 0.61 m/sec (2 ft/sec) in the case of the full rectangular tip rotor. This shift to higher descent rates in the case of the Ogee tip rotor can be attributed to a weaker and a more diffuse blade tip vortex generated by the Ogee tip rotor as well as due to a different orientation of the interacting vortex.

As is evident from the pressure-time history (Fig 8a), the spectrum of the Ogee tip rotor is dominated by broad-band noise with relatively flat spectral levels (of the order of 85 to 90 dB) for frequencies beyond 2000 Hz. With increasing descent rate, the slap or impulsive noise of the Ogee tip rotor increased reaching its highest levels around a descent rate of 4.27 m/sec (14 ft/sec) (see Fig 8b). The pressure-time history at this descent rate (Fig 8b) did not show as sharp and large impulsive noise peaks as were observed in the case of the full rectangular tip rotor (Fig 7b). The sound pressure levels in the mid-frequency region (1000-2000 Hz) were of the order of 104 dB, about 5 to 6 dB below those that were observed in the case of the full rectangular tip rotor at a descent rate corresponding to the "maximum slap" region (Fig 7b). This can again be attributed to the weaker and more diffuse tip vortex generated by the Ogee tip as well as to the different orientation of the interacting vortex. Figure 8c gives a 1/3 octave-band spectrum of the noise signature at the descent rate of 4.27 m/sec (14 ft/sec). It can be clearly seen from Figures 8b and 8c that the acoustic signature has a lot of broad-band noise, though at slightly lower levels compared to that obtained at lower descent rates (Fig 8a). However, unlike the full rectangular tip rotor, the impulsive noise levels of the Ogee tip rotor did not show any significant reduction as the descent rate was further increased. In fact, at a descent rate of 6.71 m/sec (22 ft/sec), the spectral levels (Fig 8d) were almost the same as

those at 4.27 m/sec (14 ft/sec). Since the tests were not conducted beyond the descent rate of 6.71 m/sec (22 ft/sec), it is difficult to predict the descent rate at which the spectral levels begin to show a significant drop. The impulsive noise due to blade-vortex interaction of the Ogee tip rotor reached its highest levels around a descent rate of 4.27 m/sec (14 ft/sec) and maintained these high levels through a descent rate of 6.71 m/sec (22 ft/sec). This trend is quite different from that of the full rectangular tip rotor where the impulsive noise levels reached their highest values at a descent rate of 4.27 m/sec (14 ft/sec) and decreased with further increase in the descent rate. This is most likely due to the different geometry of the interacting vortex at the descent rates in question. It is to be noted that at higher descent rates considered, the spectral levels of the Ogee tip rotor and the full rectangular tip rotor are almost the same (compare Figs 8d and 7d). The anticipated shift of the "maximum slap" region to a higher descent rate in the case of an Ogee tip rotor compared to that of a full rectangular tip rotor was not realized, though the "maximum slap" region encompassed a wider range of descent rates in the Ogee tip rotor. The higher broadband noise of the Ogee tip rotor is probably due to some of the reasons discussed earlier. However, at "maximum slap" conditions, this component of noise (see Fig 8c) did not dominate except at very high frequencies (>5 KHz).

As was noted in an earlier section, it was believed that the reduction in impulsive noise in the case of an Ogee tip rotor can be traced to the formation of the tip vortex at a more inboard station and, therefore, at a smaller Mach number compared to that of full rectangular tip. It was also argued that an effective rectangular blade tip with the same planform area as that of the Ogee tip might realize some of the advantages claimed by the Ogee tip rotor. Therefore, wind tunnel tests were conducted with an effective tip rotor running at the same rpm and developing the same total thrust as the Ogee or full rectangular tip rotor. It is to be noted that the effective tip rotor has slightly lower tip Mach number than that of either the full rectangular tip rotor or the Ogee tip rotor. Figures 9a through 9d give the acoustic spectra and pressure-time histories at microphone 2 of the effective tip rotor in descent flight. The trends noted in these figures are roughly similar to those observed in the case of the full rectangular tip rotor. The impulsive noise due to blade-vortex interaction reached its highest levels at a descent rate of 3.66 m/sec (12 ft/sec) (see Fig 9b). The spectral levels at "maximum slap" conditions (Fig 9b) were only slightly lower than those observed in the case of a full rectangular tip rotor (Fig 7b). This slight reduction in the spectral levels in the "maximum slap" region for the effective tip rotor could be due to the lower Mach number at which the tip vortex is formed. It is believed that the blade-vortex intersection in the case of an

effective tip rotor occurred at a more inboard radial station and, therefore, at a lower Mach number compared to that of a full rectangular tip rotor. The pressure-time history of the effective tip rotor at microphone 2 showed that the discrete blade-vortex intersection had occurred at the same azimuth location (compare Figs 7b and 9b) as that in the case of the full rectangular tip rotor. However, the anticipated benefits of the effective tip rotor were not realized when compared with the Ogee tip rotor. In fact, at the "maximum slap" conditions (compare Figs 8b and 9b) the effective tip rotor was found to be much noisier than the Ogee tip rotor. This could be due to the fact that in the case of the effective tip rotor, the tip vortex was stronger and more concentrated than that of the Ogee tip rotor. Therefore, it is believed that even though the blade-vortex interaction must have occurred at a more inboard station and therefore at a lower Mach number, the stronger and less diffused tip vortex of the effective tip rotor resulted in a stronger blade-vortex interaction and, therefore, higher impulsive noise than that of the Ogee tip rotor. It is also to be noted that the solidity of the effective tip rotor is about 14% higher than that of the Ogee tip rotor (see Table I) even though the total blade area between the two rotors is the same. However, it is believed that the difference in solidity between these two rotors did not contribute significantly to the differences in their acoustic signatures noted earlier.

One of the main objectives of this effort was to evaluate the relative effectiveness of TAMI and Ogee tips in reducing the impulsive noise due to blade-vortex interaction. Figures 10a through 10c show the acoustic spectra and pressure-time histories of the TAMI tip rotor with and without the air injection at the "maximum slap" condition which corresponds to a descent rate of 3.66 m/sec (12 ft/sec). It is to be noted that the TAMI tip without air injection is identical in geometry (except for the presence of air nozzle) to the effective tip. It is, therefore, not surprising that the spectral levels and trends with the TAMI tip (without air injection) are similar to those of the effective tip. A comparison of the pressure-time histories between the TAMI tip without air injection (Fig 10a) and the effective tip (Fig 9b) shows that the impulsive peaks occurred around the same azimuthal location in both cases. When air was injected through the TAMI tip at a stagnation pressure of $6.5 \times 10^5$ N/m$^2$ (94.7 PSIa) and at a descent rate of 3.66 m/sec (12 ft/sec) (which corresponds to the "maximum slap" condition), the spectral levels (see Fig 10b) showed a drop of about 3 to 5 dB for frequencies beyond 2000 Hz. In the mid-frequency region (1000-2000 Hz) where the blade-vortex interaction is supposed to have the maximum effect, the air injection did not give any reduction in the spectral levels. Air was also injected at lower stagnation pressures to find if any differences have occurred in the spectra but none could be found. A comparison of the narrow-band spectra of the TAMI tip rotor (with

air) and the Ogee tip rotor at the "maximum slap" conditions (compare Figs 10b and 8b and 8c) shows that the spectral levels in the case of the Ogee tip rotor were lower (by as much as 3 to 5 dB) than those of the TAMI tip in the frequency range 800 to 4500 Hz. At higher frequencies because of the higher broad-band noise in the case of the Ogee tip rotor, its spectral levels were slightly higher. These observed differences between the noise signatures of the TAMI (with air) and Ogee tip rotors were also found at other higher descent rates. At lower descent rates (0 to 2.4 m/sec (0 to 8 ft/sec)), because of the increased broad-band noise, the Ogee tip rotor was found to be noisier than the TAMI tip rotor. The absence of the anticipated significant reduction in the impulsive noise with tip air mass injection is puzzling. As was noted in Reference 19, the reduction in the impulsive noise due to air injection was substantial at the tip speed of 152 m/sec (500 ft/sec). However, the present tests were conducted at a higher tip speed of 233 m/sec (763 ft/sec). It is possible that at this higher tip speed, the air jet velocity at the exit of the nozzle might not have been high enough to diffuse the tip vortex. It is also possible that, despite the careful selection of the nozzle axis location based on the anticipated tip vortex position as it leaves the tip, the air jet was not properly aligned with the axis of the tip vortex to provide the maximum diffusion of the tip vortex. For the reasons mentioned above, the TAMI tip was not found to be as effective as the Ogee tip in reducing the impulsive noise due to blade-vortex interaction in descent flight.

So far, the discussion pertaining to the descent flight was limited to an advance ratio of 0.14 and to the data obtained at microphone location 2. Though the results discussed above are fairly typical, some differences were found at other microphone locations and at the other advance ratio (0.125) considered in the tests. Figures 11a through 11d give the acoustic spectra at microphone 3of the different rotors at the "maximum slap" conditions at an advance ratio of 0.14. Unlike the spectrum at microphone 2 (Fig 8b), the spectrum of the Ogee tip rotor at microphone 3 (Fig 11a) showed distinct harmonic peaks through most of the frequency range considered. In addition, the pressure-time history (Fig 11a) showed a more distinct impulsive peak characteristic of blade-vortex interaction compared to that at microphone 2 (Fig 8b). Taking into account the time lag effects, it can be shown that the blade-vortex intersection occurred somewhere around $\psi = 310°$ (in the fourth quadrant). Microphone 3 was located downstream of the rotor on the left side below the tip path plane (see Fig 3) and was therefore more sensitive to the impulsive noise due to the blade-vortex interactions on the retreating side of the blade. It is also to be noted that the "maximum slap" condition of the Ogee tip rotor at microphone 3 was observed at a higher descent rate (5.5 m/sec (18 ft/sec)) compared to that at microphone 2 (4.27 m/sec (14 ft/sec)). The reason for the stronger blade-vortex

interaction on the retreating side of the blade of the Ogee tip rotor could be due to a more parallel intersection on the retreating side. A comparison of the spectra shows that the full rectangular tip rotor has the lowest spectral levels (see Fig 11c) and the effective tip rotor has the highest levels (see Fig 11b). This could be due to the different orientations of the interacting vortex with the retreating blade. A comparison of the spectra of the Ogee and TAMI tips (Figs 11a and 11d) shows that unlike those at microphone 2, the TAMI tip is as good as the Ogee tip as far as the impulsive noise is concerned.

Figures 12a through 12d give the acoustic spectra and pressure-time histories of the different rotors at microphone 1 under the "maximum slap" conditions. Microphone 1 was located upstream (see Fig 3) and therefore was most sensitive to the impulsive noise due to either blade-vortex interaction or the compressibility effects on the advancing side of the blades. The pressure-time histories show that for all the tips considered, taking into account the time lag effects, the blade vortex intersection has occurred around the azimuthal location $\psi = 105°$. This blade-vortex intersection appeared as a secondary spike in the pressure-time histories at microphone 2 (see Figs 7b and 9b). Unlike that at microphone 2, the spectrum of the Ogee tip rotor at microphone 1 showed a more distinct impulsive noise (compare Figs 12a and 8b). This could be due to the directivity of the impulsive noise on the advancing blades. A comparison of the spectra at microphone 1 shows that as in the case of microphone 2 at the "maximum slap" condition, the Ogee tip rotor had the lowest spectral levels. However, at the descent rates corresponding to the "maximum slap" condition, the spectral levels of the effective tip rotor were slightly higher than those of the full rectangular tip rotor (compare Figs 12b and 12c) and the TAMI tip rotor had the highest spectral levels.

The wind tunnel tests were also conducted at a lower advance ratio of 0.125. Under all flight conditions tested at this advance ratio, the rotor shaft was tilted slightly away from the flow compared to that at the advance ratio of 0.14. This resulted in a different wake geometry and therefore the characteristics of blade-vortex interaction were slightly different. Figures 13a through 13h give the acoustic spectra and the pressure-time histories at microphone 2 of different rotors under "maximum slap" conditions. A comparison of these spectra with those at the advance ratio of 0.14 shows that the essential characteristics of the impulsive noise remain the same regardless of the change in the advance ratio. However, the "maximum slap" conditions were found at lower rates of descent for advance ratio of 0.125. This could be due to the slightly different wake and tip vortex geometry at this advance ratio. Also, the pressure-time histories showed two distinct spikes (see Figs 13a and 13e). This suggests

two different blade-vortex intersections, both occurring in the first quadrant. Once again, this could be attributed to the different vortex geometry. A comparison of the spectra shows that unlike those at the advance ratio of 0.14, the spectral levels of the effective tip rotor are higher than those of the full rectangular tip rotor. This reversal can be attributed to different vortex geometry and, therefore, possibly a more parallel blade-vortex intersection in the case of the effective tip rotor at the advance ratio of 0.125. The Ogee tip rotor, however, showed the same characteristics (less intense impulsive noise and high broad-band noise) as it did at the advance ratio of 0.14. Also, the TAMI tip was not effective in reducing the impulsive noise at the advance ratio of 0.125. The acoustic trends observed at microphone 1 were similar to those observed at the advance ratio of 0.14. However, the trends observed at microphone 3 were somewhat different. Unlike that at advance ratio of 0.14, the full rectangular tip showed as high spectral levels at microphone 3 as those of the effective tip rotor. The spectral levels of the Ogee tip rotor at microphone 3 were lower than those of either the effective or full rectangular tip rotors.

Summarizing, it can be said that at both the advance ratios considered in the tests, the "maximum slap" was found at moderate rate of descents (of the order of 3.05 to 4.27 m/sec (10 to 14 ft/sec)) and the Ogee tip seemed to be more effective in reducing the impulsive noise. The TAMI tip was not found to be effective in reducing the impulsive noise at both the advance ratios considered. Also, despite the small differences in solidity of the different rotors tested (see Table I), it cannot be concluded that solidity played a major role in the impulsive noise characteristics of these rotors in descent flight.

Analysis Based on a Weighted dBA Approach: - The analysis of narrow-band spectra and pressure-time histories has given us a comparative evaluation of the acoustic data of different rotor tips. However, these results cannot be directly utilized to provide the subjective human response to the different rotor tips as regards their effectiveness in reducing the impulsive noise during descent flight. In order to obtain such an evaluation, the acoustic spectra of different rotor tips were compared on a dBA basis. To determine the full-scale effect of rotor tips, the acoustic spectra were first converted to those based on equivalent full-scale frequencies and the SPLs were then converted to dBA values using the A-weighted averaging curve. The equivalent full-scale frequencies were obtained by dividing the model frequencies by 6.13 which is equal to the ratio of model rotor rpm (1985) and the full-scale UH-1H rotor rpm (324). Figures 14 through 18 give these spectra (dBA vs. equivalent full-scale frequencies) of rotors with different tips under different flight conditions. These spectra are presented in bands of constant bandwidth of

100 Hz. It is believed that a comparison based on these spectra will give a more subjective evaluation of different rotor tips as regards annoyance and will therefore have a more practical significance.

Figure 14 gives the spectra in terms of dBA vs. equivalent full-scale frequency for the full rectangular tip rotor at an advance ratio of 0.14. These were obtained from the data taken at microphone 2. These spectra show that the peak dBA value increased from a value of 87.5 in steady level flight to a value of about 108 under "maximum slap" conditions at a descent rate of 4.27 m/sec (14 ft/sec). As the descent rate was increased further, the peak value decreased and reached a value of about 101 at a descent rate of 6.1 m/sec (20 ft/sec). This trend clearly establishes the annoying characteristics of impulsive noise in descent flight. It is also seen from Figure 14 that over most of the equivalent full-scale frequency range considered (100 to 800 Hz) the spectral levels at "maximum slap" condition (corresponds to a descent rate of 4.27 m/sec (14 ft/sec)) were about 15 to 20 dBA higher than those in steady level flight. It is also to be noted that the spectral curves in Figure 14 reached their peak values around an equivalent full-scale frequency of about 250 Hz and have similar shapes. Figure 15 gives the spectra of an Ogee tip rotor at microphone 2 at an advance ratio of 0.14. These spectra clearly show some of the characteristics of the Ogee tip rotor discussed earlier. In contrast to the full rectangular tip rotor (Fig 14), the Ogee tip rotor shows a relatively flat spectrum at equivalent full-scale frequencies beyond 400 Hz under different rates of descent. These spectra show that for equivalent full-scale frequencies beyond 400 Hz, the dBA levels remain almost the same with descent rate. This implies that the broad-band noise which contributed to the flat portion of the spectra is not significantly affected by the descent rate. These spectra also show that for full-scale frequencies below 400 Hz, the difference in dBA levels between the curves at descent rates corresponding to 4.27 m/sec (14 ft/sec) and 6.71 m/sec (22 ft/sec) are quite small. In fact, between a descent rate of 4.27 m/sec (14 ft/sec) and 6.71 m/sec (22 ft/sec), the peak dBA level changed by only about 1 dBA. As was the case with the full rectangular tip rotor, the peak dBA levels for the Ogee tip rotor also occurred around an equivalent full-scale frequency of about 250 Hz. The trends observed in the case of the effective and TAMI tip rotors were similar to that shown for the full rectangular tip rotor (Fig 14). Similar trends were also observed at the other microphone locations as well as at the other advance ratio (0.125) considered in the tests.

Figure 16 gives the spectra of rotors with different tips in terms of dBA vs. equivalent full-scale frequency at "maximum slap" conditions at microphone 2 and at the advance ratio of 0.14. It

is to be noted that these "maximum slap" conditions correspond to different rates of descent. All these spectra show the typical hump pattern characteristic of impulsive noise due to blade-vortex interaction. The dBA levels corresponding to different rotor tips at equivalent full-scale frequencies below 100 Hz are approximately the same since these levels are mainly due to the steady loads on the rotor. The dBA levels increase with frequency reaching their peak values (due to impulsive noise of blade-vortex interaction) around equivalent full-scale frequencies of 200 to 300 Hz. The dBA levels then drop with further increase in the frequency. However, as shown in Figure 16, the dBA levels in the case of the Ogee tip rotor remain almost constant for frequencies beyond 400 Hz, mainly due to the presence of a large component of broad-band noise. These spectra clearly show that over most of the frequency range considered, the full rectangular tip rotor had the highest dBA levels, while the Ogee tip rotor had the lowest dBA levels. As shown in Figure 16, the peak dBA value in the case of the full rectangular tip rotor is about 108.5. The effective tip reduces that value to about 105 while the Ogee tip reduces it to 100.5 dBA. The TAMI tip rotor (with air injected at 6.65 $N/m^2$ (94.7 PSIa)) had the same peak value as that of the effective tip rotor, but showed a drop of about 2 to 3 dB at higher frequencies compared to the effective tip rotor. Based on these spectra, it can be concluded that at least at the advance ratio of 0.14, the Ogee tip was the most effective in reducing the impulsive noise at microphone 2. Also, for this microphone location, it can be concluded that the TAMI system was not as effective as the Ogee tip in reducing the impulsive noise. It was also evident that the high level of broad-band noise observed in the case of the Ogee tip rotor did not undermine its effectiveness. However, the Ogee tip was not always the most effective. Figure 17 shows the spectra in terms of dBA vs. equivalent full-scale frequency obtained from the data taken at microphone 3 at an advance ratio of 0.14. These spectra correspond to rates of descent at which "maximum slap" was found and clearly show that, on a dBA basis, the Ogee tip rotor is almost as noisy as the effective tip rotor and that the full rectangular tip rotor is the quietest. This trend was observed only at microphone 3 at the advance ratio of 0.14. This shows that at least as far as the impulsive noise due to blade-vortex interaction on the retreating side is concerned, the Ogee tip need not necessarily be the quietest. However, the noise at microphone 3 is not representative of cabin noise. It is also to be noted that the peak dBA levels between different rotor tips differ by only about 3 dBA at microphone 3. The trends observed at microphone 1 are similar to those at microphone 2 but with smaller differences (of the order of 3 to 4 dBA) between the peak dBA levels of different tips.

Figure 18 gives the weighted spectra of different rotors at microphone 2 at the advance ratio of 0.125 at "maximum slap" conditions. The shapes of these curves are the same as those at the advance ratio of 0.14 (see Fig 16). Also, the Ogee tip continues to be the most effective. In addition at this advance ratio, the effective tip rotor showed the highest dBA levels reaching a peak value of about 107.5 dBA at a full-scale frequency of about 200 Hz. The full rectangular tip rotor showed (see Fig 18) a drop of about 3 dBA in the peak dBA level, while the Ogee tip showed a drop of about 8 dBA in its peak level, compared to the effective tip rotor. The TAMI tip once again proved to be marginally effective compared to the effective tip rotor. It is also to be noted that at this advance ratio, the spectral levels peaked at a lower equivalent full-scale frequency compared to that at the advance ratio of 0.14 (compare Figs 16 and 18). The trends observed at other microphone locations at the advance ratio of 0.125 were similar to those observed at microphone 2, except that the difference in the peak dBA levels between different tips is much smaller (of the order of only 2 to 3 dBA).

In conclusion, it can be said that despite its high broad-band noise levels, the Ogee tip was found to be the most effective in reducing impulsive noise on a "subjective" as well as "scientific basis" at least as far as the data at microphones 1 and 2 are concerned. The TAMI tip was found to be relatively ineffective, possibly due to a misalignment of the airjet and the axis of the tip vortex. The anticipated equivalence between the effective tip rotor and Ogee tip rotor was not realized, possibly due to the presence of a more concentrated tip vortex in the case of the effective tip rotor. As expected, the full rectangular tip rotor was found to be the noisiest both on a "subjective" and "scientific basis" in most of the flight conditions tested. However, under some flight conditions (advance ratio 0.125) the effective tip was found to be noisier than the full rectangular tip. This could probably be attributed to the different orientation of the interacting tip vortex. Despite the differences in solidity of the different rotors tested, it could not be concluded that solidity played a major role in the impulsive noise characteristics of these rotors in descent flight.

Performance Characteristics: - As was noted earlier, the rotors with all the different tips were tested such that they developed the same total lift of about 900 N (202 lb) at all the simulated descent rates. The power input to the driving motor was measured at all the flight conditions. A motor efficiency of about 80% was assumed (based on motor power characteristics) to obtain the power absorbed by the rotor. Figures 19 and 20 show the power absorbed vs. rate of descent curves for the rotors with different tips at the two advance ratios considered in the tests. The linear variation of these curves was expected since

the parasite power to be supplied by the motor reduces linearly with the descent rate at a given advance ratio.

Figure 19 gives the power curves for an advance ratio of 0.125. As shown in Figure 19, the power absorbed by the Ogee tip rotor was the highest followed by the full rectangular tip, TAMI tip (including the compressor power) and the effective tip rotors at all the descent rates considered. It is to be noted that the Ogee tip rotor and the full rectangular tip rotor had the same tip Mach number. However, the Ogee tip rotor absorbed on an average 2.5 KW (3.35 hp) more power compared to the full rectangular tip rotor. This suggests an increased drag at the Ogee tip which could be due to separated flow at the Ogee tip. It is to be noted that the Reynolds numbers in the Ogee tip region are much lower than those in the corresponding region for the full rectangular tip. It is also possible that since the blades are untwisted, both the full rectangular tip and the Ogee tip rotors might have had relatively large angles of attack near their blade tips for the thrust values at which they were tested. A combination of relatively high angle of attack and low Reynolds numbers might have resulted in a tip stall in the case of an Ogee tip rotor. The high drag associated with the tip stall could explain the increase in the power absorbed by the Ogee tip rotor compared to that of the full rectangular tip rotor. It is also to be noted that because of the large torque arm, small changes in the drag near the Ogee tip would result in relatively large changes in the torque absorbed by the rotor. The tip stall and the associated separated flow might also explain the increased broad-band noise found in the case of the Ogee tip rotor.

As shown in Figure 19, the power absorbed by the effective tip rotor was on an average 1.3 KW (1.76 hp) lower than that absorbed by the full rectangular tip rotor. It is believed that this is mainly due to the lower tip Mach number of the effective tip rotor compared to that of the full rectangular tip rotor. It is believed that at the angles of attack corresponding to the operating conditions (thrust and advance ratio) both the full and effective rectangular tips would be in the supercritical region. In the supercritical region, small changes in Mach number could result in relatively larger changes in the drag. It is, therefore, believed that despite a relatively small difference in the tip Mach number between the full rectangular tip and effective tip rotors (of the order of 7%), the larger tip Mach number and the higher torque-weighted solidity resulted in higher power absorption for the full rectangular tip rotor than that for the effective rectangular tip rotor.

The power absorbed by the TAMI tip rotor is on an average 3.5 KW (4.7 hp) lower than that of the effective tip rotor. Both of these rotors were run at the same tip speed and developed the same amount of thrust. This reduction in power is partly due to the power recovery from the pressure jet effect of the air mass injection system. However, in order to make a valid comparison, it is necessary to add the power required to obtain the necessary air jet for the TAMI system. An estimate of this power was made based on the kinetic energy of the air jet at the exit of the nozzle in the TAMI tip. It was found that approximately 4.5 KW (6 hp) may be required to drive the air mass injection system. As shown in Figure 19 for the same tip Mach number and thrust, the total power required for the TAMI tip rotor (including the power required to drive the air mass injection system) is more (by about 10% of the steady level flight power) than that of the effective tip rotor at most of the descent rates considered.

Figure 20 gives the power curves at the advance ratio of 0.14. As shown in Figure 20, the trends are similar to those observed at the advance ratio of 0.125. As expected, the power levels at 0.14 are slightly higher than those at 0.125. These increased levels are mainly due to the increased parasite drag of the assumed scaled fuselage at the higher forward velocity corresponding to the advance ratio of 0.14.

## CONCLUSIONS

It is believed that the controlled wind tunnel test program has provided a comparative assessment of the effectiveness of different blade tips in reducing the impulsive noise due to blade-vortex interaction in simulated descent flight. Specifically, the following conclusions were drawn:

1. Generally, for most of the flight conditions considered, the Ogee tip was the most effective in reducing the impulsive noise in descent flight. However, at advance ratio 0.14, the data at microphone 3 showed that the Ogee tip was not very effective in reducing the impulsive noise. In addition, at low rates of descent, because of the presence of strong broad-band noise, the Ogee tip was as noisy as the other blade tips considered.

2. At most of the flight conditions and microphone locations considered, the full rectangular tip had the highest impulsive noise levels. However, at an advance ratio 0.14, the data at microphone 3 showed that the full rectangular tip had the lowest impulsive noise levels.

3. In general, the TAMI tip was found to be ineffective in reducing the impulsive noise due to blade-vortex interaction in descent flight. It is believed that the TAMI system is very sensitive to the rotor operating conditions and that unless the nozzle location is carefully selected consistent with the tip vortex location at the blade trailing edge for the rotor operating conditions of interest, the TAMI system will not be as effective as the Ogee tip in reducing the impulsive noise due to blade-vortex interaction.

4. A "subjective" evaluation of the acoustic spectra of rotors with different blade tips in terms of dBA versus equivalent full-scale frequency confirmed the acoustic trends observed in the spectral data.

5. For the same tip Mach number and thrust, TAMI tip rotor required more power than the effective tip rotor and the Ogee tip rotor required more power than the full rectangular tip rotor.

6. The increased power absorption in the case of an Ogee tip rotor may have been caused by a possible tip stall due to very low Reynolds numbers and high angles of attack in the Ogee tip region. The tip stall and the associated turbulent flow may also have been responsible for the higher broad-band noise observed for the Ogee tip rotor.

## REFERENCES


1. Tangler, James L., "Schlieren and Noise Studies of Rotors in Forward Flight", 33rd Annual National Forum of the American Helicopter Society, Preprint No. 77, 33-05, Washington, D.C., May 1977.

2. Widnall, S., "Helicopter Noise due to Blade-Vortex Interaction", Journal of the Acoustical Society of America, Vol. 50, No. 1 (Part 2), 1971, pp. 354-365.

3. Schieman, J. and Shivers, J., "Exploratory Investigation of the Structure of the Tip Vortex of a Semi-span Wing for Several Wing Modifications", NASA/Langley Research Center, NASA TND-6101, February 1971.

4. Chigier, N. and Corsiglia, V., "Tip Vortices - Velocity Distributions", 27th Annual National Forum of the American Helicopter Society, Preprint No. 522, Washington, D.C., May 1971.

5. Spencer, R., Sternfeld, H. and McCormick, B., "Tip Vortex Core Thickening for Application to Helicopter Rotor Noise Reduction", US Army Material Laboratories, R-403-A, September 1966.

6. White, R.P., Jr., Patent: "Vortex Dissipator", US Patent No. 3,845,918; Issued November 5, 1974.

7. Balcerak, J.C. and Feller, R., "Vortex Modification by Mass Injection and by Tip Geometry", USAAMRDL Contract No. DAAJ02-72-C-0097, RASA Report 73-01, USAAMRDL Technical Report 73-45, June 1973.

8. Balcerak, J.C. and Feller, R., "Effect of Sweep Angle on the Pressure Distributions and Effectiveness of the Ogee Tip in Diffusing a Line Vortex", RASA Report No. 73-07, NASA CR-132355, September 1973.

9. Landgrebe, Anton J. and Bellinger, E. Dean, "Experimental Investigation of Model Variable Geometry and Ogee Tip Rotors", NASA CR-2275, 1974.

10. Rorke, J.B., Moffitt, R.C. and Ward, J.F., "Wind Tunnel Simulation of Full-Scale Vortices", 28th Annual National Forum of the American Helicopter Society, Preprint No. 623, May 1972.

11. Mantay, W.R., Campbell, R.L. and Shidler, P.A., "Full-Scale Testing of an Ogee Tip Rotor", Presented at Specialists Meeting on Helicopter Acoustics, Hampton, Virginia, May 1978.

12. Rinehart, S.A., "Theoretical Study of Modifications of Rotor Tip Vortex by Aerodynamic Means", RASA Report 70-02, ONR Contract N00014-69-C-0169, January 1970.

13. White, R.P. Jr., Balcerak, J.C. and Rinehart, S.A., "An Experimental Study of Tip Vortex Modification by Mass Flow Injection", RASA Report 71-01, ONR Contract N00014-69-C-0169, AD 726736, 1971.

14. White, R.P. Jr. and Balcerak, J.C., "An Investigation of the Mixing of Linear and Swirling Flows", RASA Report 72-04, ONR Contract N00014-71-C-0226, 1972.

15. Balcerak, J.C. and Zalay, A.D., "Investigation of the Effect of Mass Injection to Restructure a Trailing Tip Vortex at Transonic Speeds", RASA Report 73-03, ONR Contract N00014-71-C-0226, February 1973.

16. White, R.P. Jr. and Balcerak, J.C., "Investigation of the Dissipation of the Tip Vortex of a Rotor Blade by Mass Injection", USAAMRDL TR-72-43, August 1972.

17. White, R.P. Jr., Balcerak, J.C. and Zalay, A.D., "Investigation of Viscous Line Vortices With and Without the Injection of Core Turbulence", RASA Report 74-01, ONR Contract N000-14-71-C-0226, February 1974.

18. Balcerak, J.C., White, R.P. Jr. and Pegg, R.J., "Summary of Results Indicating the Beneficial Effects of Rotor Vortex Modifications", AHS National Symposium on Helicopter Aerodynamic Efficiency", Hartford, Connecticut, March 1975.

19. White, R.P. Jr., "Wind Tunnel Tests of a Two-Bladed Model Rotor to Evaluate the TAMI System in Descending Forward Flight", NASA CR-145195, May 1977.

TABLE I

GEOMETRIC CHARACTERISTICS OF ROTORS

| | |
|---|---|
| Chord | 10.67 cm (4.2 in) |
| Number of Blades | 2 |
| Type of Hub | Teetering |
| Blade Airfoil | 0015 |
| Blade Twist | 0 (No Twist) |
| Rotor Radius with Ogee Tip | 1.194 m (3.9175 ft) |
| Rotor Radius with Full Rectangular Tip | 1.194 m (3.9175 ft) |
| Rotor Radius with Effective Tip | 1.12 m (3.673 ft) |
| Rotor Radius with TAMI Tip | 1.12 m (3.673 ft) |
| Solidity with Ogee Tip | 0.0533 |
| Solidity with Full Rectangular Tip | 0.0569 |
| Solidity with Effective Tip/TAMI Tip | 0.0607 |

TABLE II

TEST CONDITIONS

| | |
|---|---|
| Rotor rpm | 1985 |
| Rotor Tip Speed (with Full Rectangular or Ogee Tip) | 248 m/sec (814 ft/sec) |
| Rotor Tip Speed (with Effective or TAMI Tip) | 233 m/sec (763 ft/sec) |
| Rotor Thrust | 900 N (202 lbs) |
| Thrust Coefficient (with Full Rectangular or Ogee Tip) | 0.002664 |
| Thrust Coefficient (with Effective or TAMI Tip) | 0.003446 |
| Assumed Equivalent Fuselage Flat-Plate Drag Area | 0.093 $m^2$ (1 sq ft) |
| Advance Ratios Considered | 0.125, 0.140 |
| Range of Rates of Descent Considered | 0 - 6.1 m/sec (0 - 20 ft/sec) |

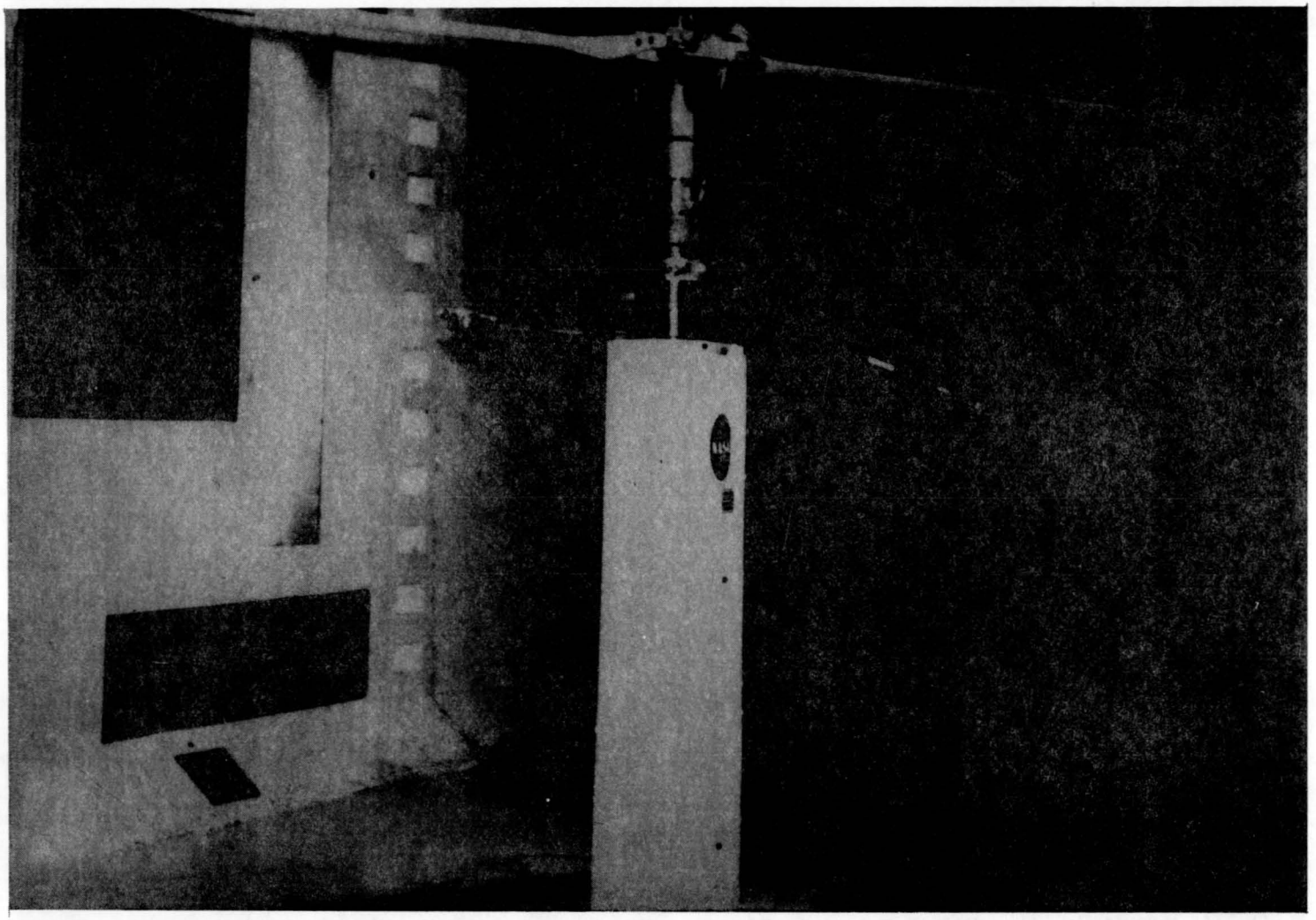

FIGURE 1. Tami Rotor Test Model in the Wind Tunnel.

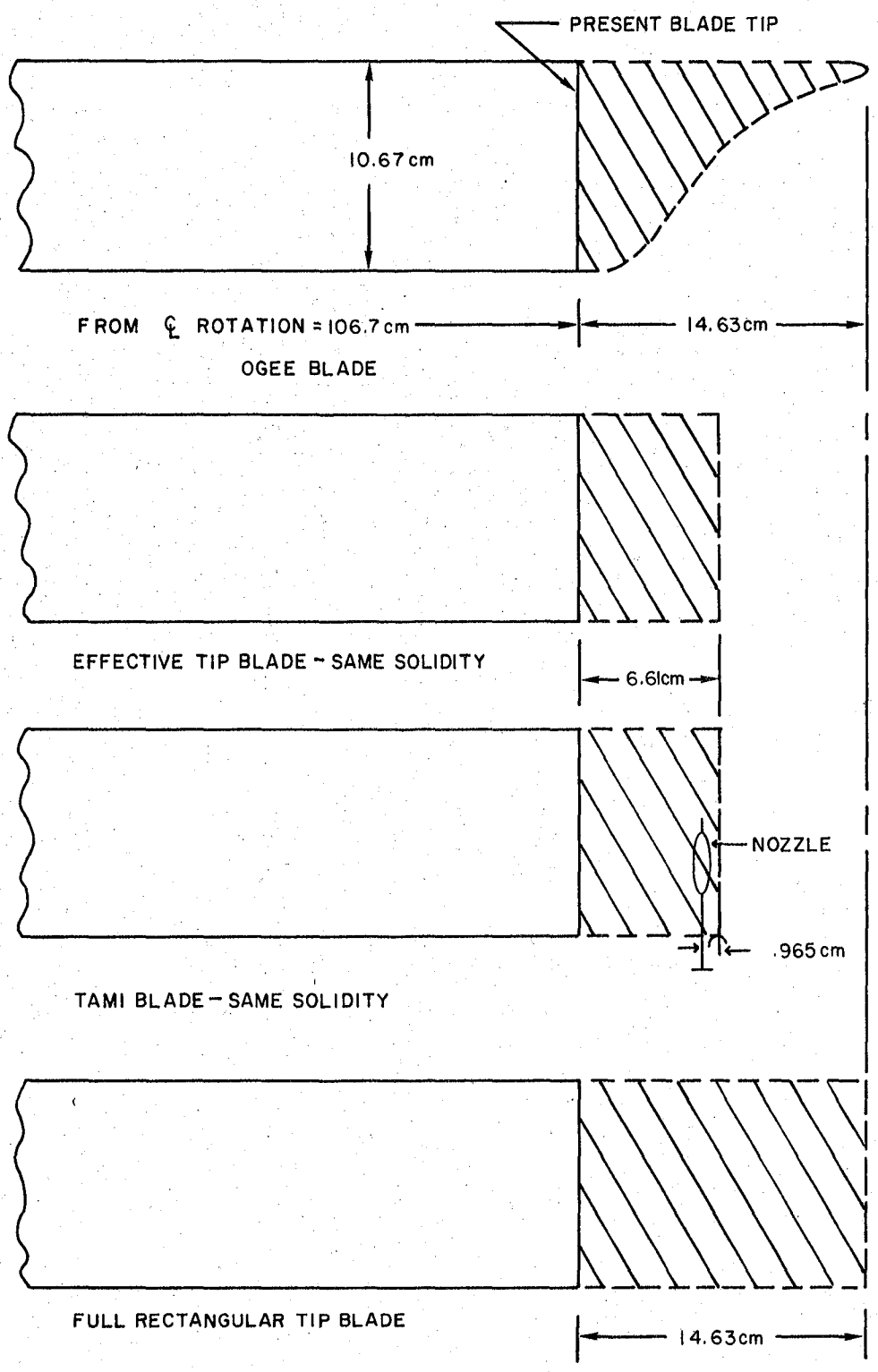


FIGURE 2. Blade Tip Modifications.

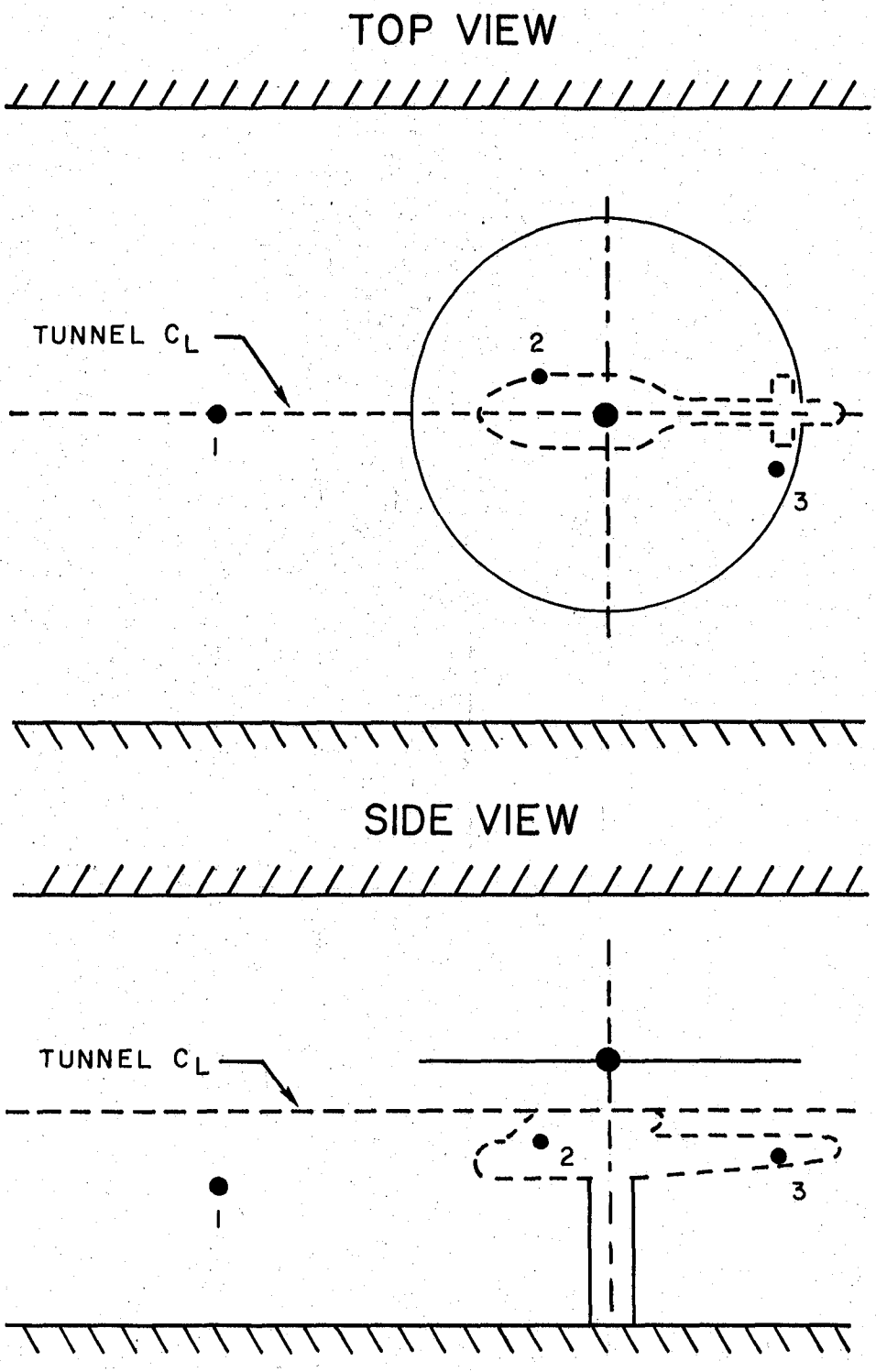


FIGURE 3. Microphone Locations (NOTE: Mikes 2 and 3 Move with Rotor Support Structure).

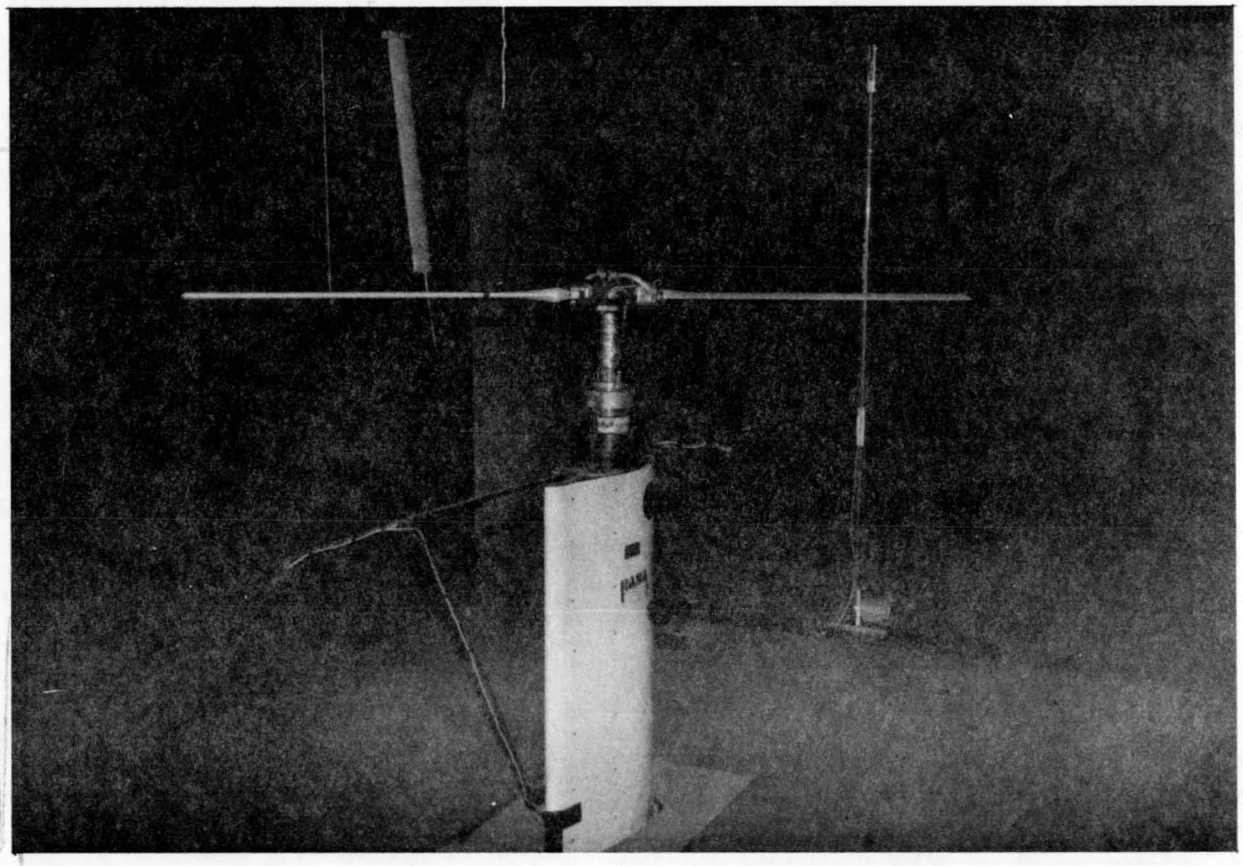

FIGURE 4. Rotor Model in the Acoustically Treated Wind Tunnel Test Section.

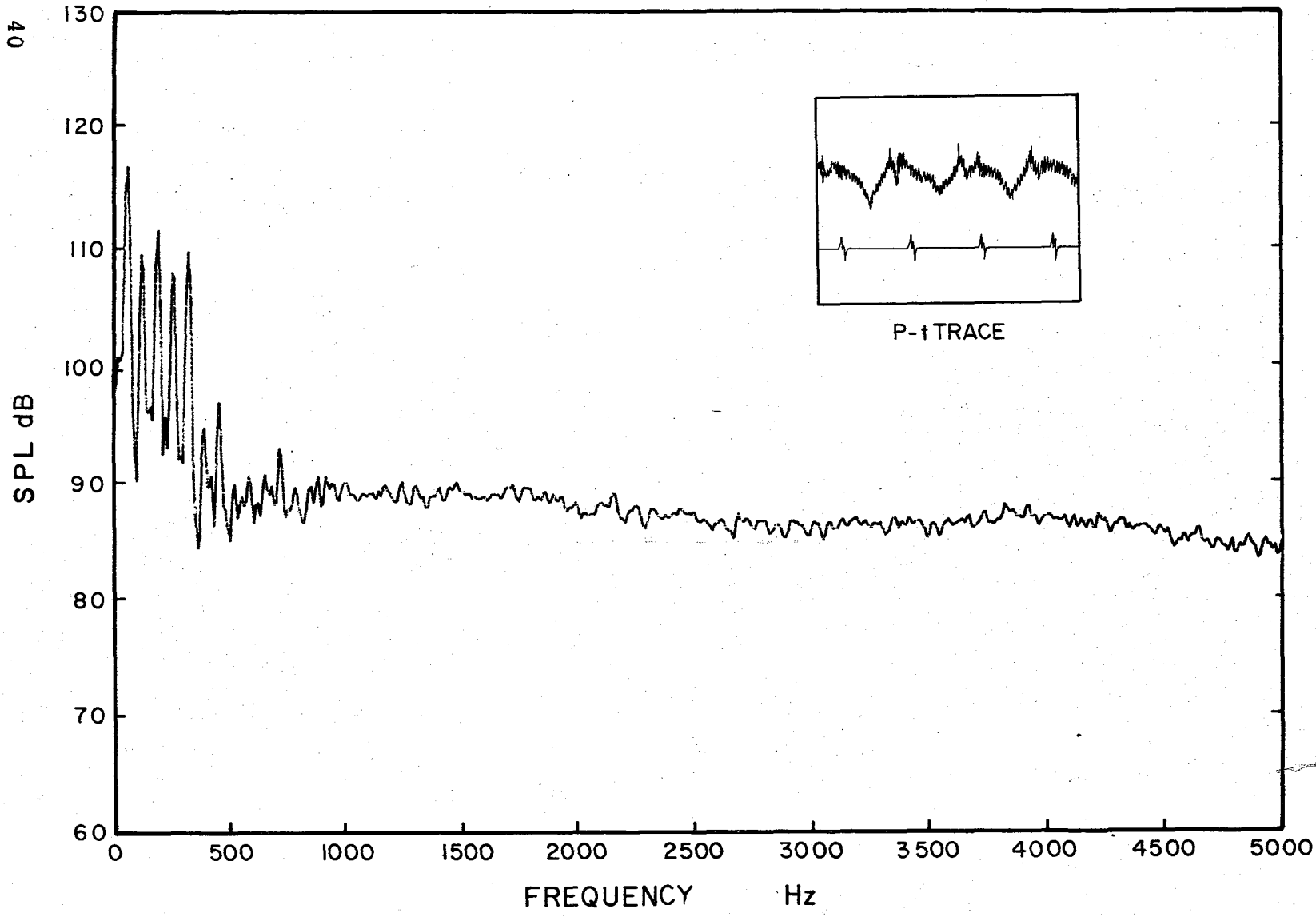


FIGURE 5a. Narrow-Band Spectrum of the Ogee Tip Rotor in Steady Level Flight at Microphone 2 and Advance Ratio 0.14.

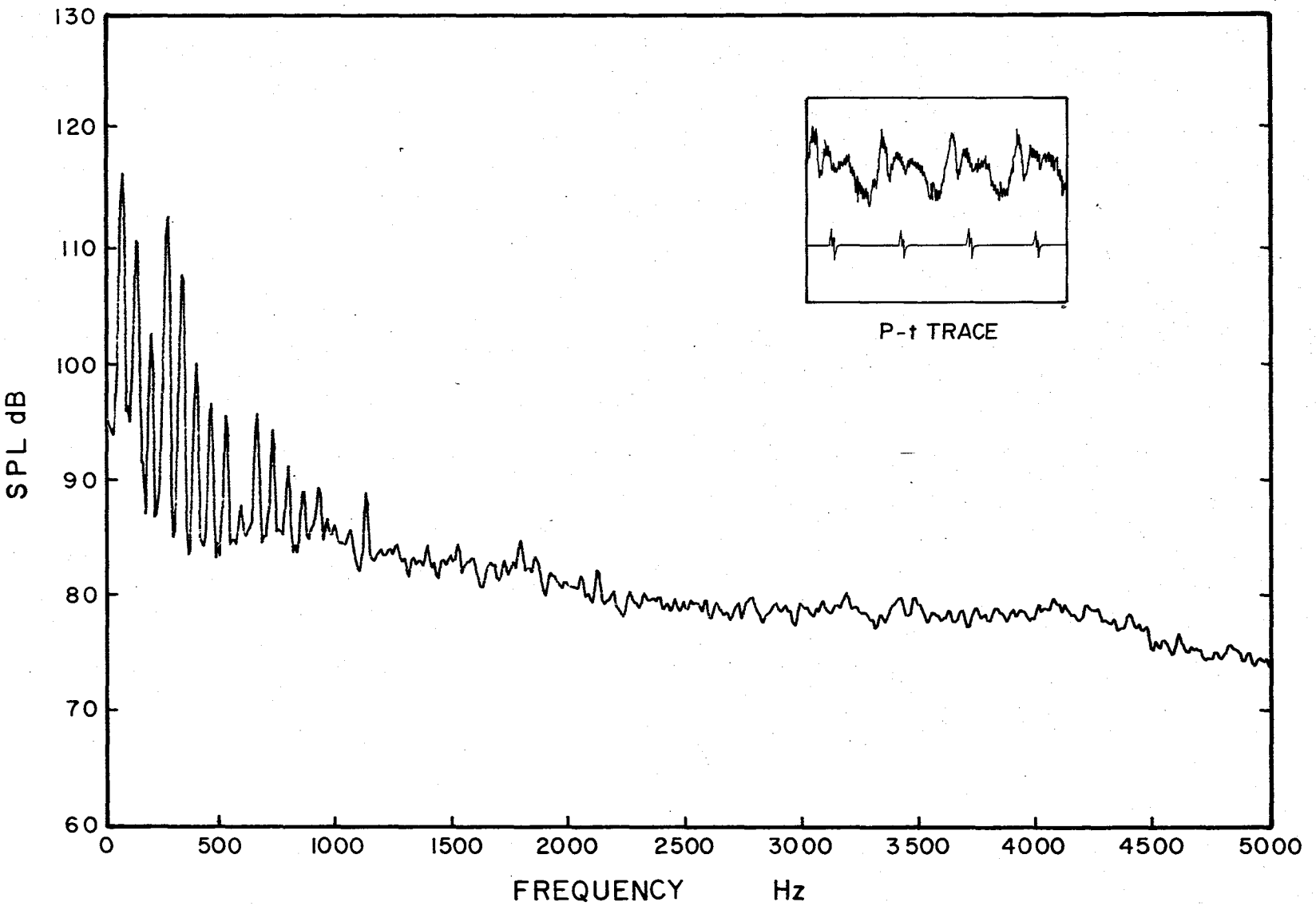


FIGURE 5b. Narrow-Band Spectrum of the Effective Tip Rotor in Steady Level Flight at Microphone 2 and Advance Ratio 0.14.

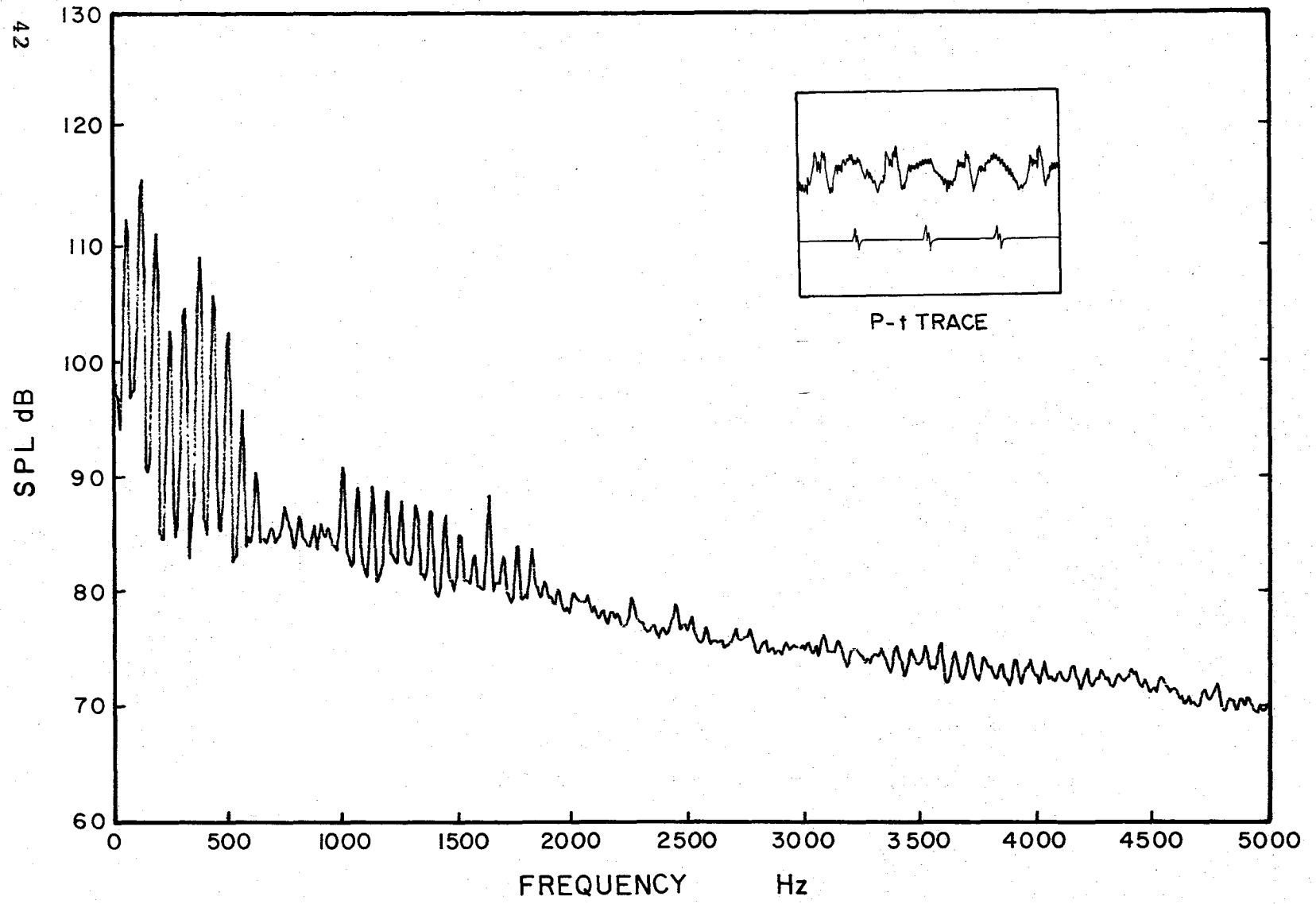


FIGURE 5c. Narrow-Band Spectrum of the Full Rectangular Tip Rotor in Steady Level Flight at Microphone 2 and Advance Ratio 0.14.

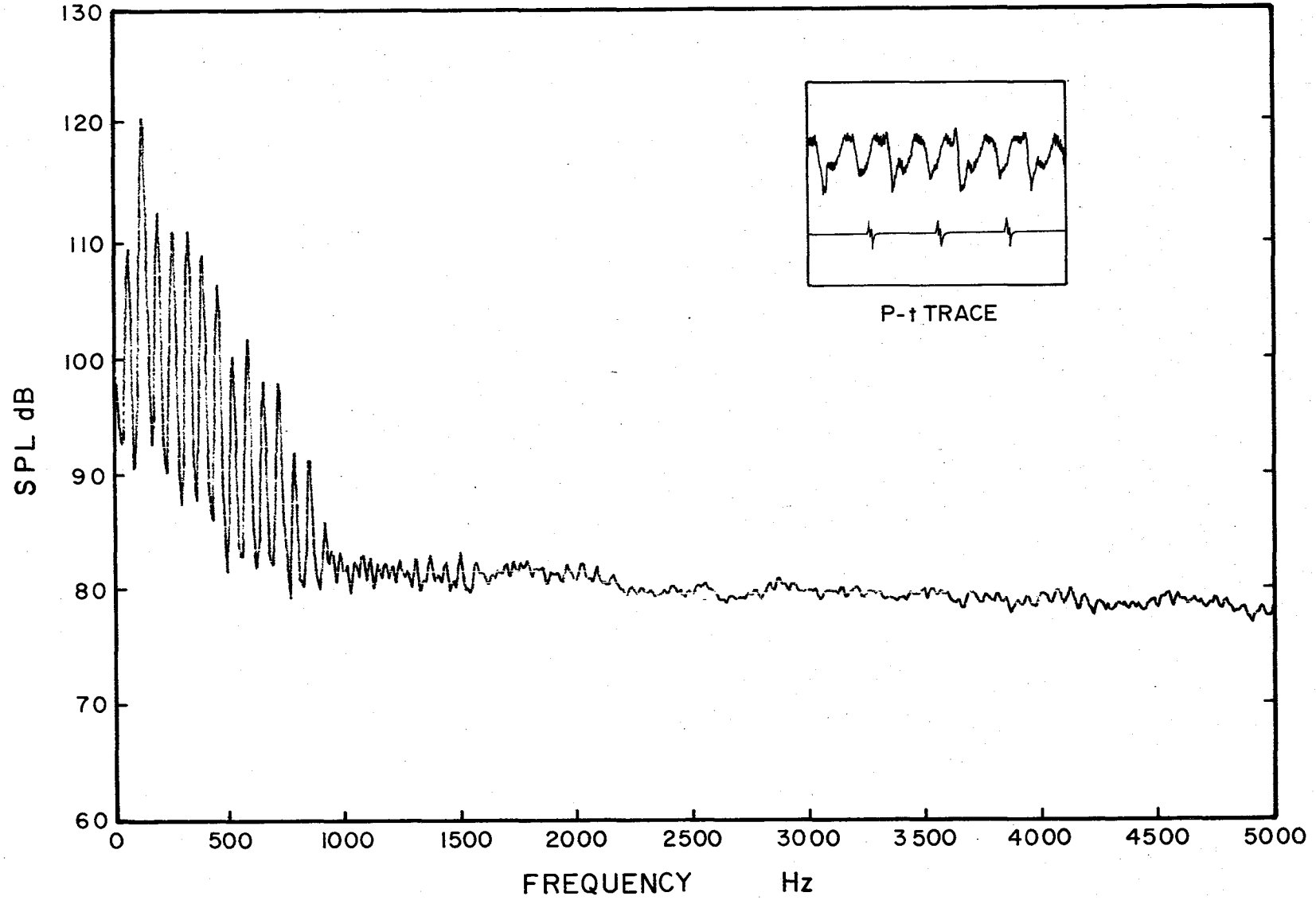


FIGURE 6a. Narrow-Band Spectrum of the Ogee Tip Rotor in Steady Level Flight at Microphone 1 and Advance Ratio 0.14.

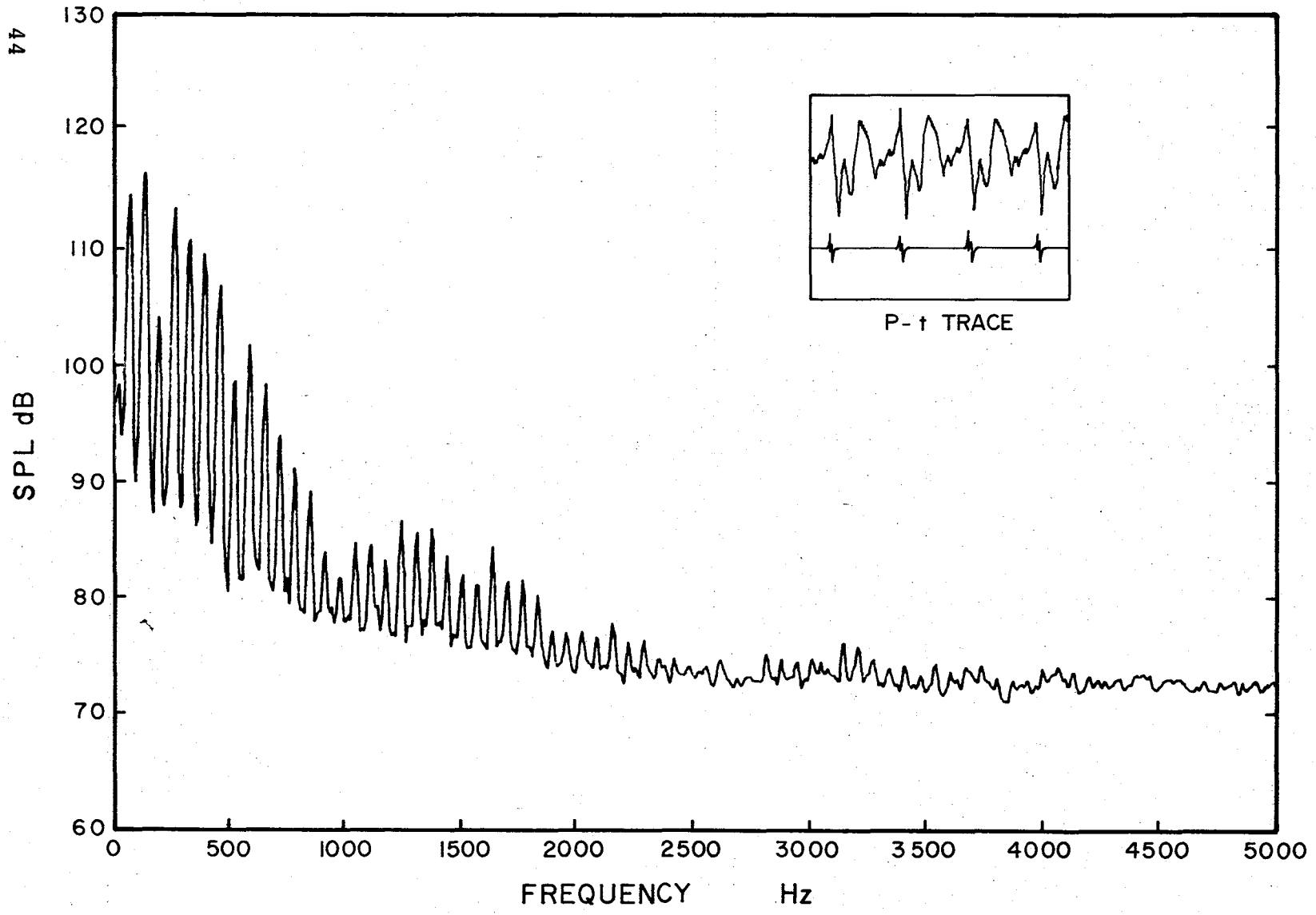


FIGURE 6b. Narrow-Band Spectrum of the Effective Tip Rotor in Steady Level Flight at Microphone 1 and Advance Ratio 0.14.

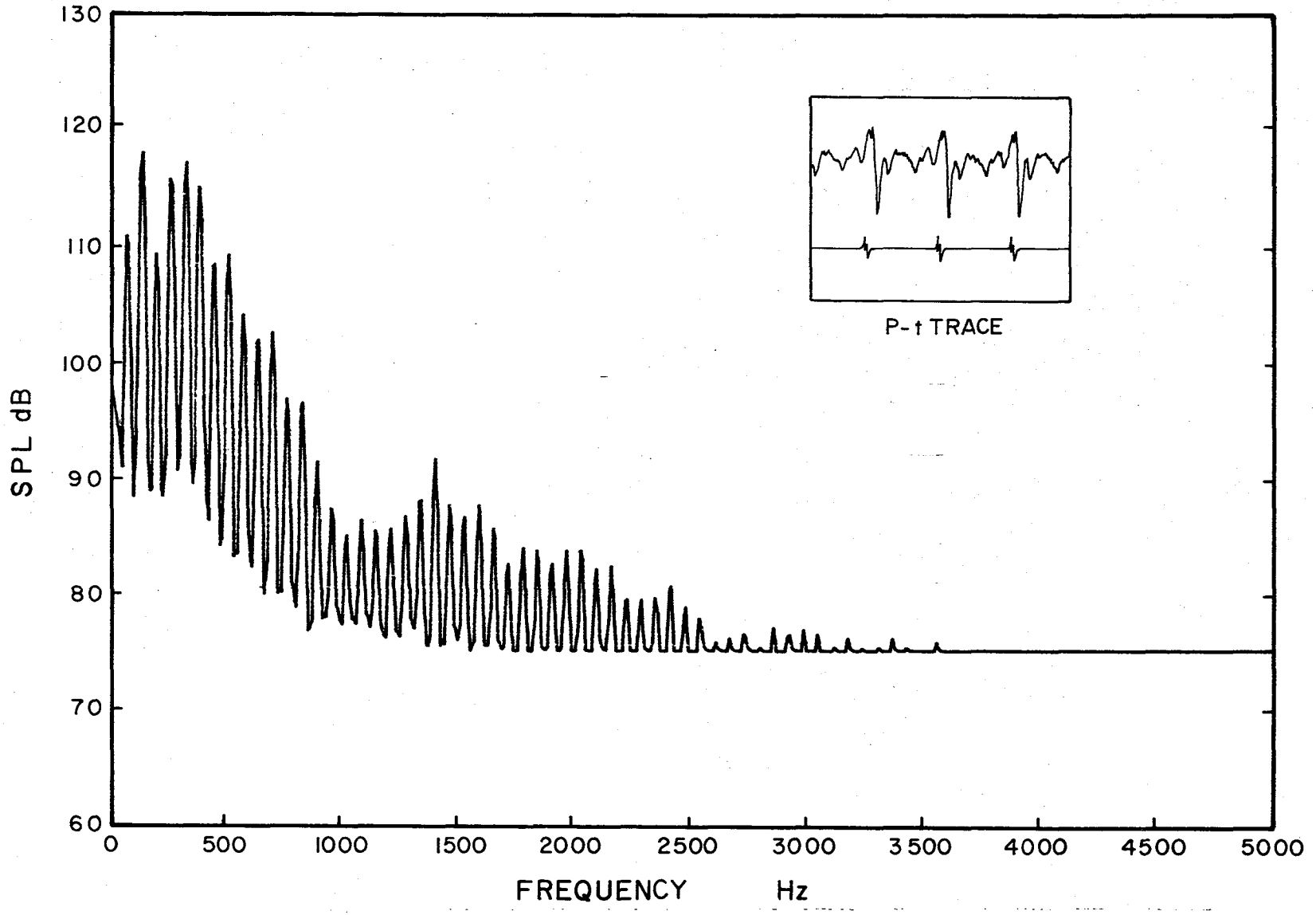


FIGURE 6c. Narrow-Band Spectrum of the Full Rectangular Tip Rotor in Steady Level Flight at Microphone 1 and Advance Ratio 0.14.

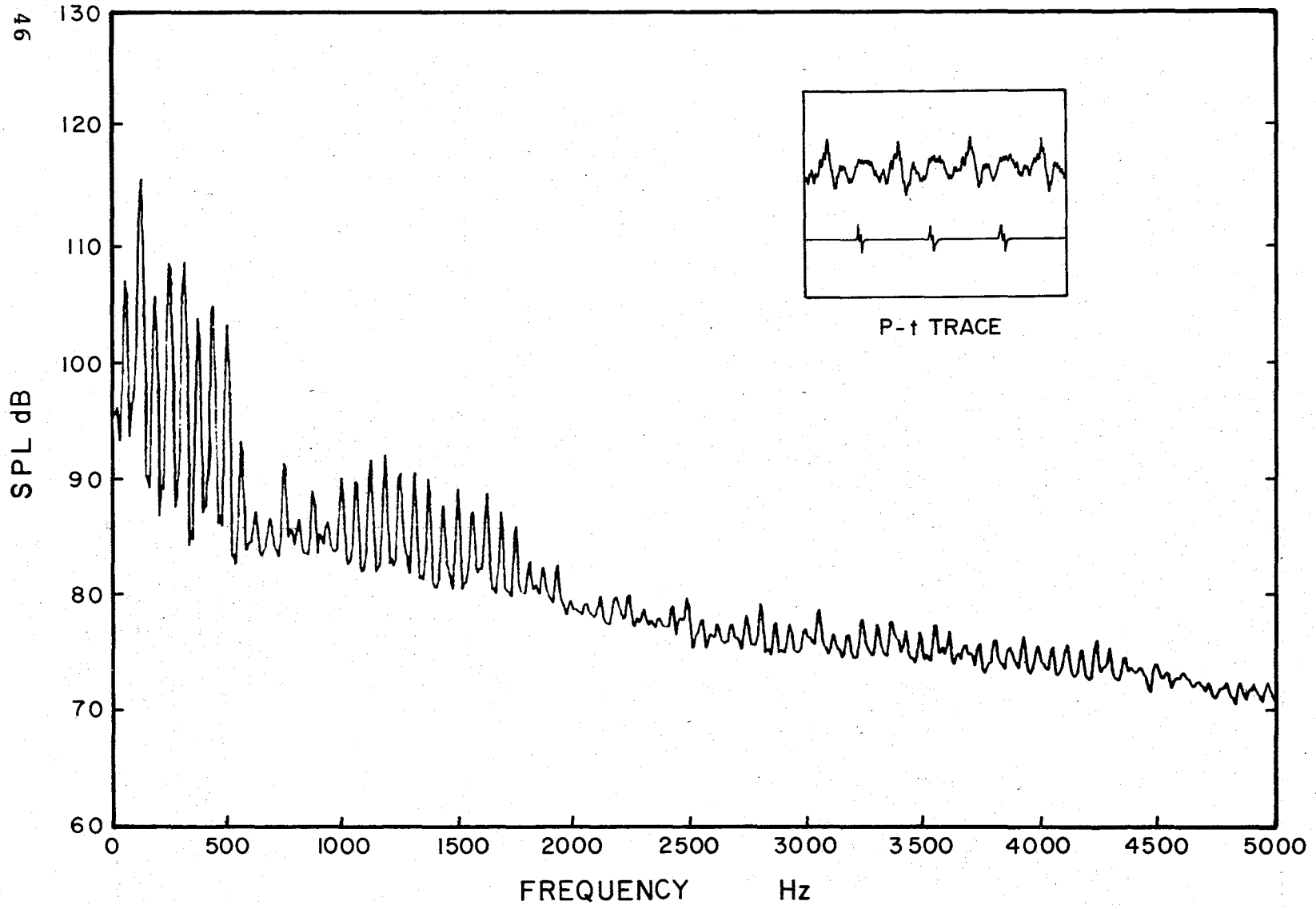


FIGURE 7a. Narrow-Band Spectrum of the Full Rectangular Tip Rotor in Descent Flight at Microphone 2 and Advance Ratio 0.14; Descent Rate = 0.61 m/sec.

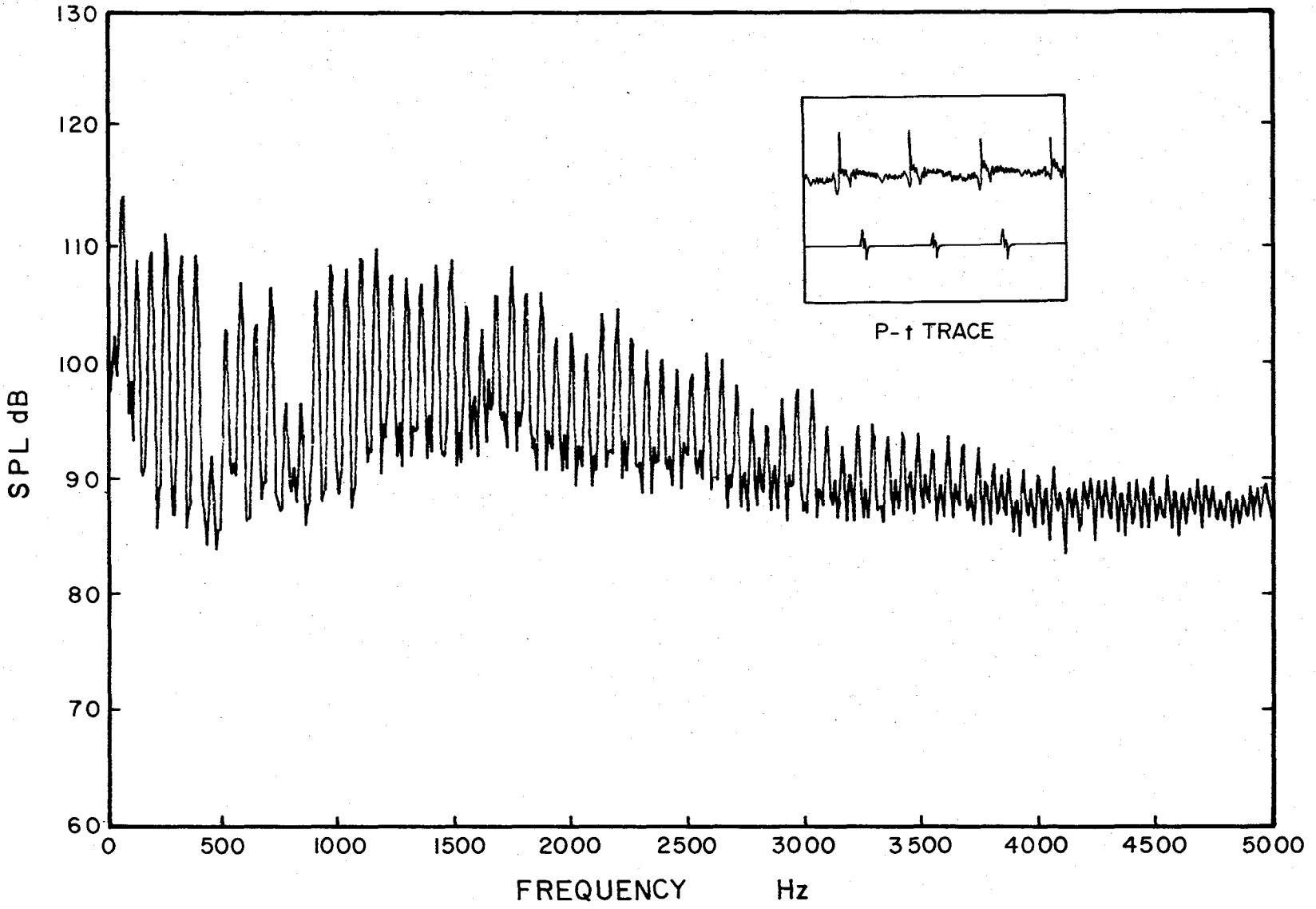


FIGURE 7b. Narrow-Band Spectrum of the Full Rectangular Tip Rotor in Descent Flight at Microphone 2 and Advance Ratio 0.14; Descent Rate = 4.27 m/sec.

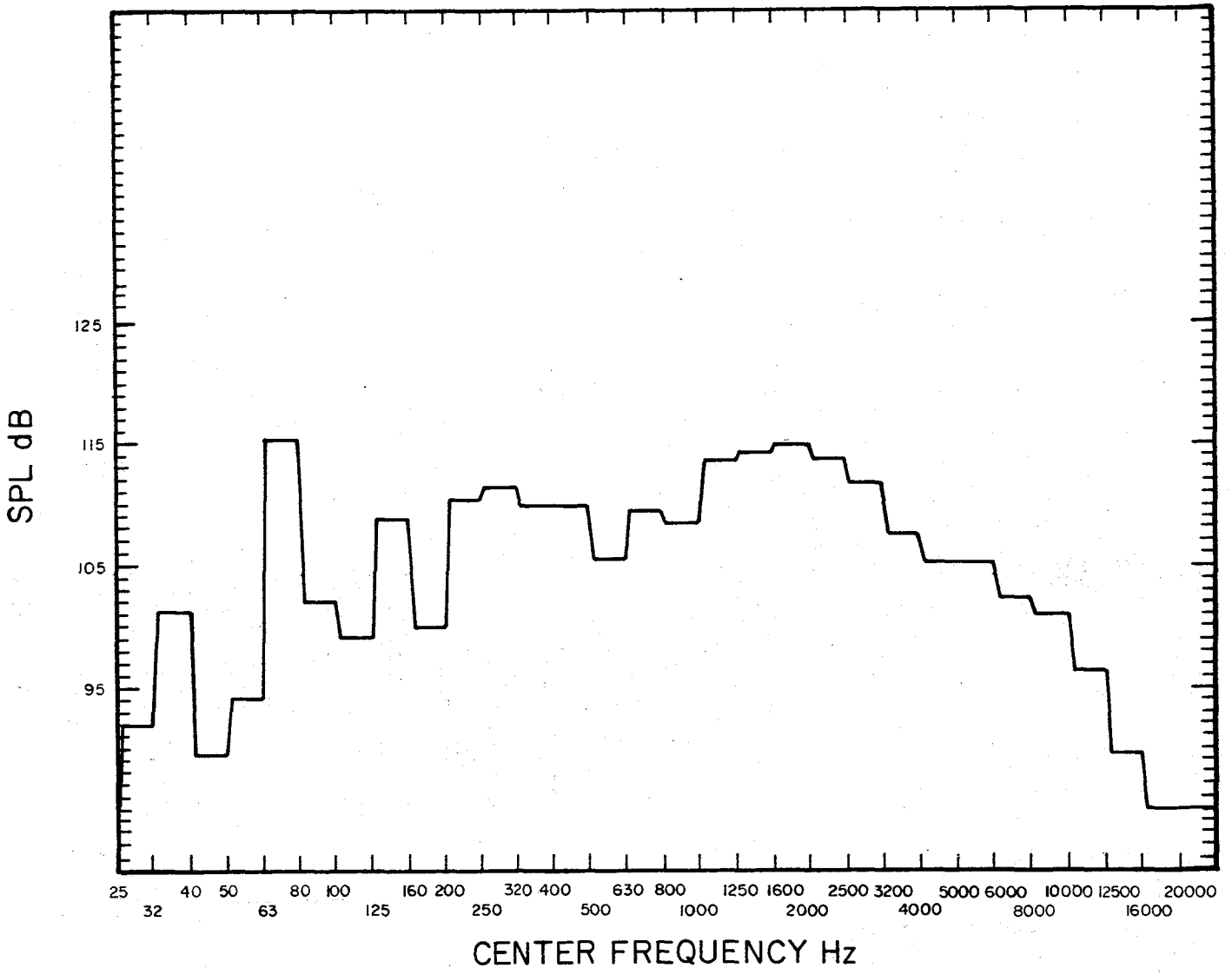


FIGURE 7c. 1/3 Octave-Band Spectrum of the Full Rectangular Tip Rotor in Descent Flight at Microphone 2 and Advance Ratio 0.14; Descent Rate = 4.27 m/sec.

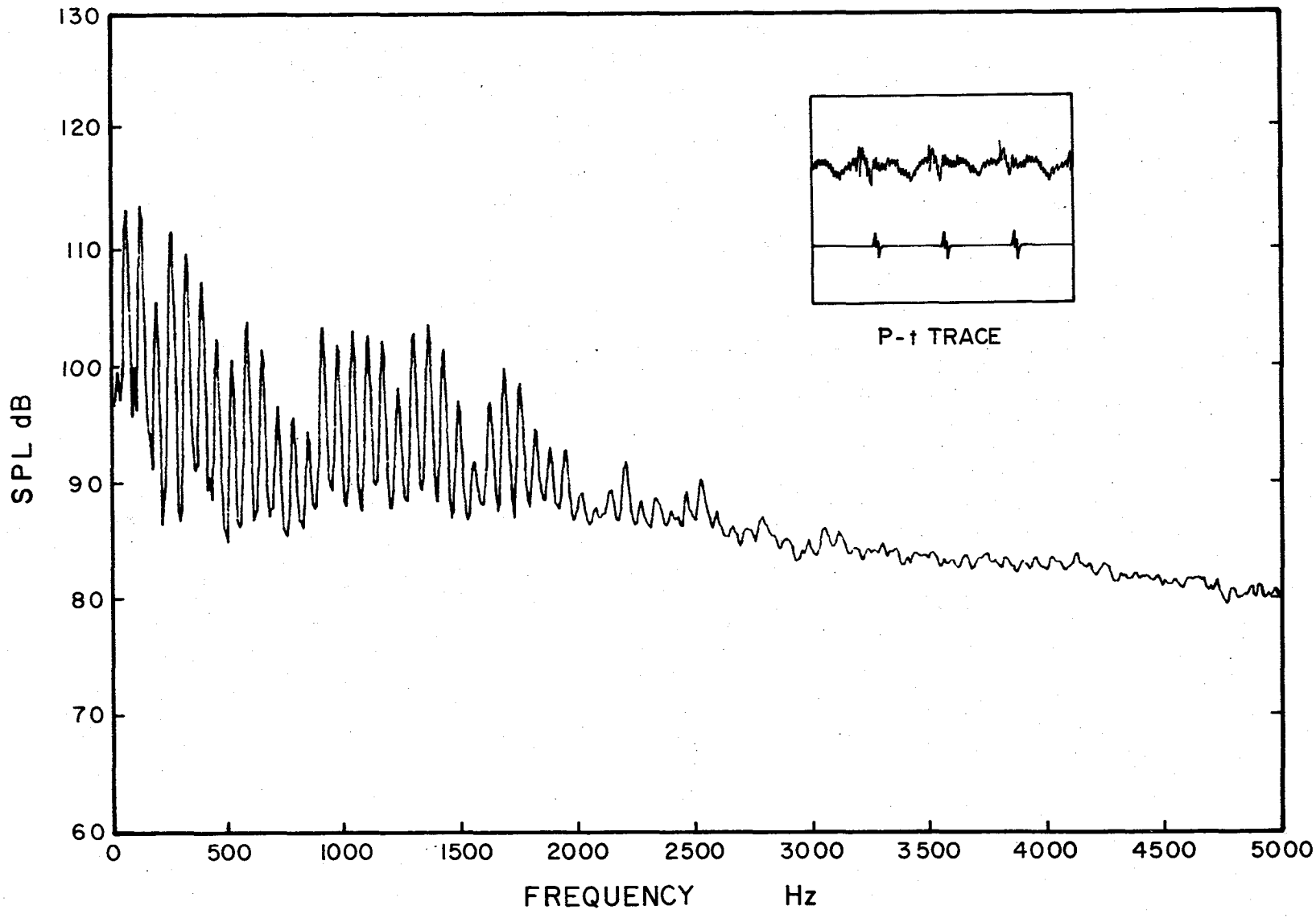


FIGURE 7d. Narrow-Band Spectrum of the Full Rectangular Tip Rotor in Descent Flight at Microphone 2 and Advance Ratio 0.14; Descent Rate = 6.10 m/sec.

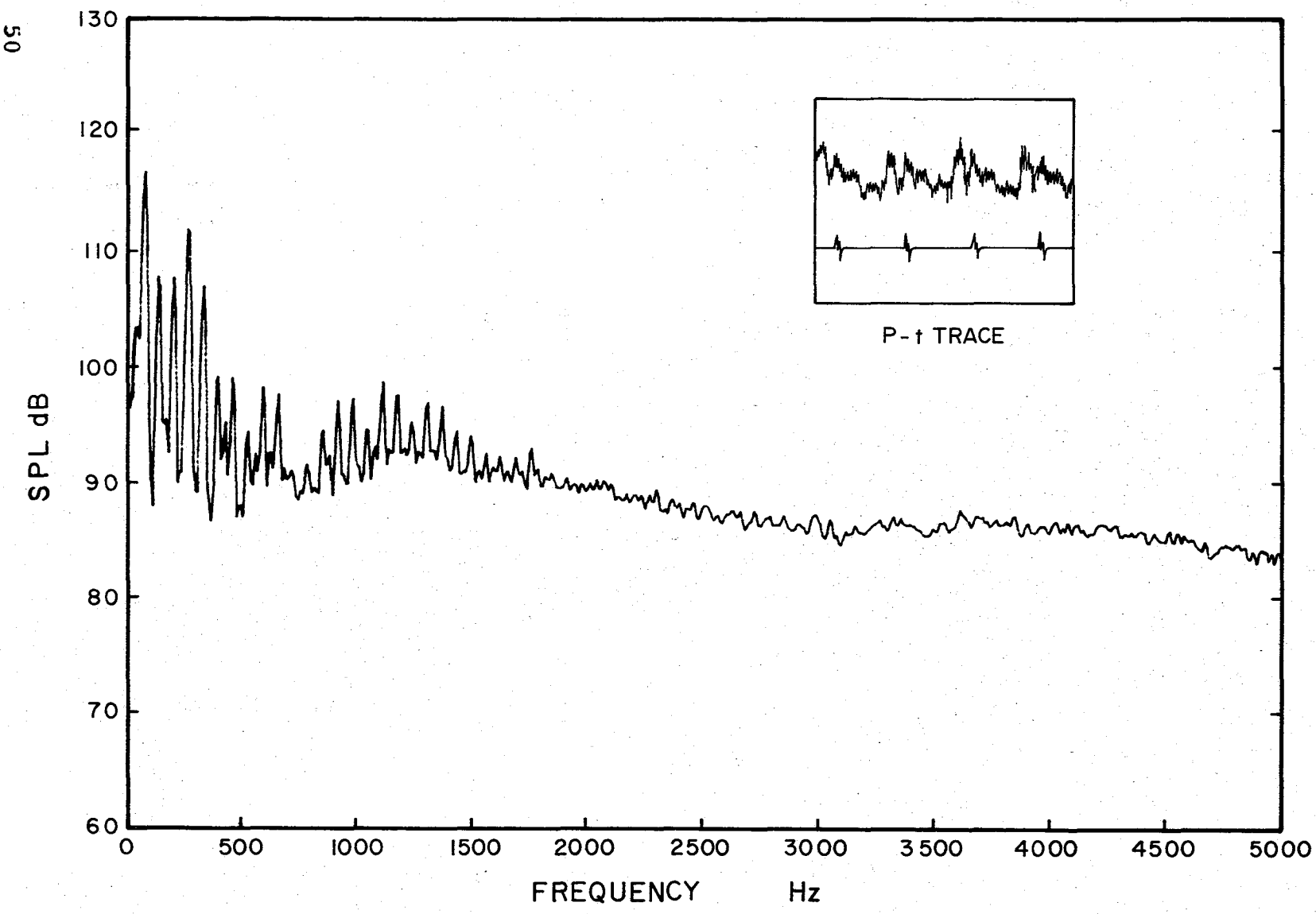


FIGURE 8a. Narrow-Band Spectrum of the Ogee Tip Rotor in Descent Flight at Microphone 2 and Advance Ratio 0.14; Descent Rate = 3.05 m/sec.

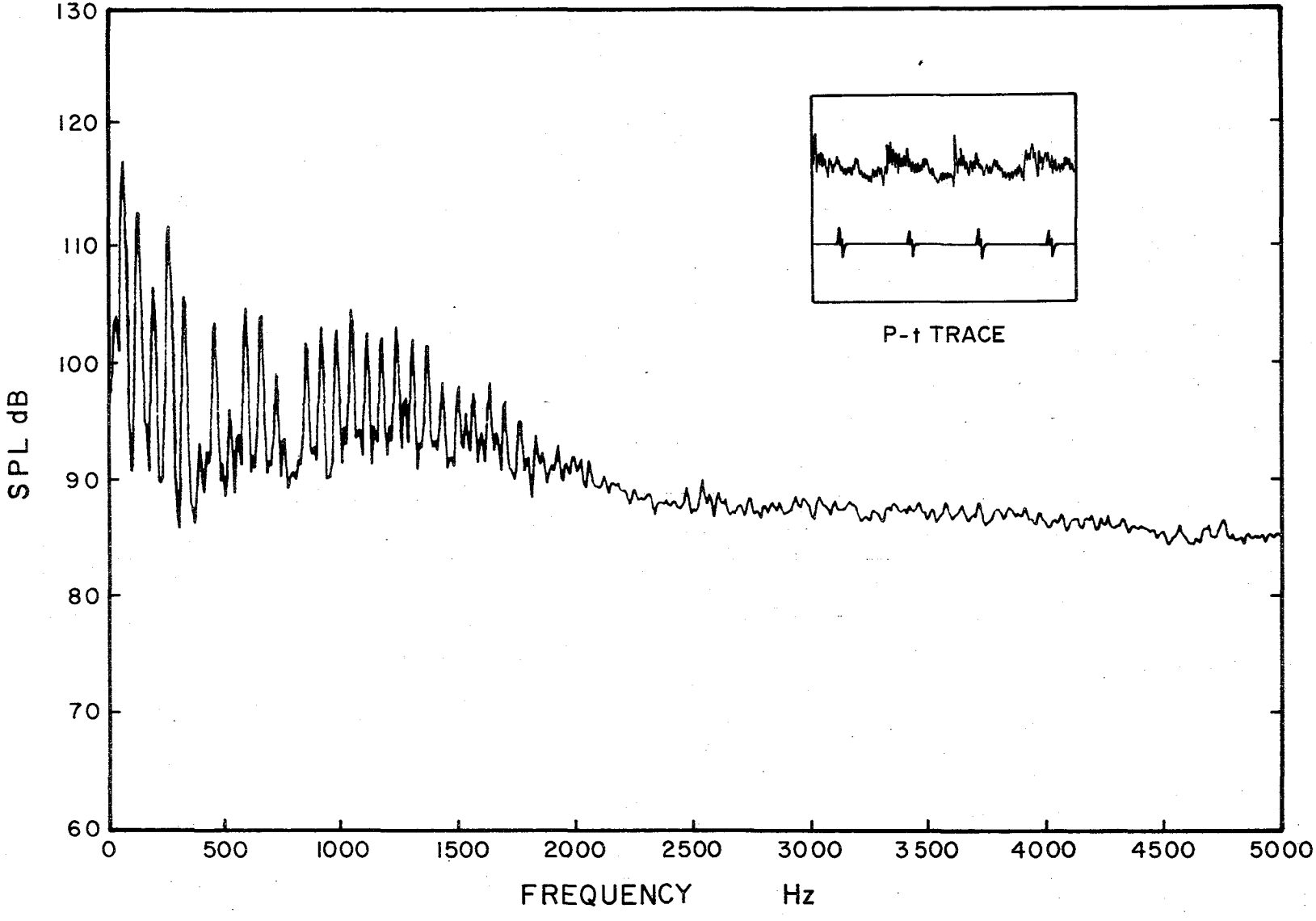


FIGURE 8b. Narrow-Band Spectrum of the Ogee Tip Rotor in Descent Flight at Microphone 2 and Advance Ratio 0.14; Descent Rate = 4.27 m/sec.

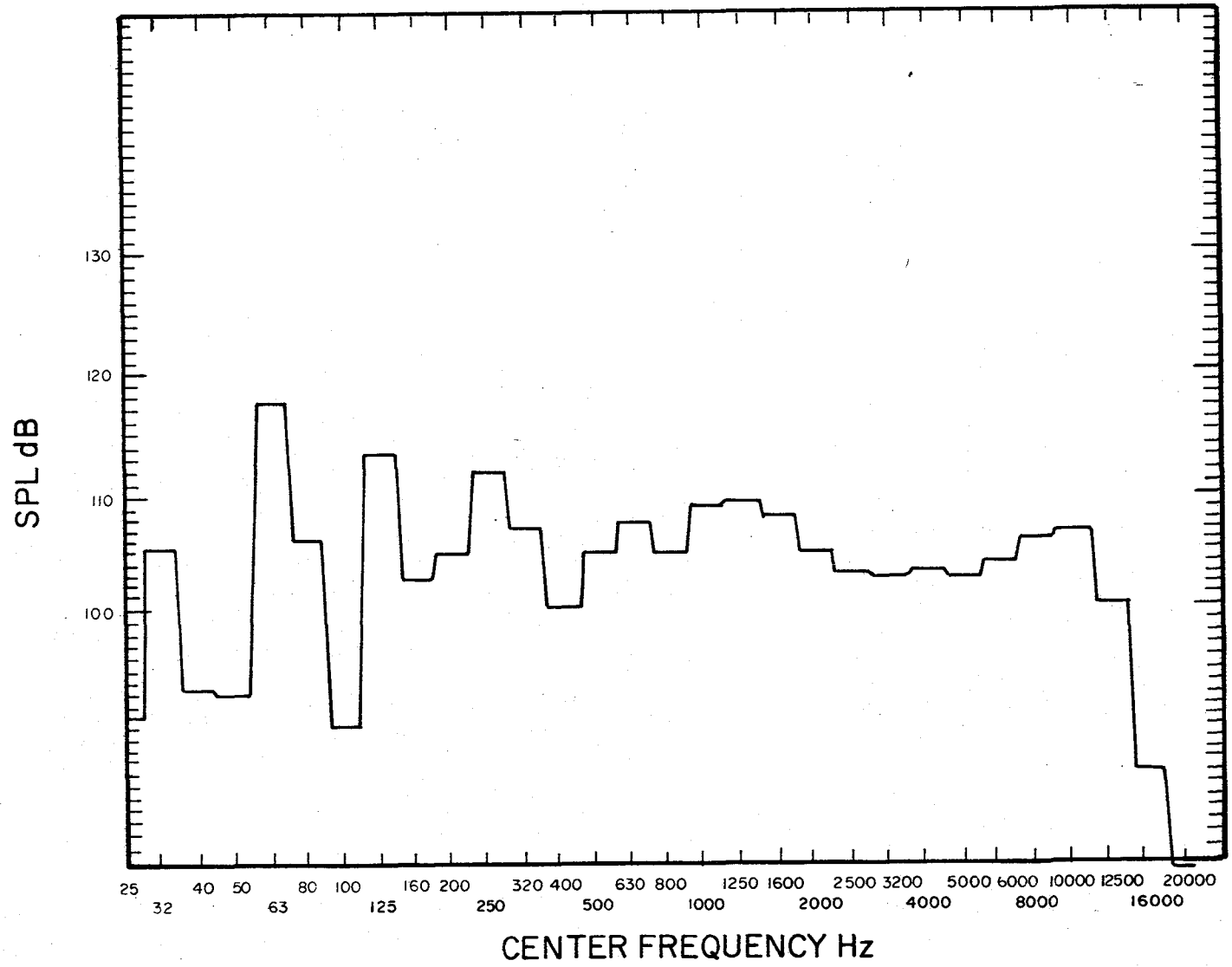


FIGURE 8c. 1/3 Octave-Band Spectrum of the Ogee Tip Rotor in Descent Flight at Microphone 2 and Advance Ratio 0.14; Descent Rate = 4.27 m/sec.

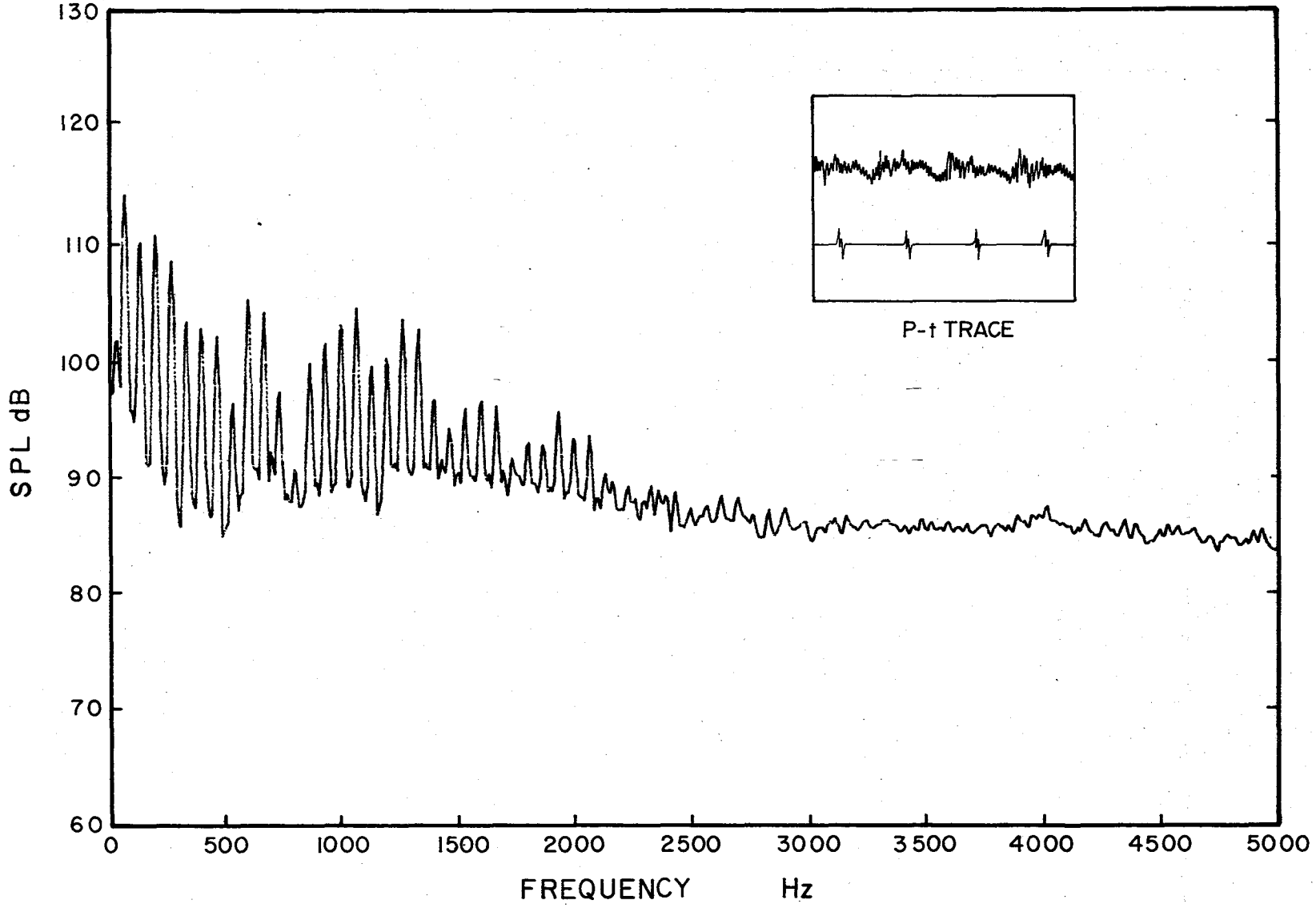


FIGURE 8d. Narrow-Band Spectrum of the Ogee Tip Rotor in Descent Flight at Microphone 2 and Advance Ratio 0.14; Descent Rate = 6.71 m/sec.

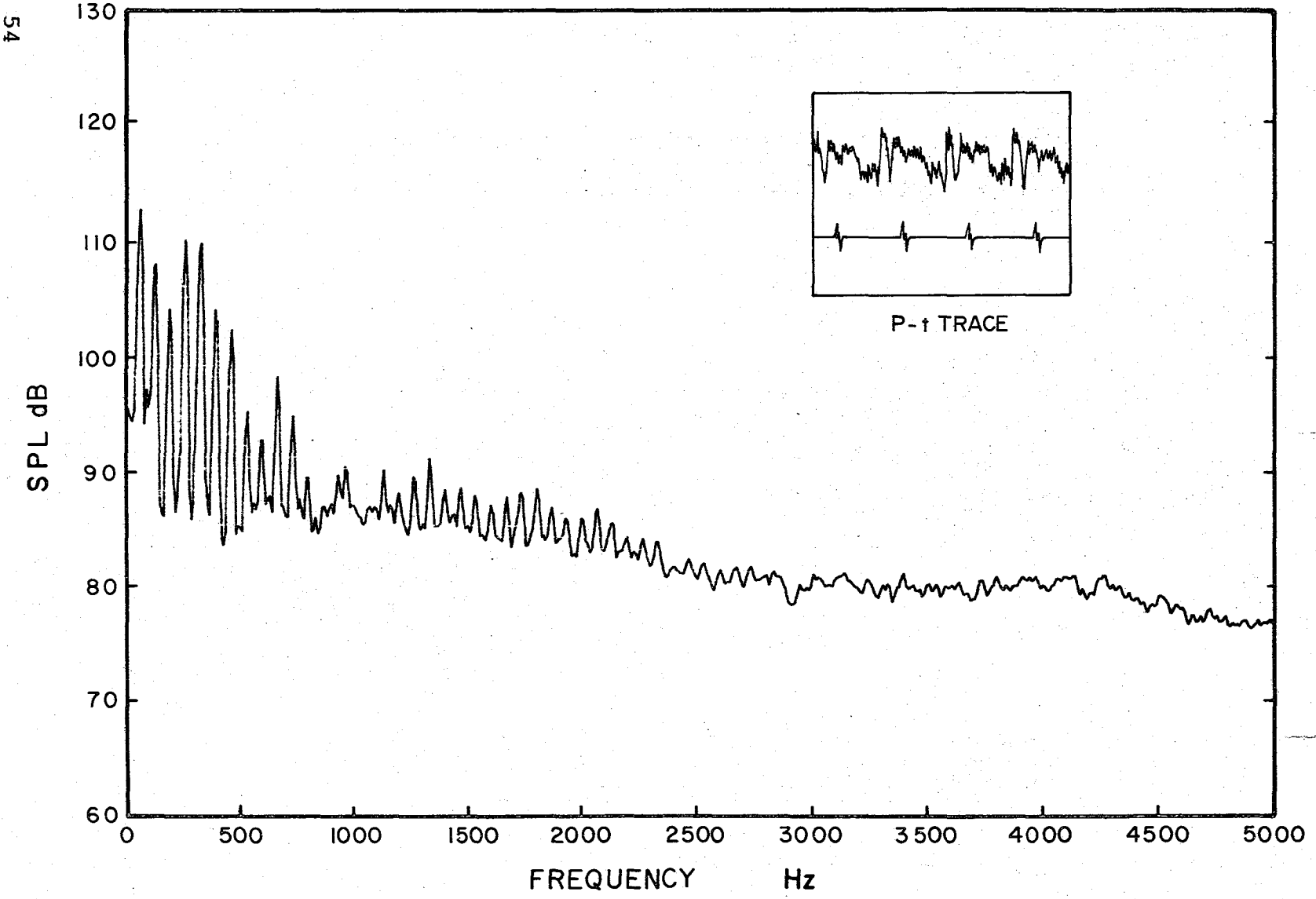


FIGURE 9a. Narrow-Band Spectrum of the Effective Tip Rotor in Descent Flight at Microphone 2 and Advance Ratio 0.14; Descent Rate = 1.22 m/sec.

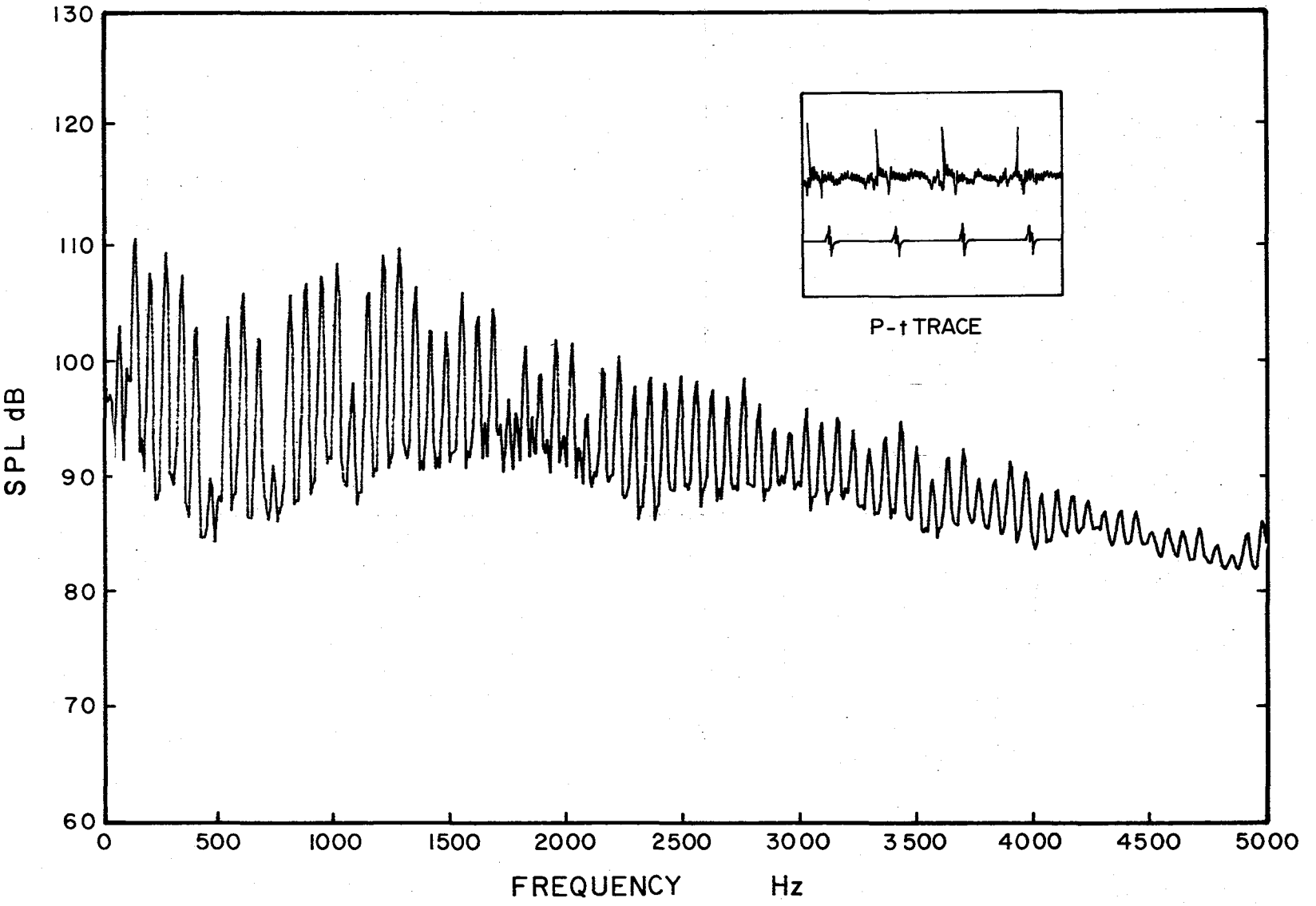


FIGURE 9b. Narrow-Band Spectrum of the Effective Tip Rotor in Descent Flight at Microphone 2 and Advance Ratio 0.14; Descent Rate = 3.66 m/sec.

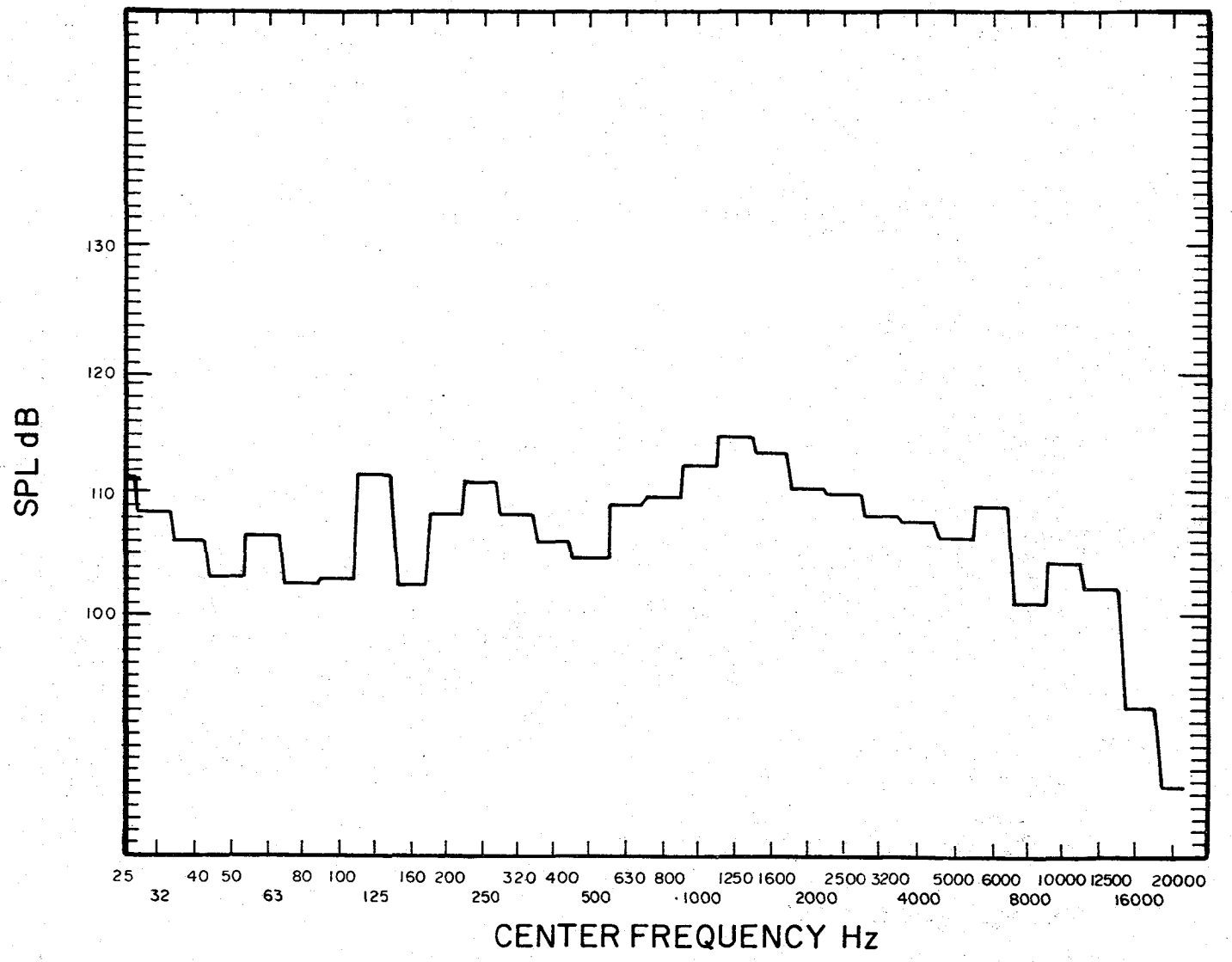


FIGURE 9c. 1/3 Octave Band Spectrum of the Effective Tip Rotor in Descent Flight at Microphone 2 and Advance Ratio 0.14; Descent Rate = 3.66 m/sec.

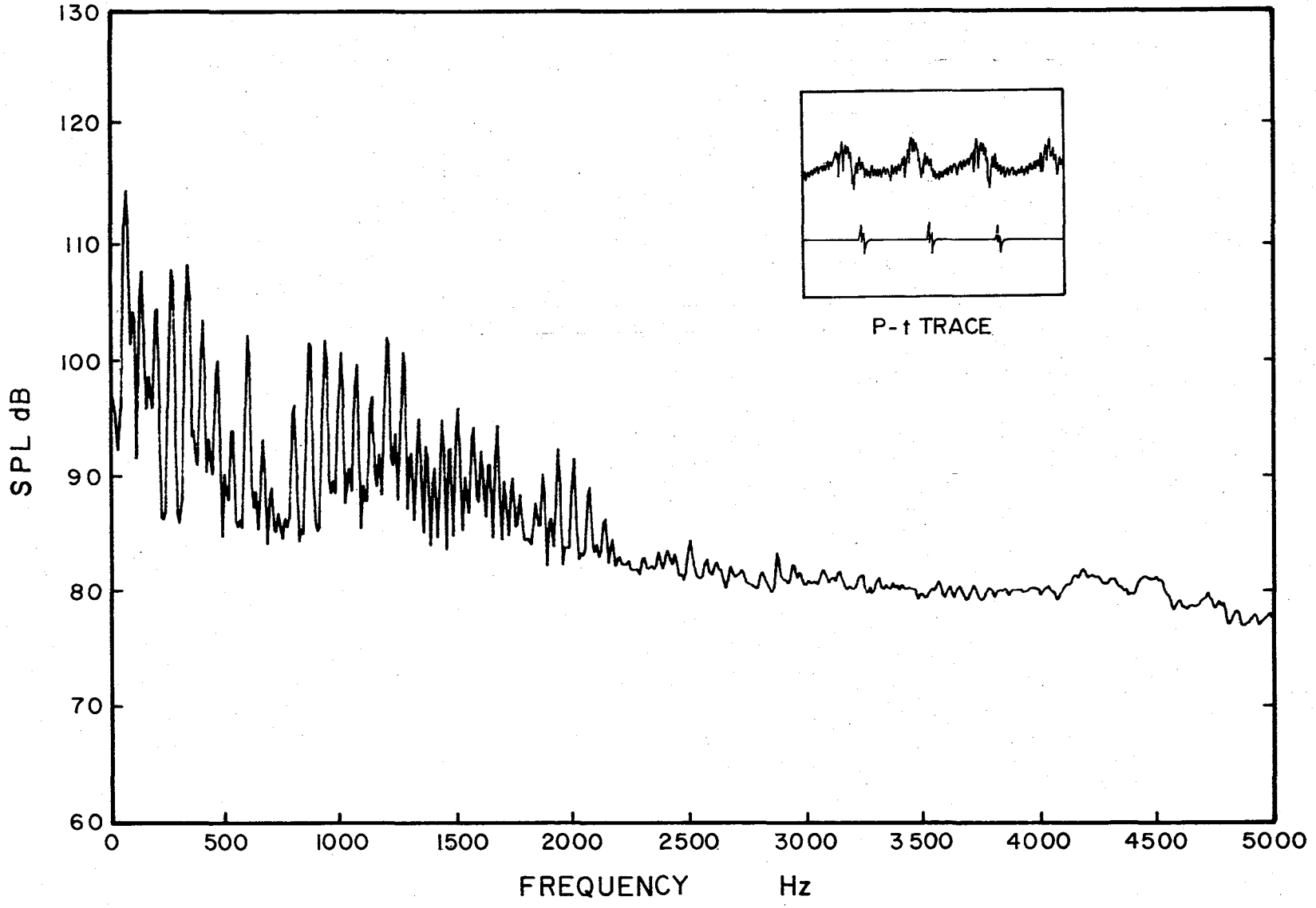


FIGURE 9d. Narrow-Band Spectrum of the Effective Tip Rotor in Descent Flight at Microphone 2 and Advance Ratio 0.14; Descent Rate = 6.71 m/sec.

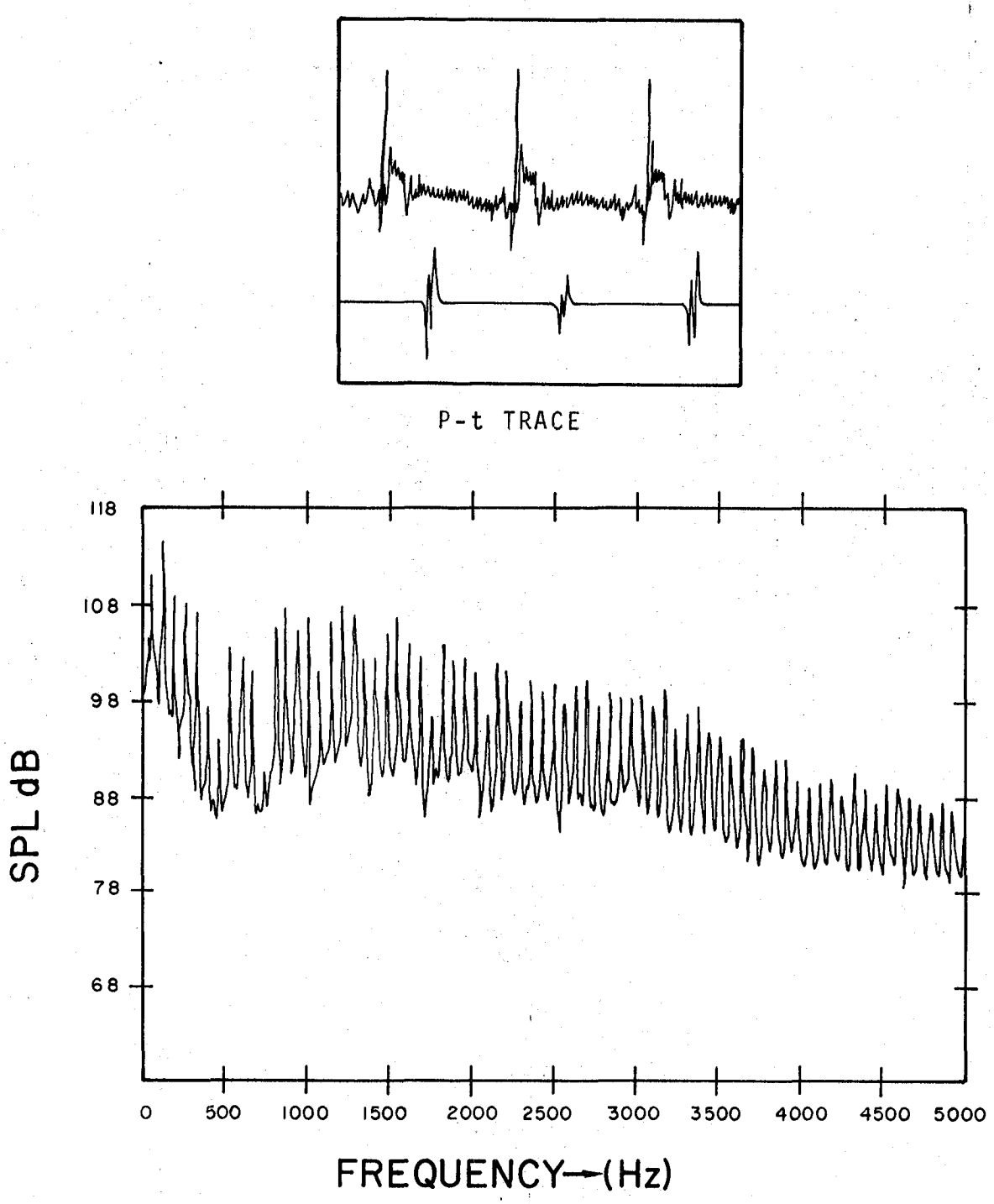


FIGURE 10a. Narrow-Band Spectrum of the TAMI Tip Rotor Without Air Injection in Descent Flight at Microphone 2 and Advance Ratio 0.14; Descent Rate = 3.66 m/sec.

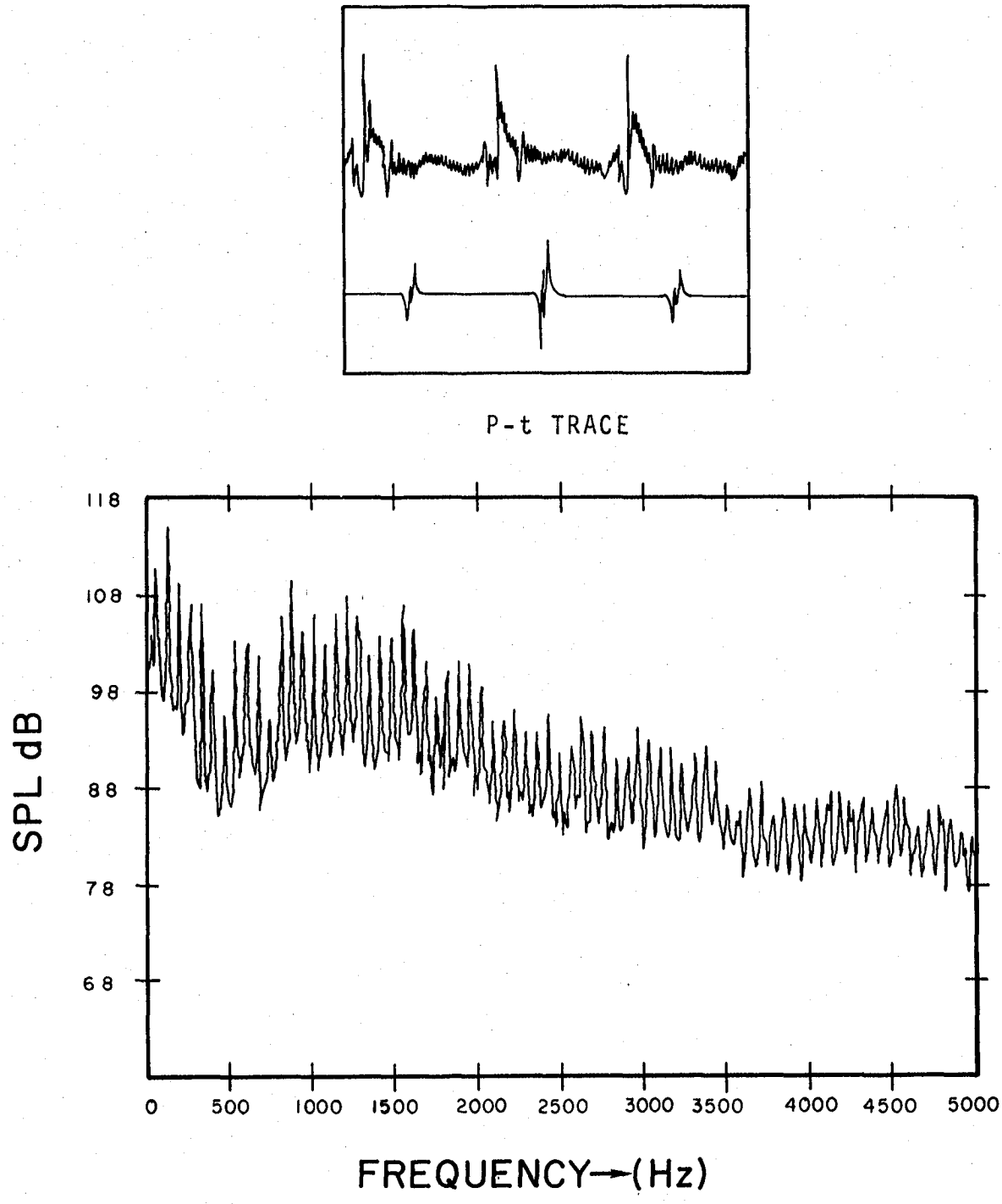


FIGURE 10b. Narrow-Band Spectrum of the TAMI Tip Rotor in Descent Flight (with Air Injected at $6.5 \times 10^5 N/m^2$) at Microphone 2 and Advance Ratio 0.14; Descent Rate = 3.66 m/sec.

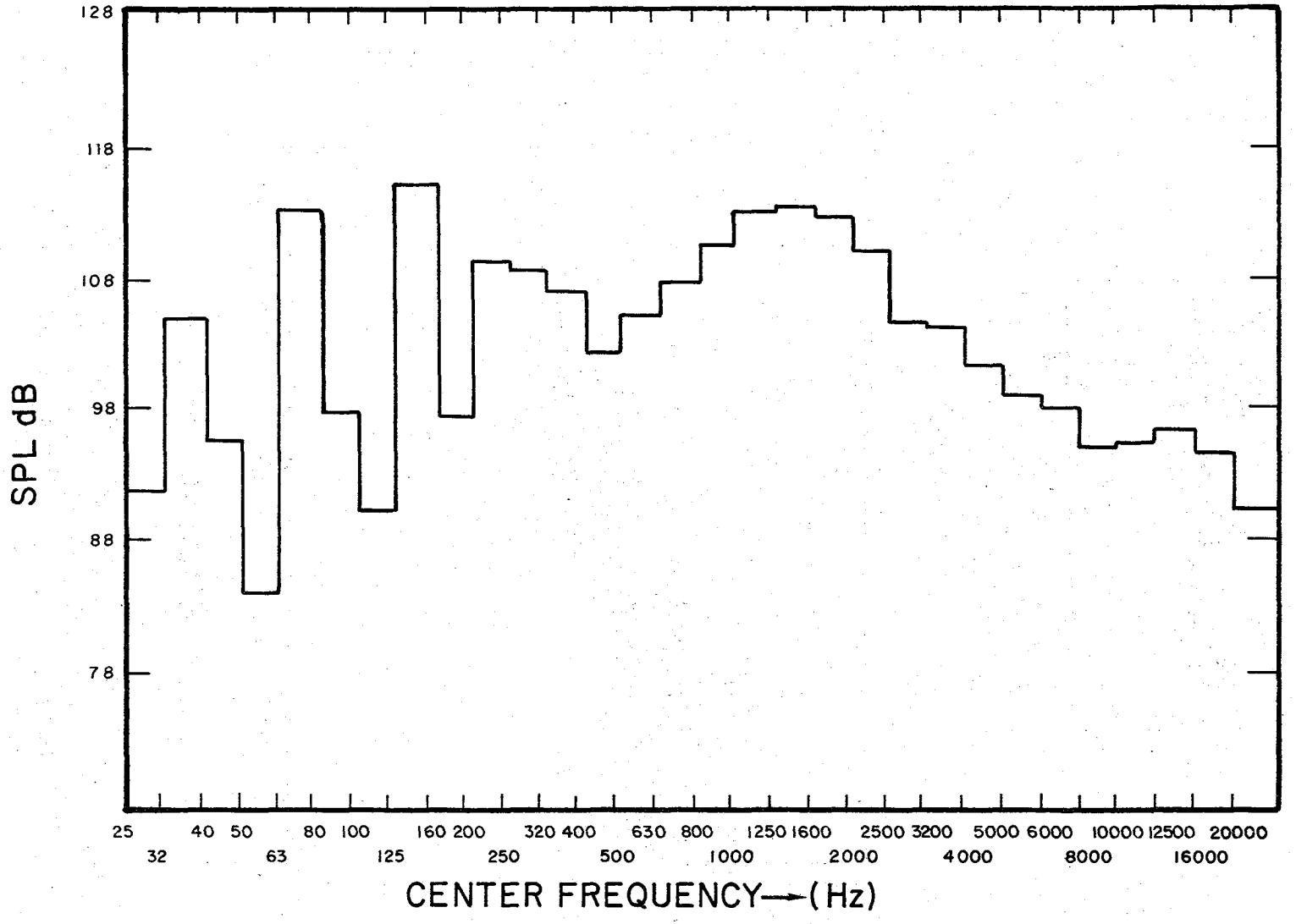


FIGURE 10c. 1/3 Octave Band Spectrum of the TAMI Tip Rotor in Descent Flight (with Air Injected at $6.5 \times 10^5$ N/m$^2$) at Microphone 2 and Advance Ratio 0.14; Descent Rate = 3.66 m/sec.

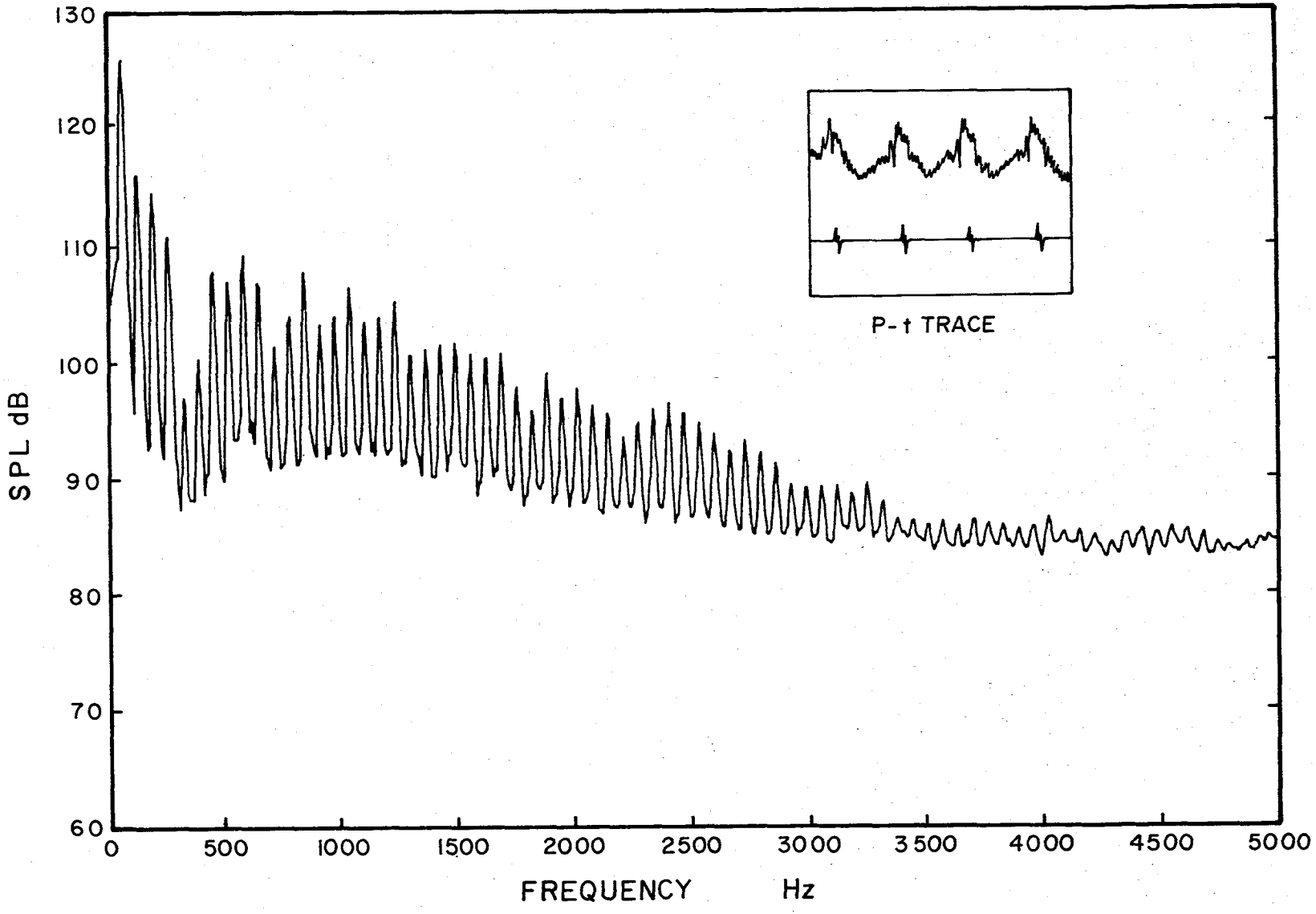


FIGURE 11a. Narrow-Band Spectrum of the Ogee Tip Rotor in Descent Flight at Microphone 3 and Advance Ratio 0.14; Descent Rate = 5.5 m/sec.

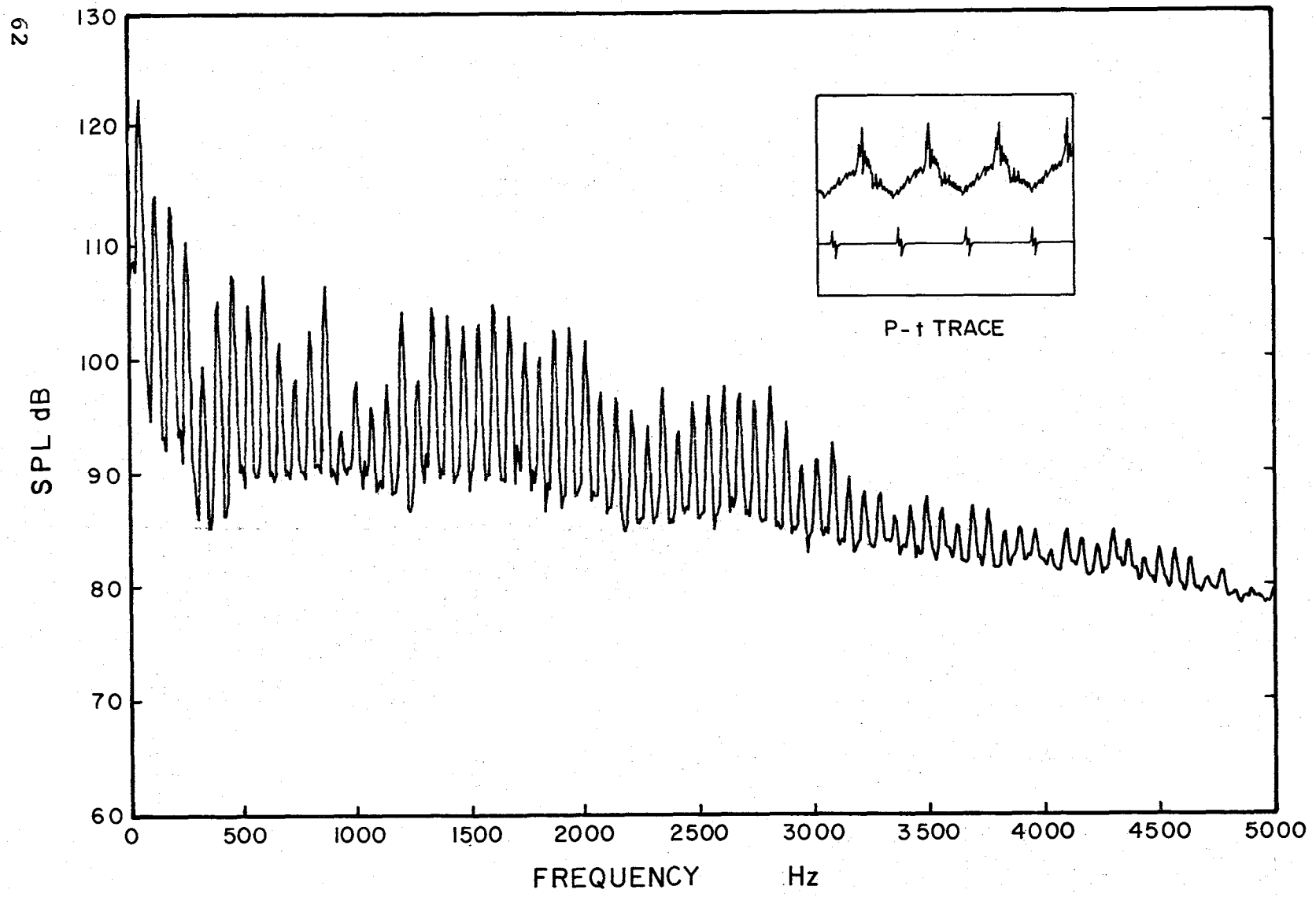


FIGURE 11b. Narrow-Band Spectrum of the Effective Tip Rotor in Descent Flight at Microphone 3 and Advance Ratio 0.14; Descent Rate = 4.27 m/sec.

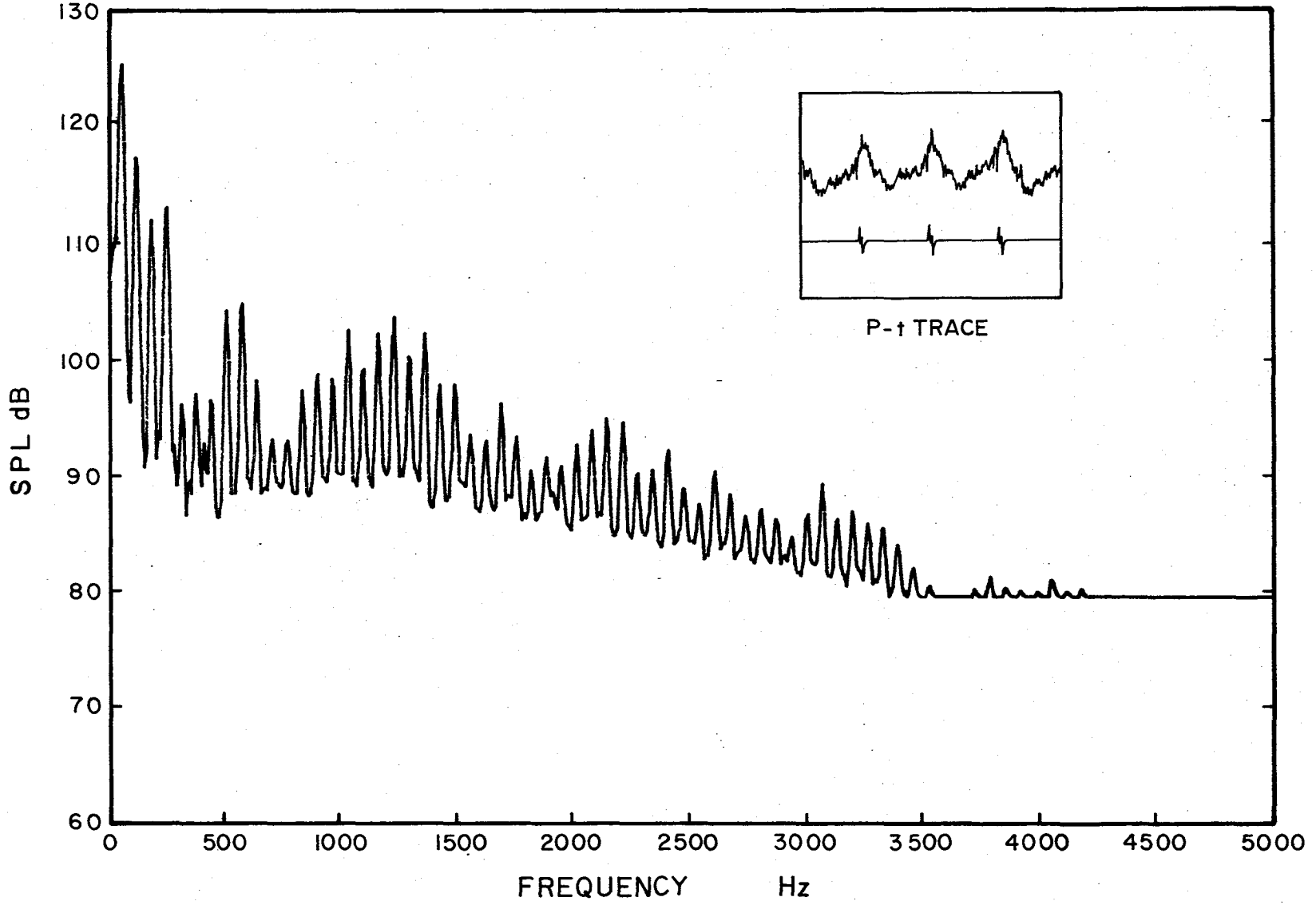


FIGURE 11c. Narrow-Band Spectrum of the Full Rectangular Tip Rotor in Descent Flight at Microphone 3 and Advance Ratio 0.14; Descent Rate = 5.5 m/sec.

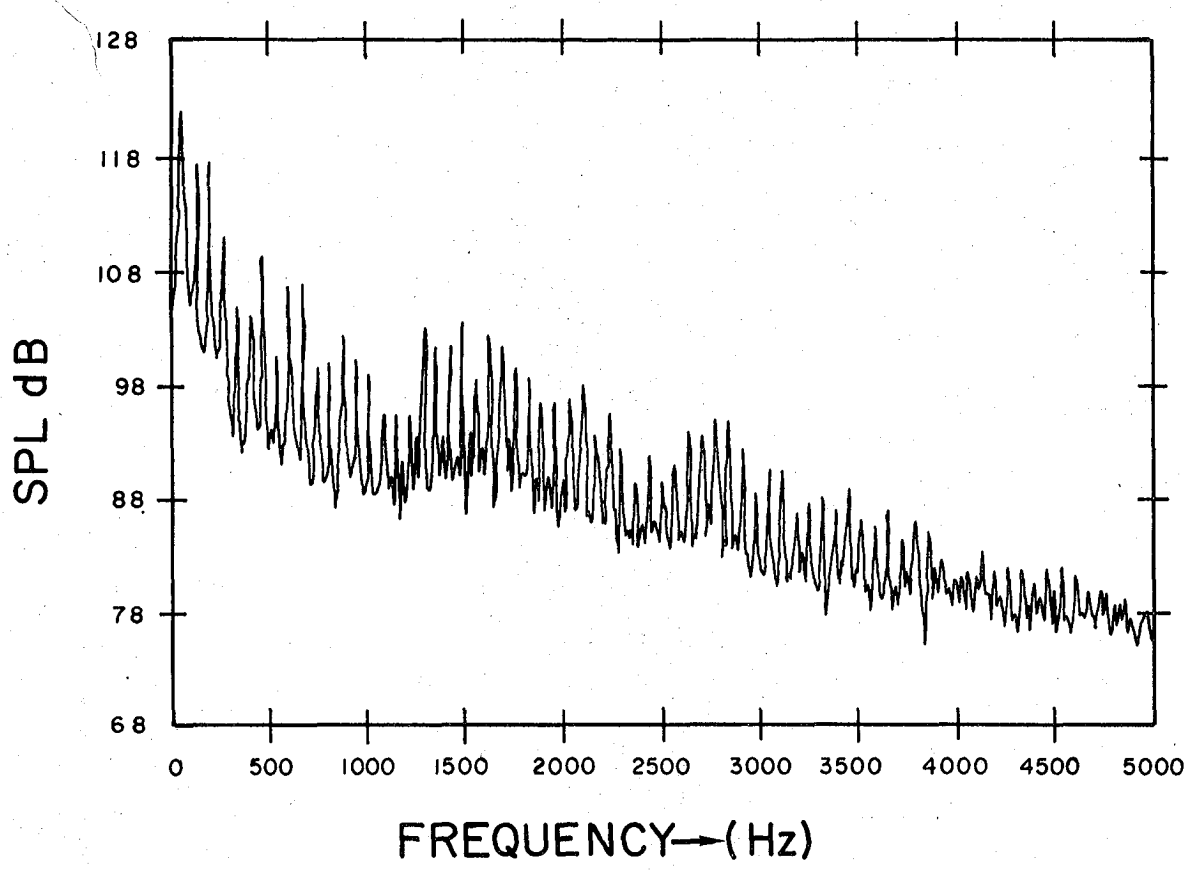


FIGURE 11d. Narrow-Band Spectrum of TAMI Tip Rotor (with Air Injected at $6.5 \times 10^5$ N/m$^2$) at Microphone 3 and Advance Ratio of 0.14; Descent Rate = 4.27 m/sec

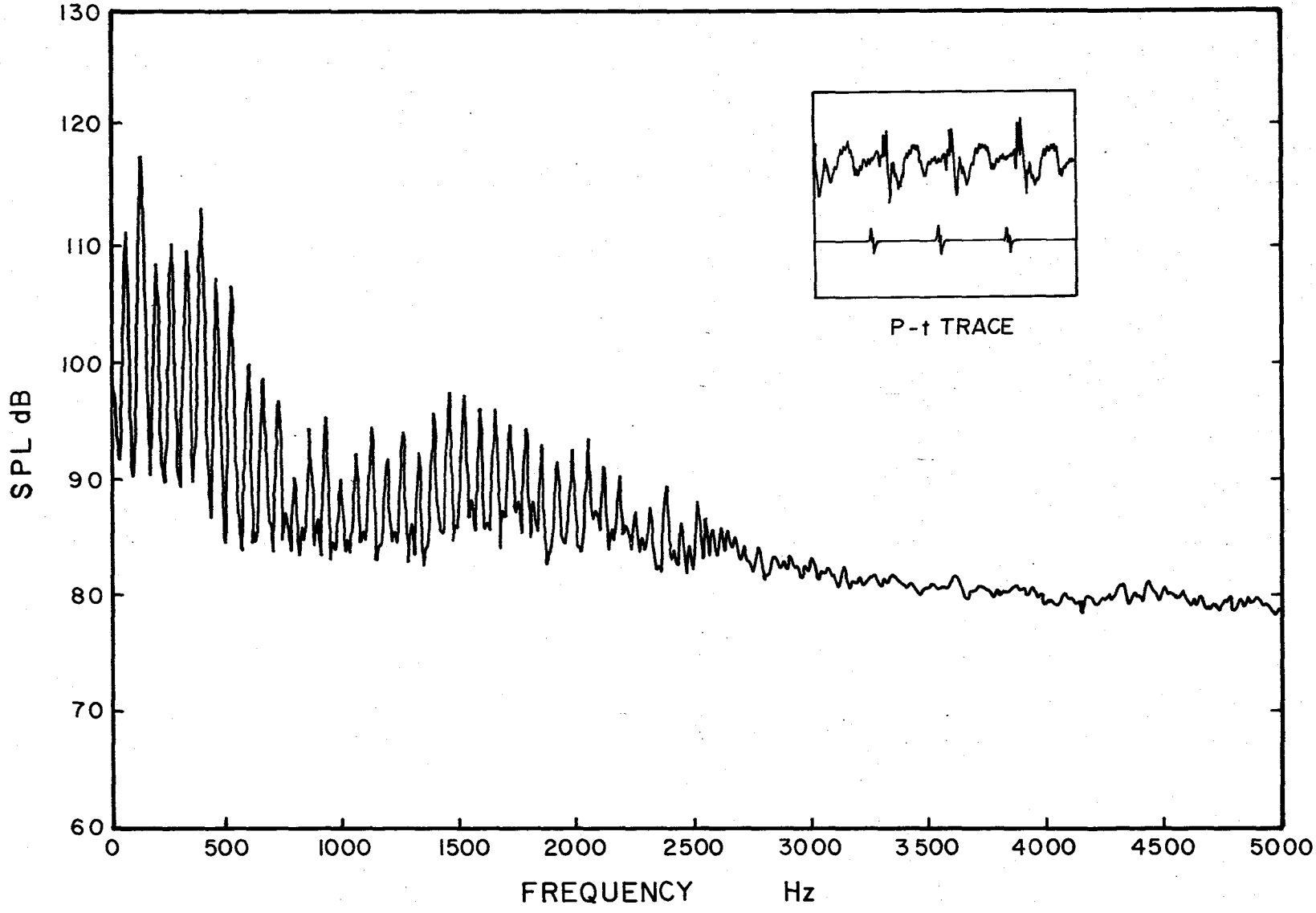


FIGURE 12a. Narrow-Band Spectrum of the Ogee Tip Rotor in Descent Flight at Microphone 1 and Advance Ratio 0.14; Descent Rate = 4.27 m/sec.

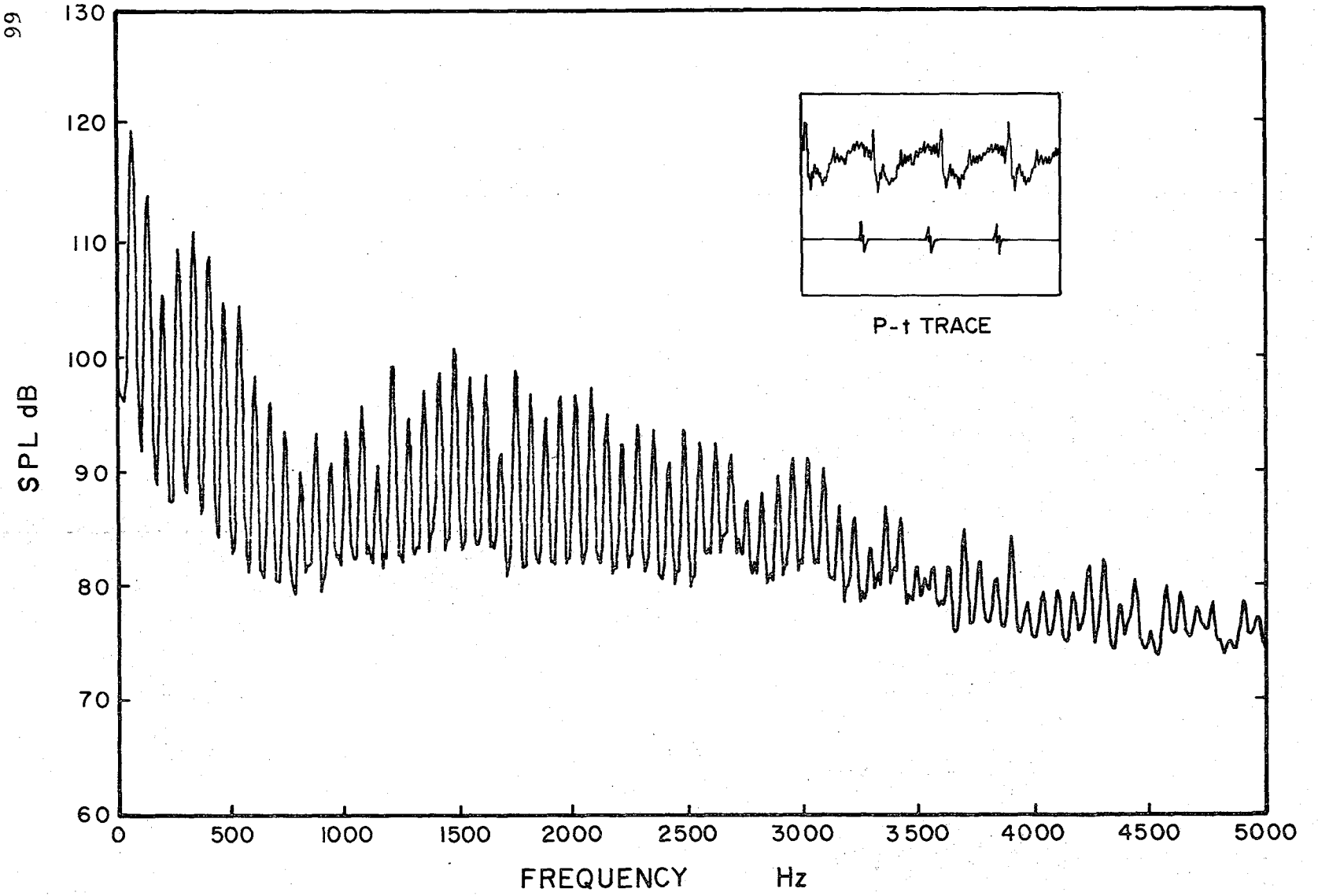


FIGURE 12b. Narrow-Band Spectrum of the Effective Tip Rotor in Descent Flight at Microphone 1 and Advance Ratio of 0.14; Descent Rate = 3.66 m/sec.

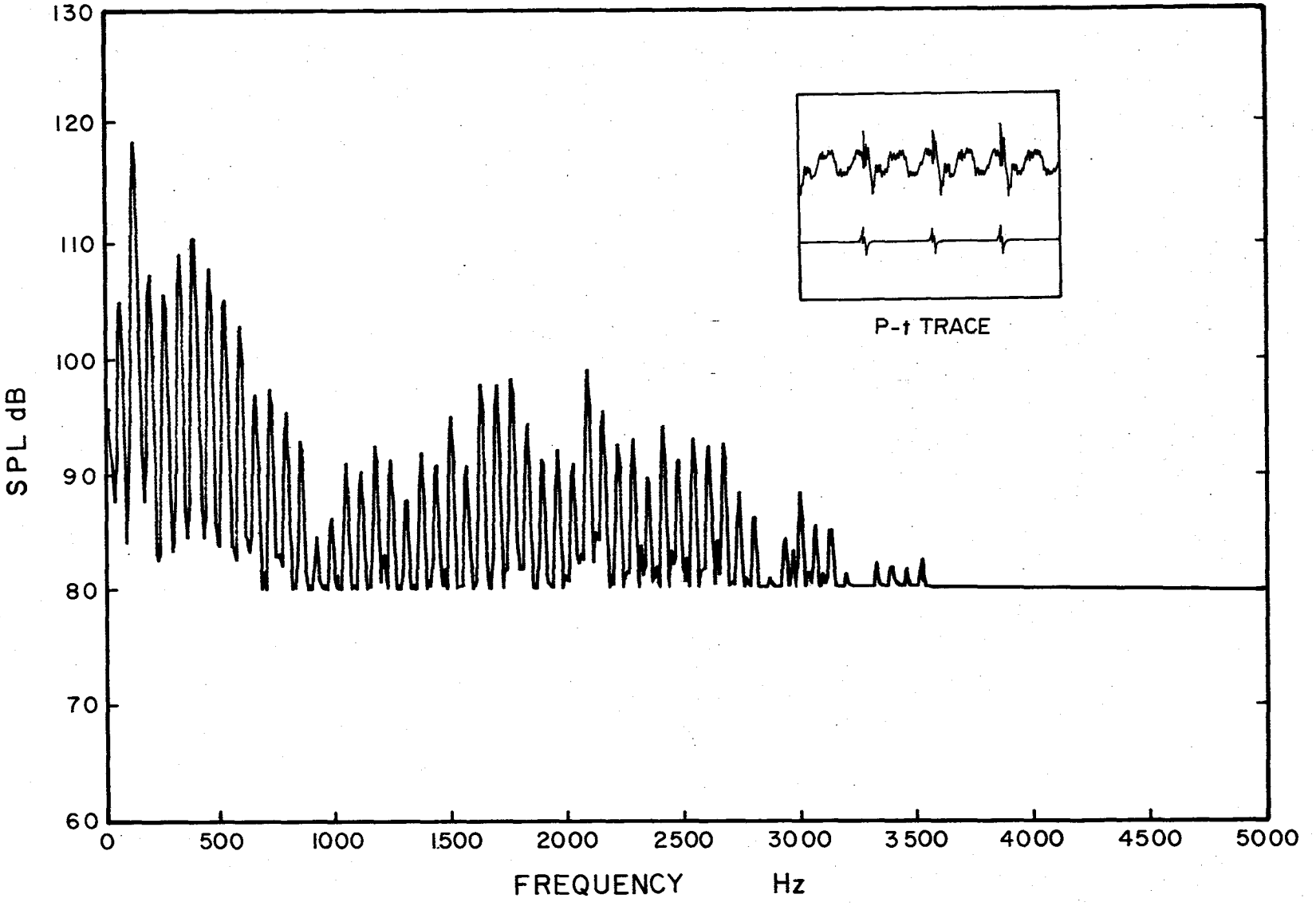


FIGURE 12c. Narrow-Band Spectrum of the Full Rectangular Tip Rotor in Descent Flight at Microphone 1 and Advance Ratio 0.14; Descent Rate = 4.27 m/sec.

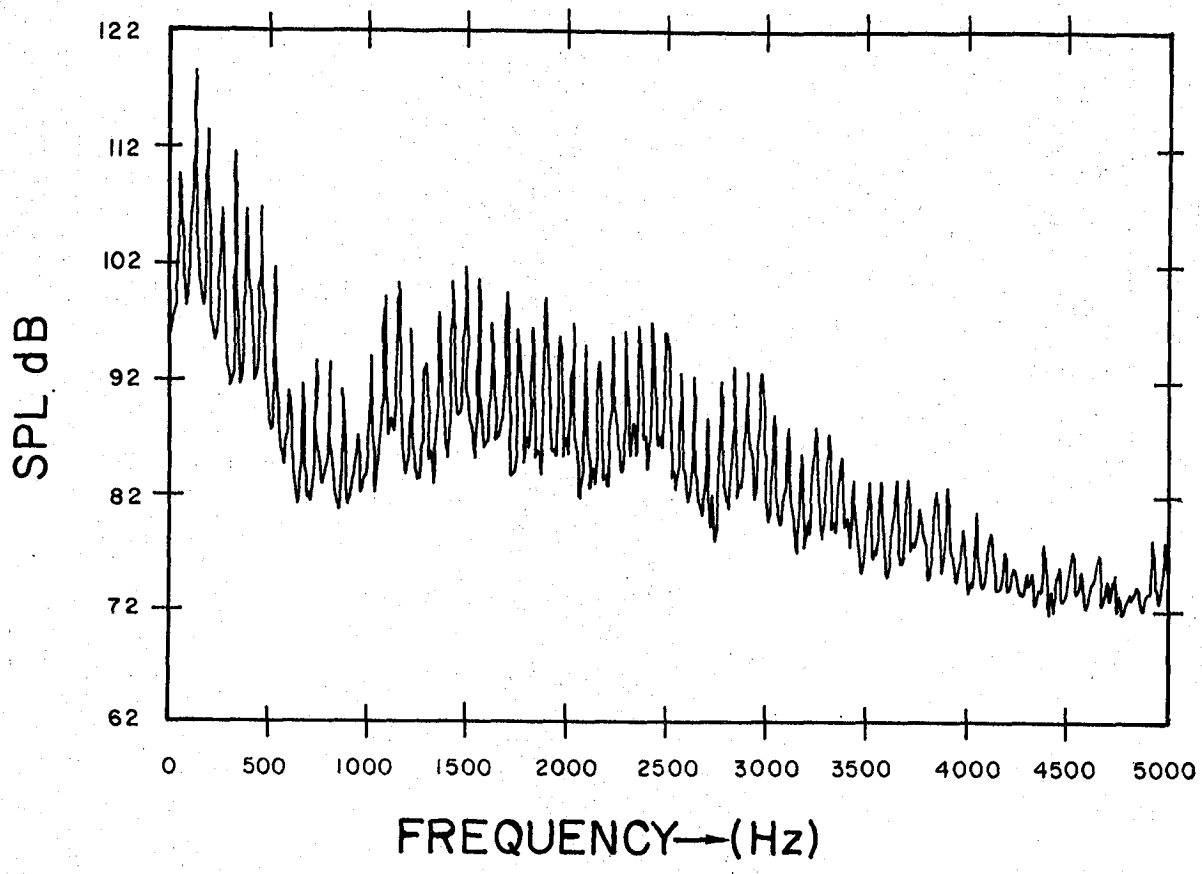


FIGURE 12d. Narrow-Band Spectrum of TAMI Tip Rotor in Descent Flight (with Air Injected at $6.5 \times 10^5$ N/m$^2$) at Microphone 1 and Advance Ratio 0.14; Descent Rate = 3.66 m/sec.

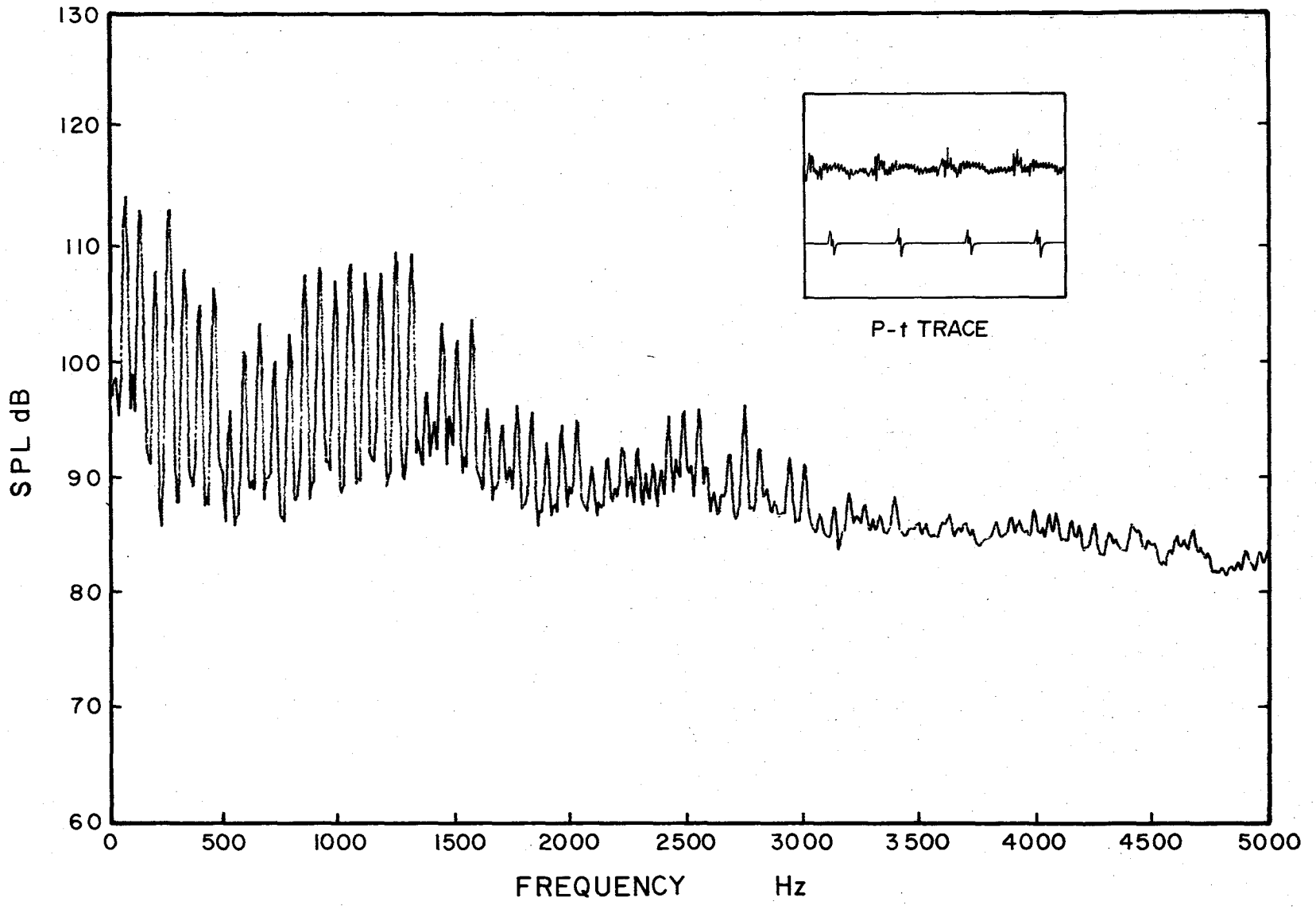


FIGURE 13a. Narrow-Band Spectrum of the Full Rectangular Tip Rotor in Descent Flight at Microphone 1 and Advance Ratio 0.125; Descent Rate = 3.66 m/sec.

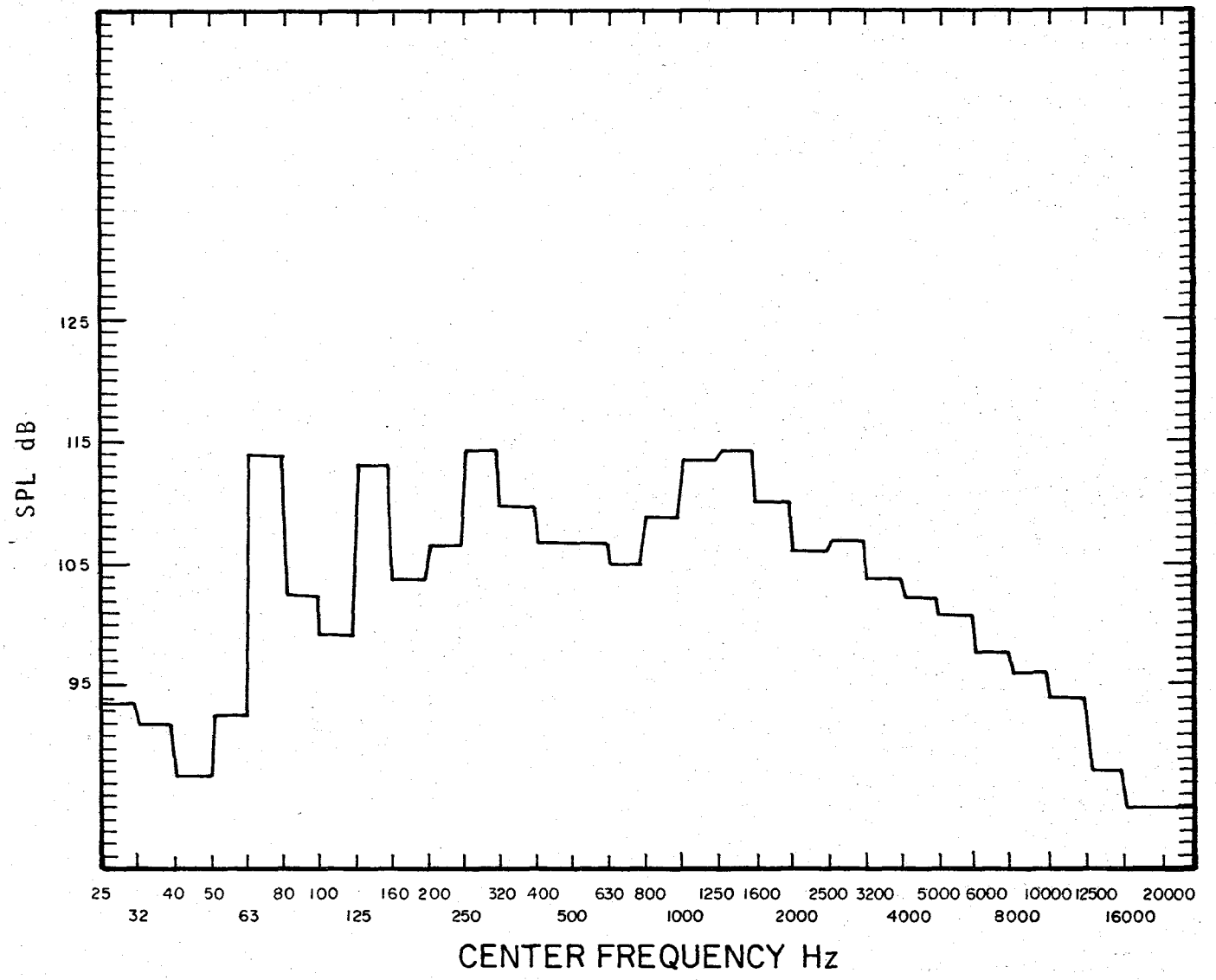


FIGURE 13b. 1/3 Octave-Band Spectrum of the Full Rectangular Tip Rotor in Descent Flight at Microphone 2 and Advance Ratio 0.125; Descent Rate = 3.66 m/sec.

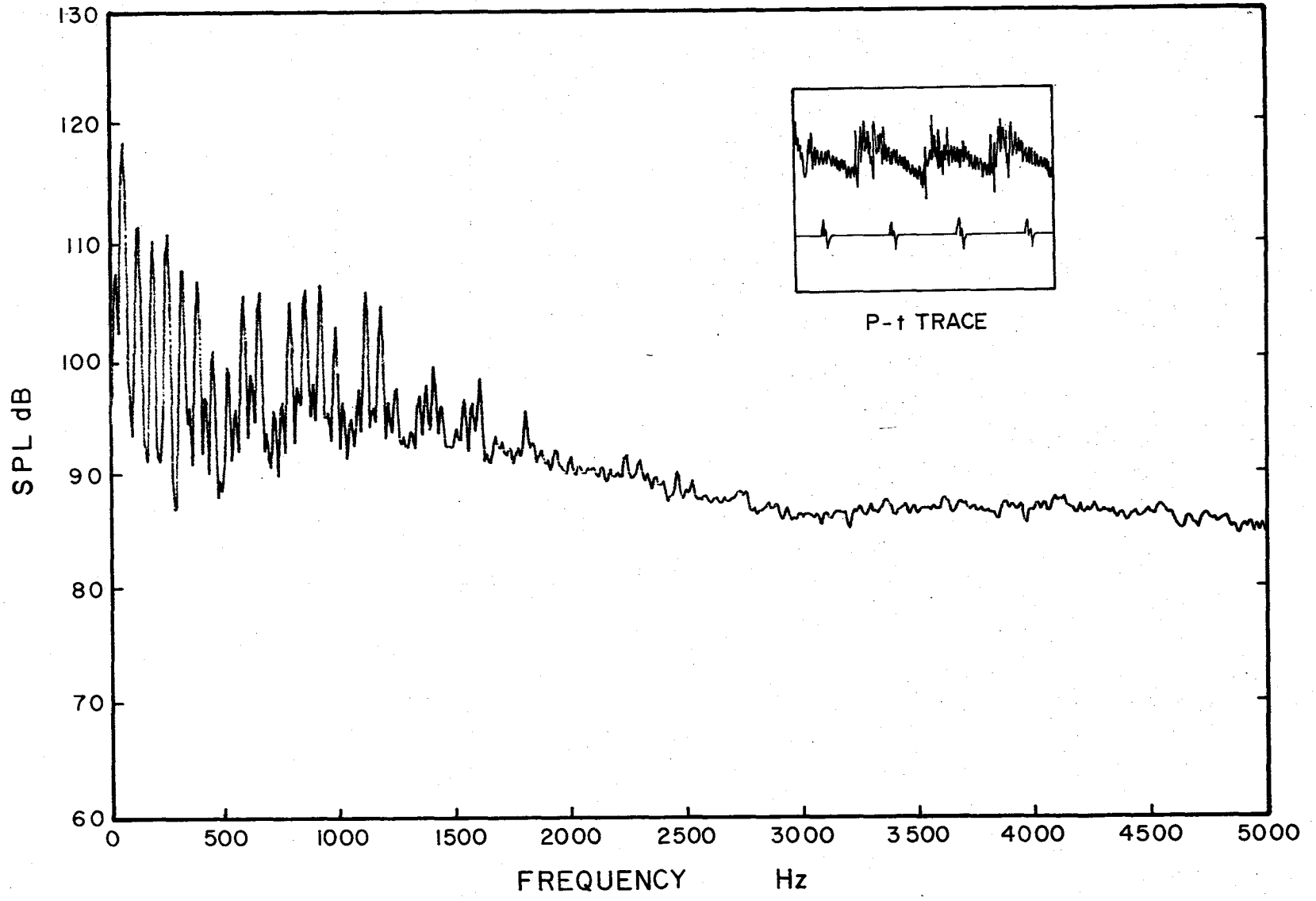


FIGURE 13c. Narrow-Band Spectrum of the Ogee Tip Rotor in Descent Flight at Microphone 2 and Advance Ratio 0.125; Descent Rate = 3.66 m/sec.

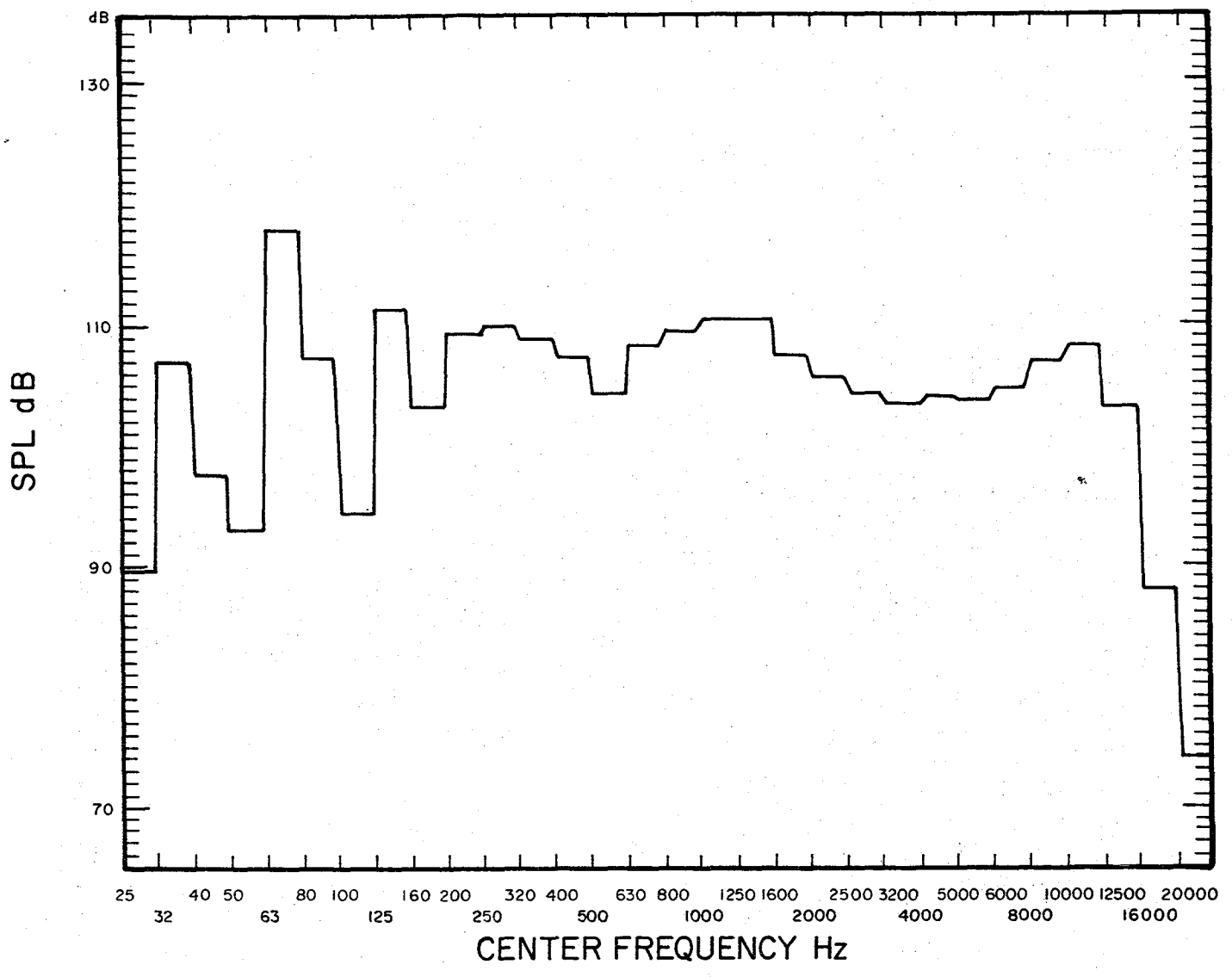


FIGURE 13d. 1/3 Octave-Band Spectrum of the Ogee Tip Rotor in Descent Flight at Microphone 2 and Advance Ratio 0.125; Descent Rate = 3.66 m/sec.

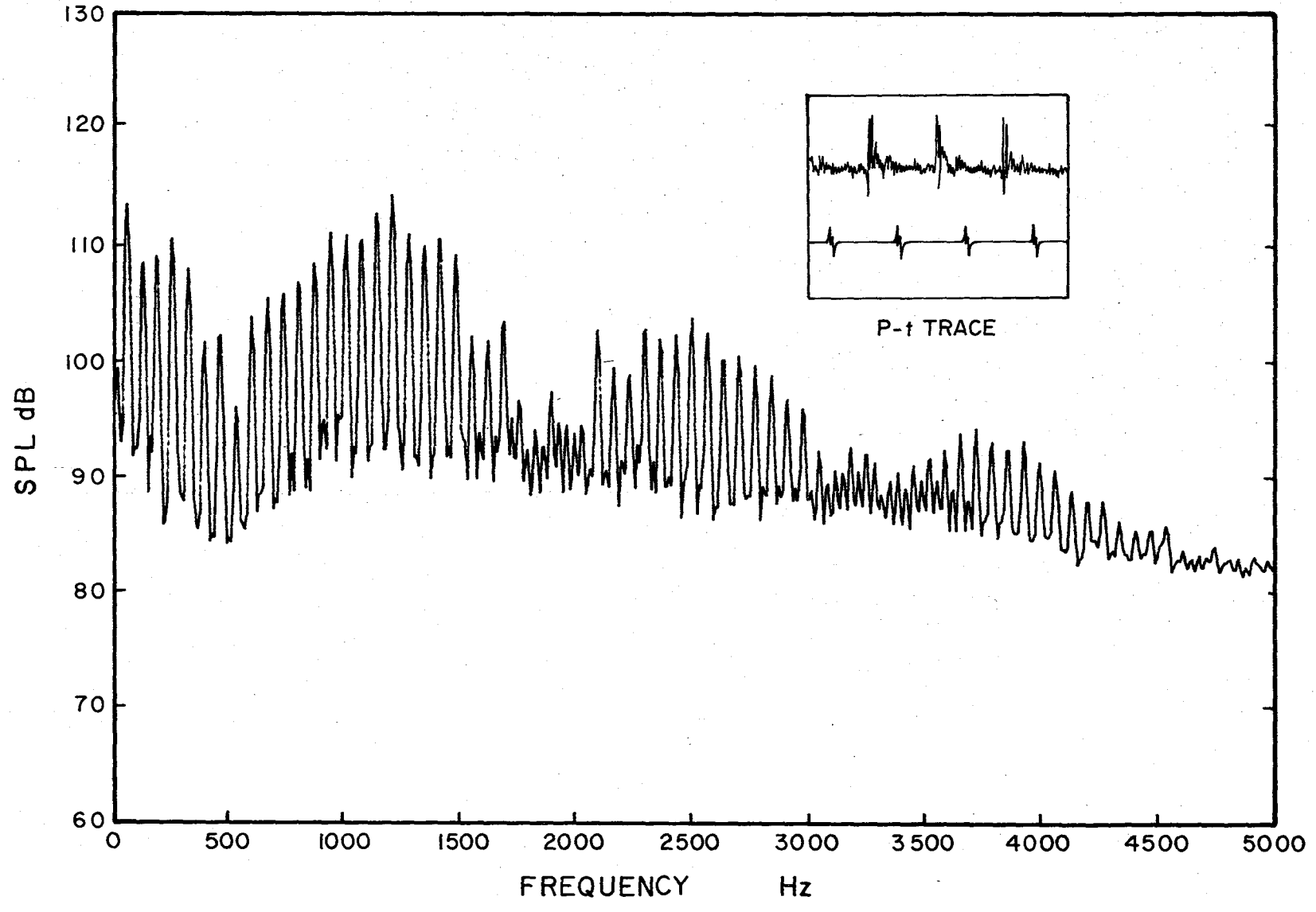


FIGURE 13e. Narrow-Band Spectrum of the Effective Tip Rotor in Descent Flight at Microphone 2 and Advance Ratio 0.125; Descent Rate = 3.05 m/sec.

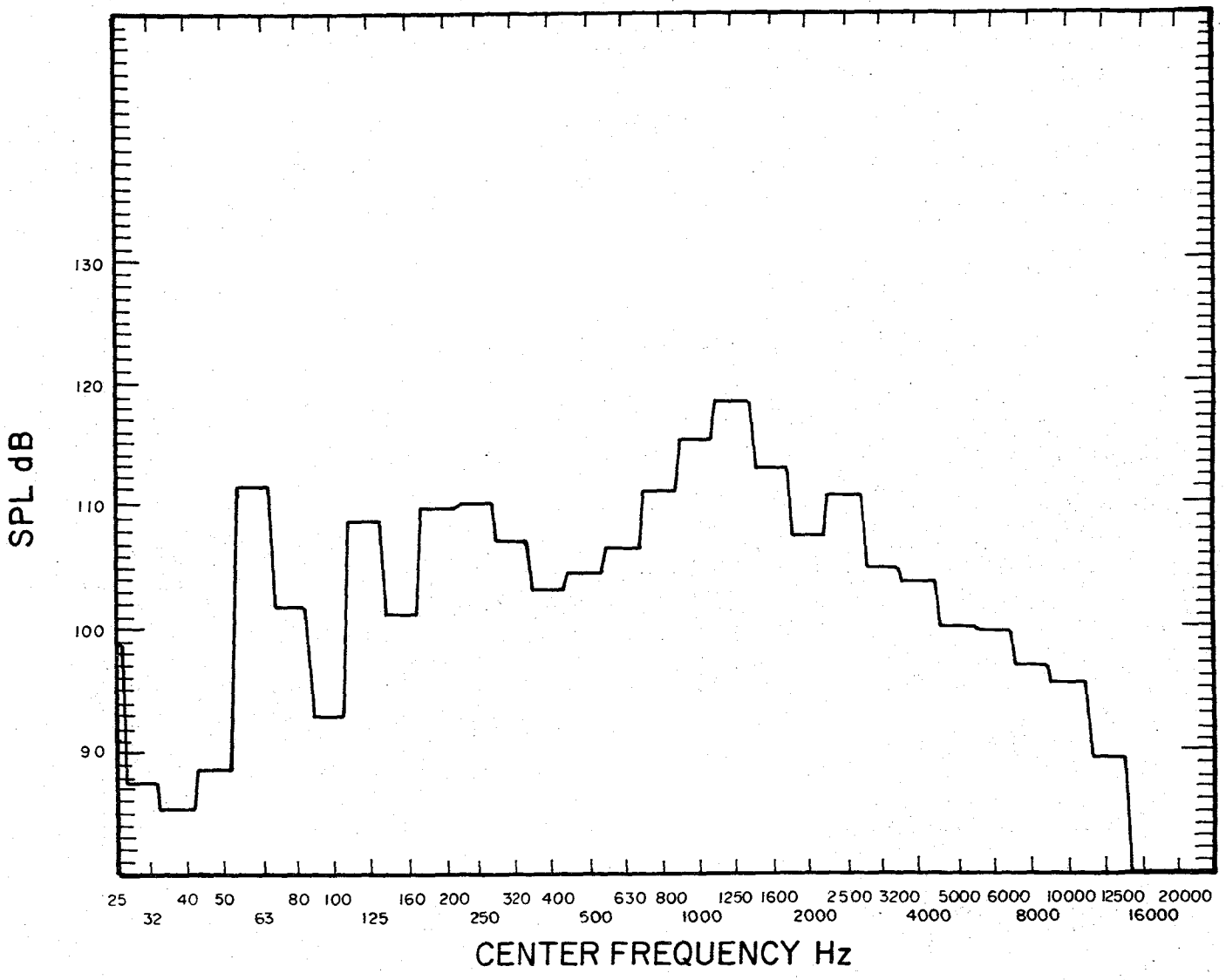


FIGURE 13f. 1/3 Octave-Band Spectrum of the Effective Tip Rotor in Descent Flight at Microphone 2 and Advance Ratio 0.125; Descent Rate = 3.05 m/sec.

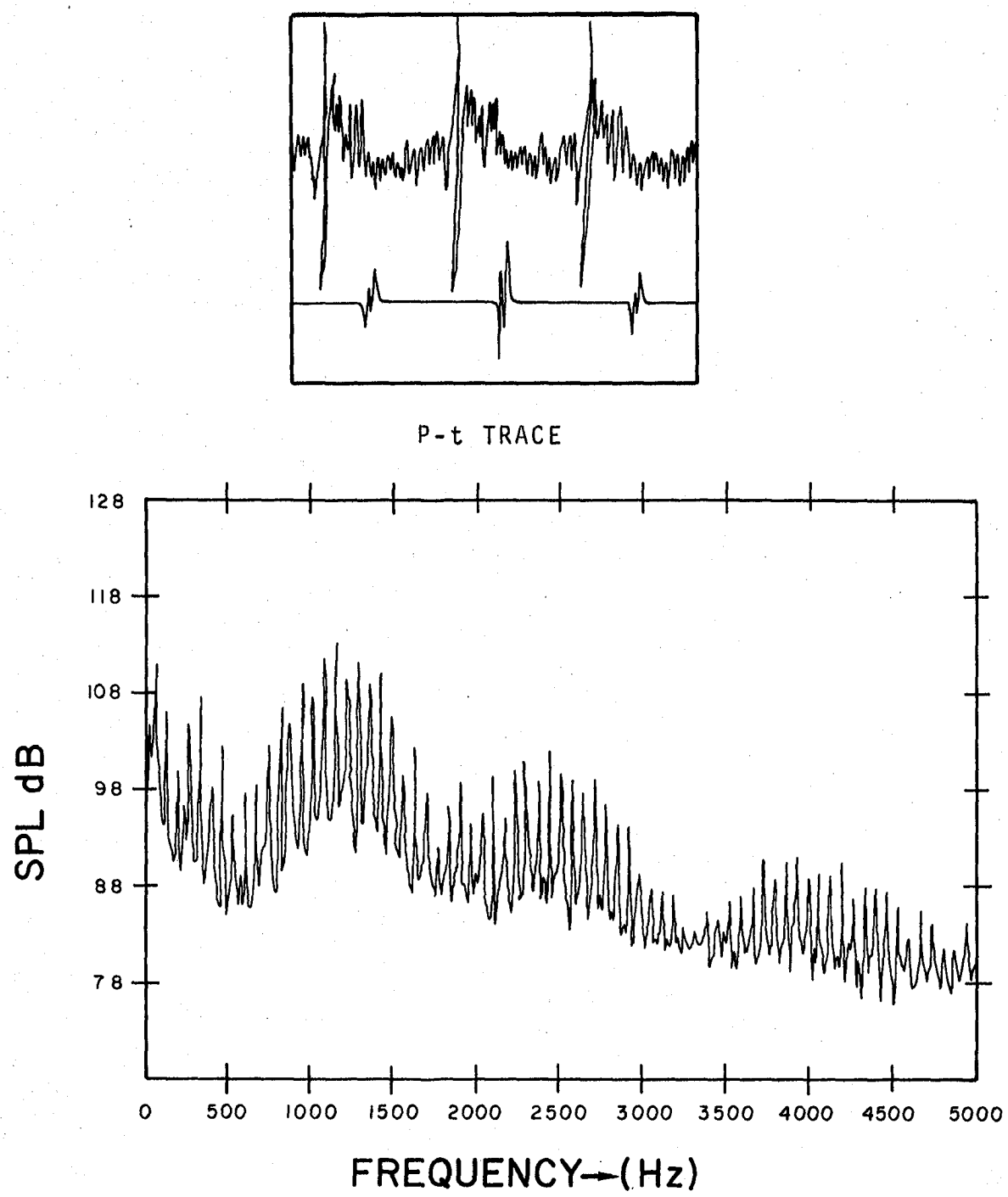


FIGURE 13g. Narrow-Band Spectrum of the TAMI Tip Rotor in Descent Flight (with Air Injected at $6.5 \times 10^5$ N/m$^2$) at Microphone 2 and Advance Ratio 0.125; Descent Rate = 3.05 m/sec.

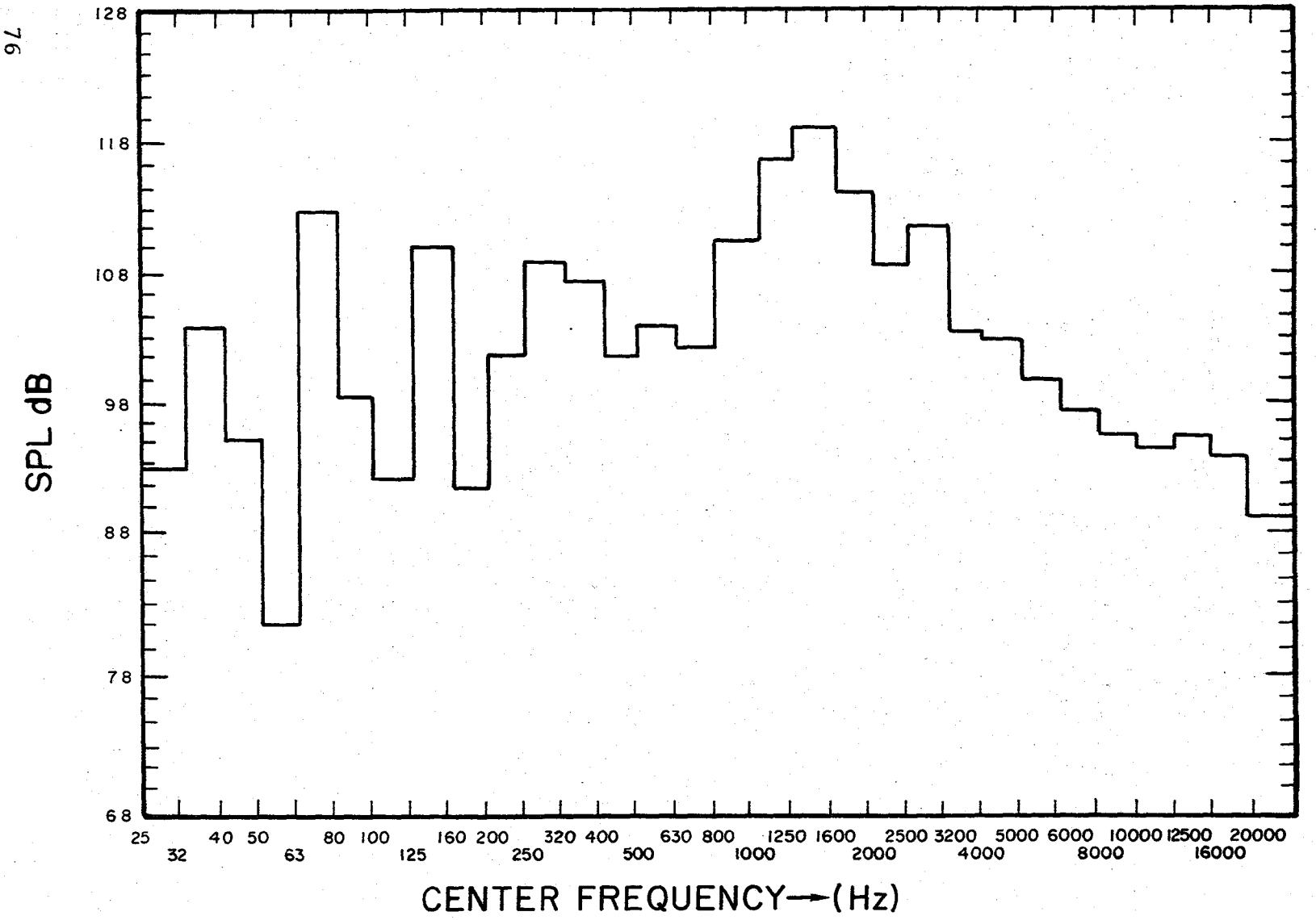


FIGURE 13h. 1/3 Octave-Band Spectrum of the TAMI Tip Rotor in Descent Flight (with Air Injected at $6.5 \times 10^5$ N/m$^2$) at Microphone 2 and Advance Ratio 0.125; Descent Rate = 3.05 m/sec.

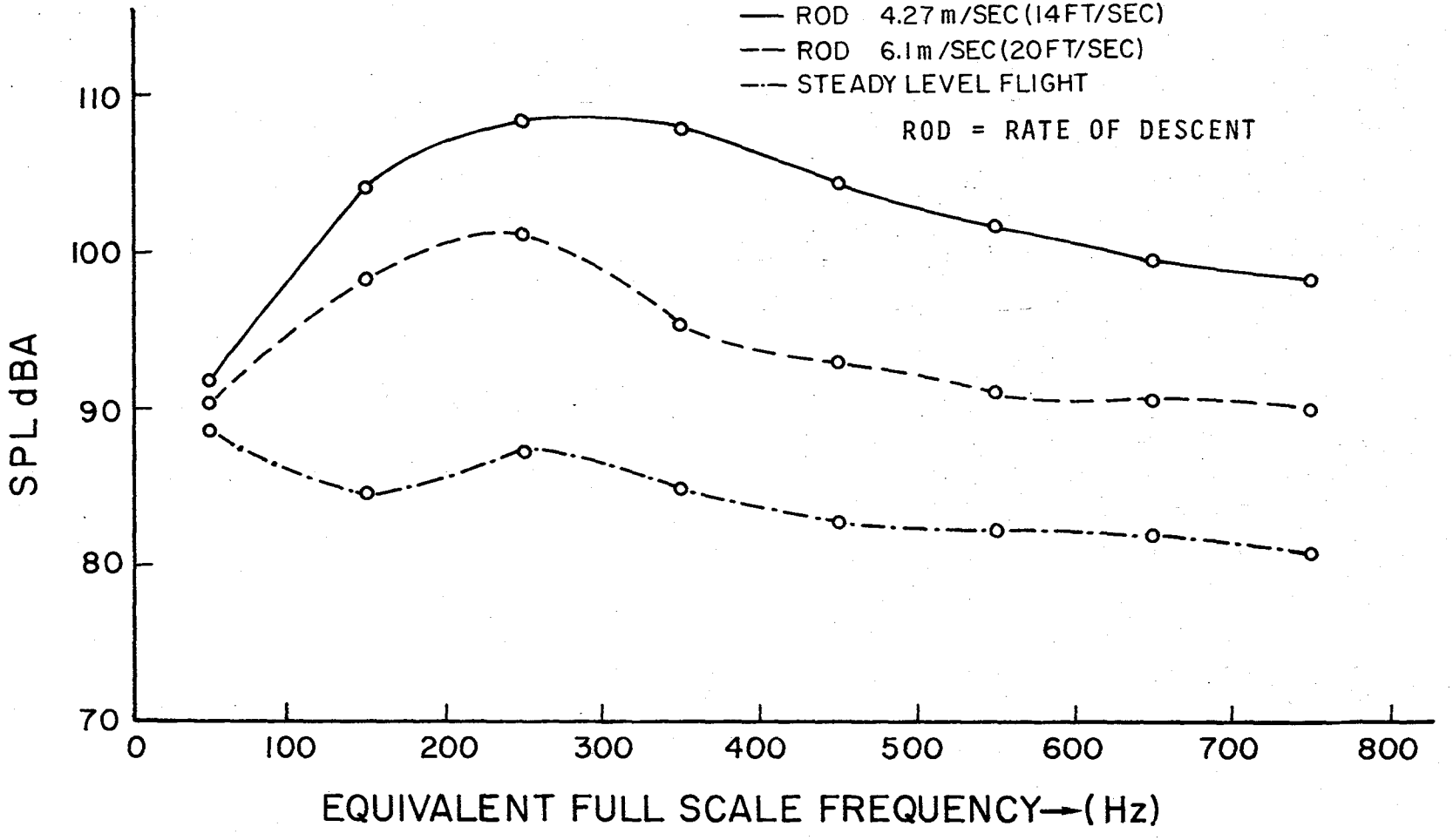


FIGURE 14. dBA vs. Frequency of a Full Rectangular Tip Rotor at Microphone 2 and at Advance Ratio of 0.14.

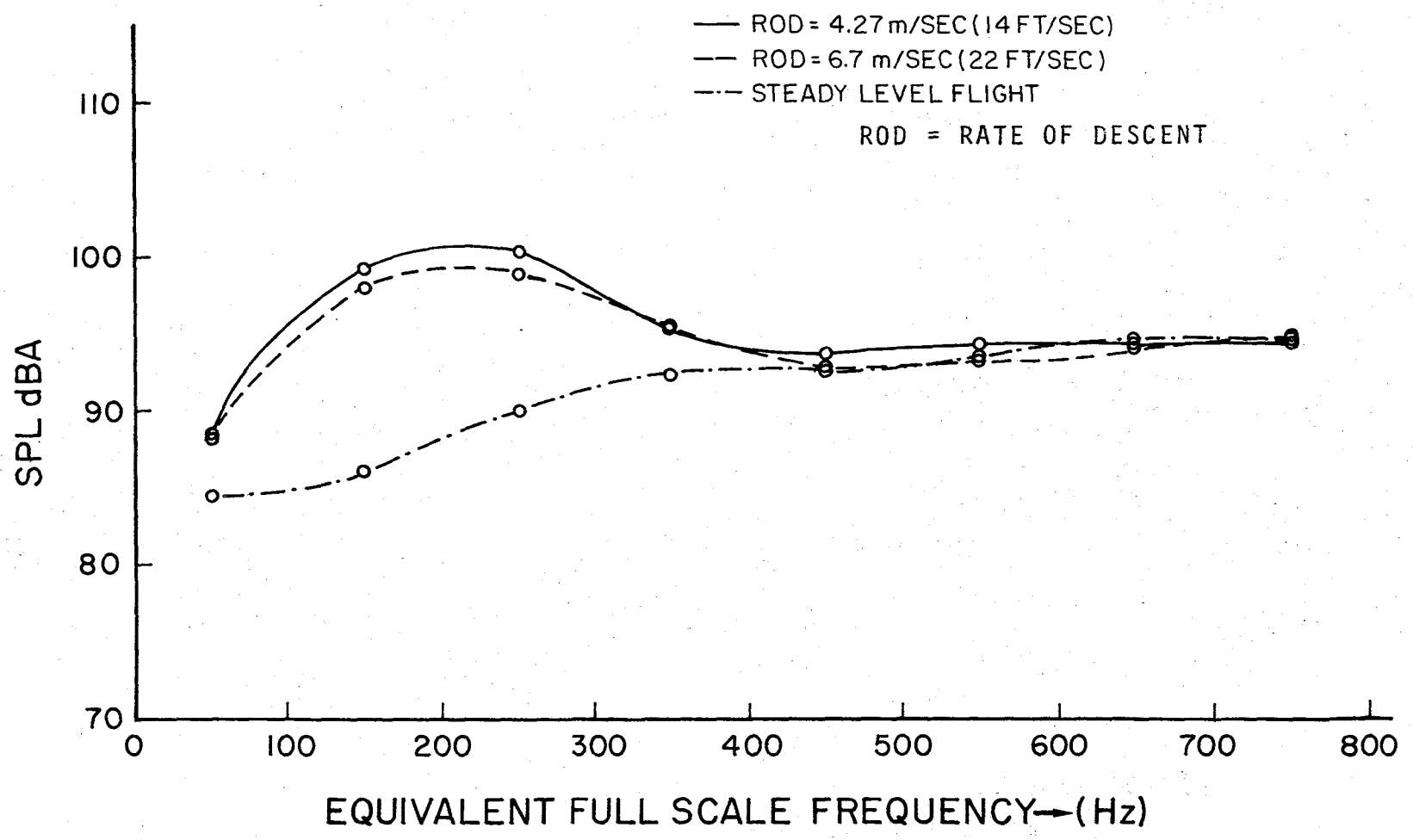


FIGURE 15. dBA vs. Frequency of an Ogee Tip Rotor at Microphone 2 and at Advance Ratio of 0.14.

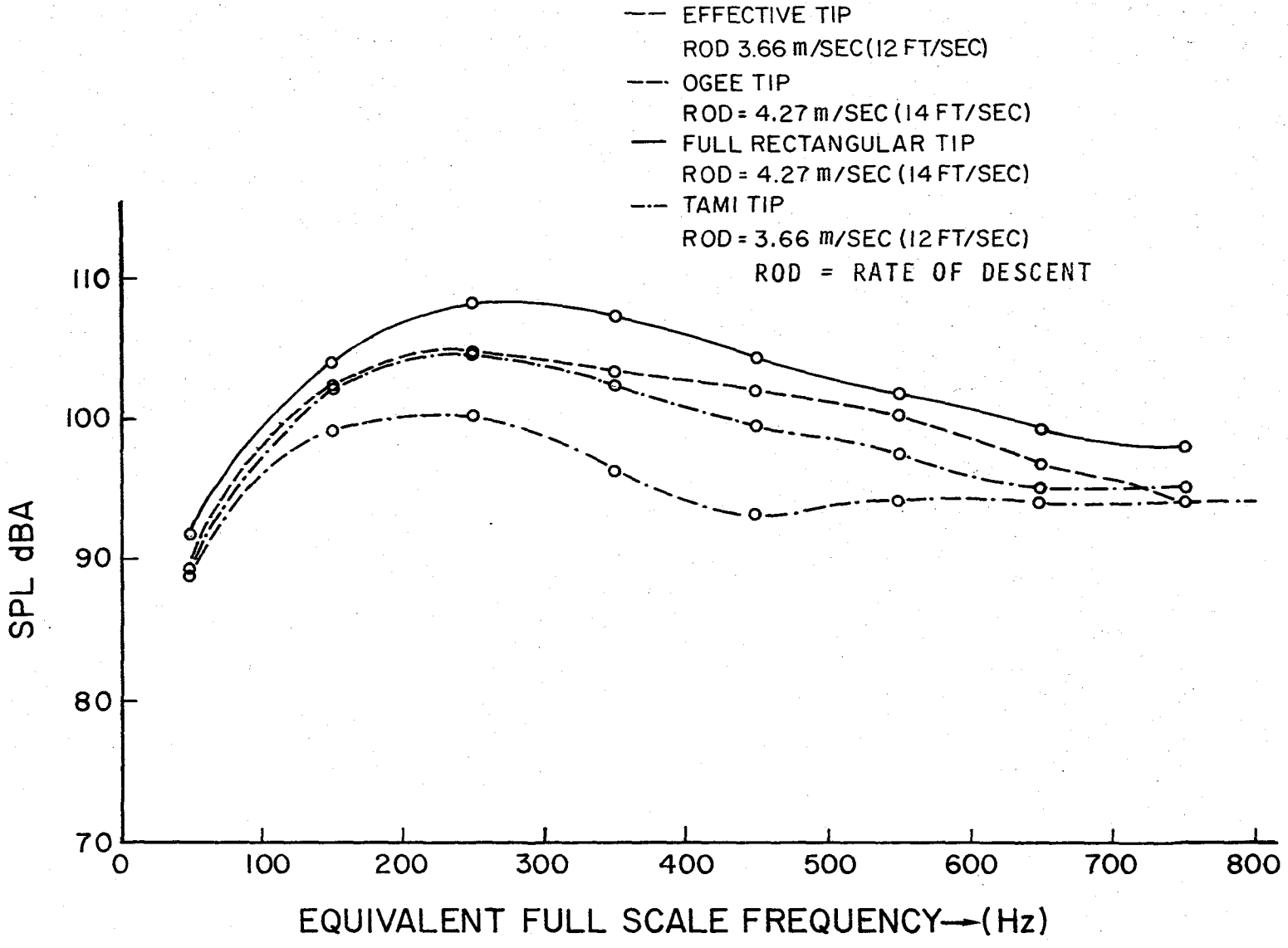


FIGURE 16. dBA vs. Frequency for Maximum Slap Conditions at Microphone 2 and at Advance Ratio of 0.14.

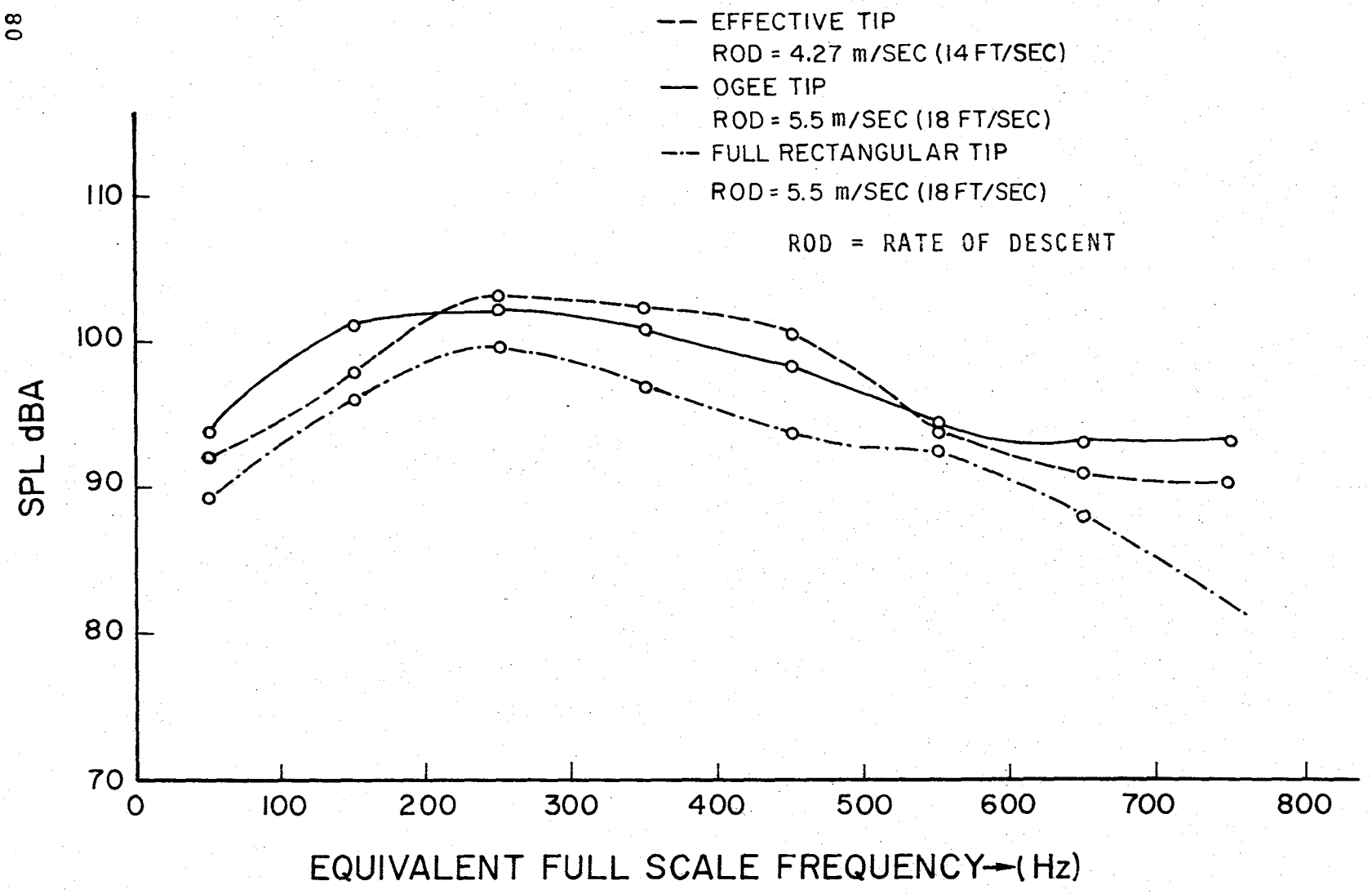


FIGURE 17. dBA vs. Frequency for Maximum Slap Conditions at Microphone 3 and at Advance Ratio of 0.14.

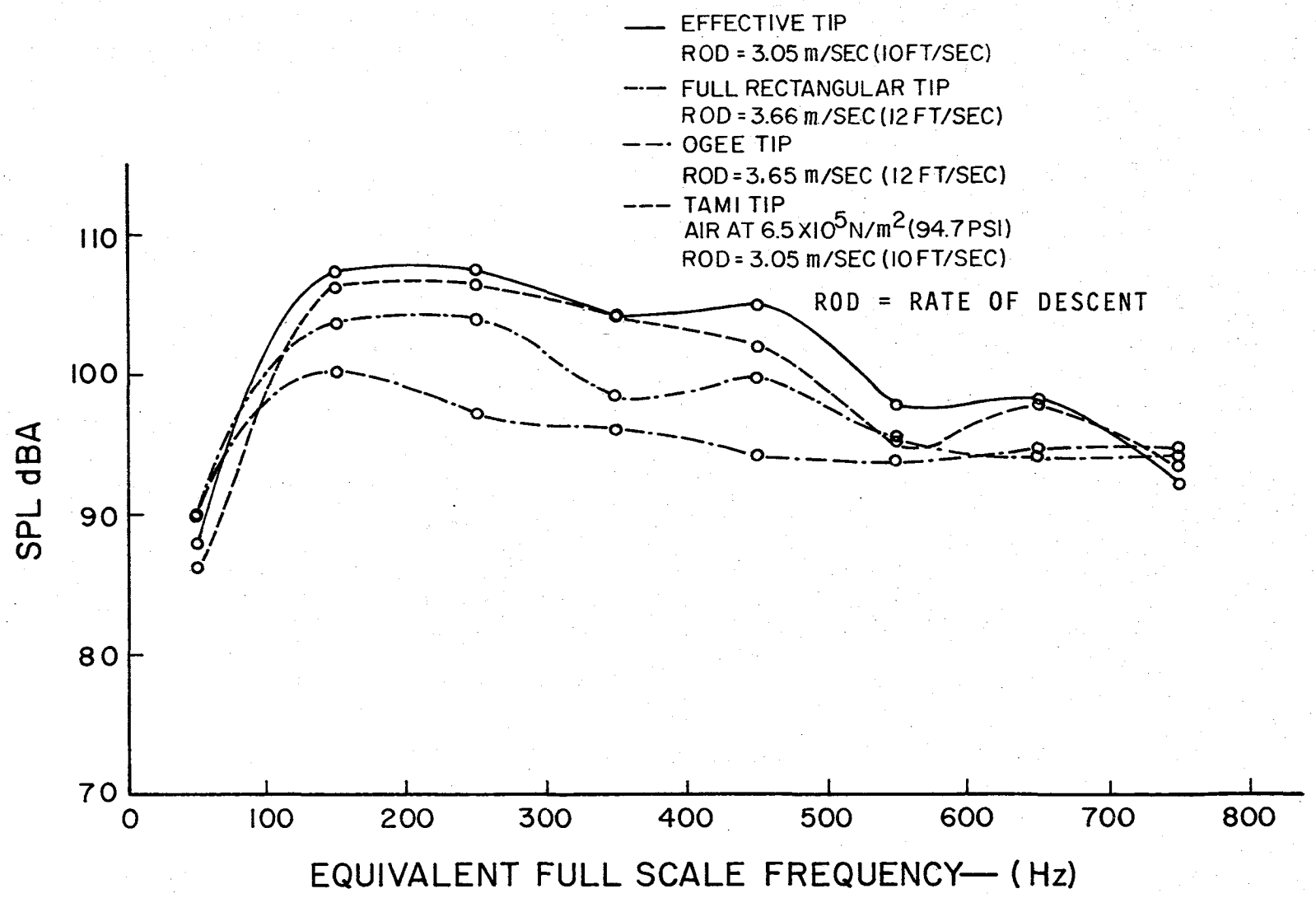


FIGURE 18. dBA vs. Frequency for Maximum Slap Conditions at Microphone 2 and at Advance Ratio of 0.125.

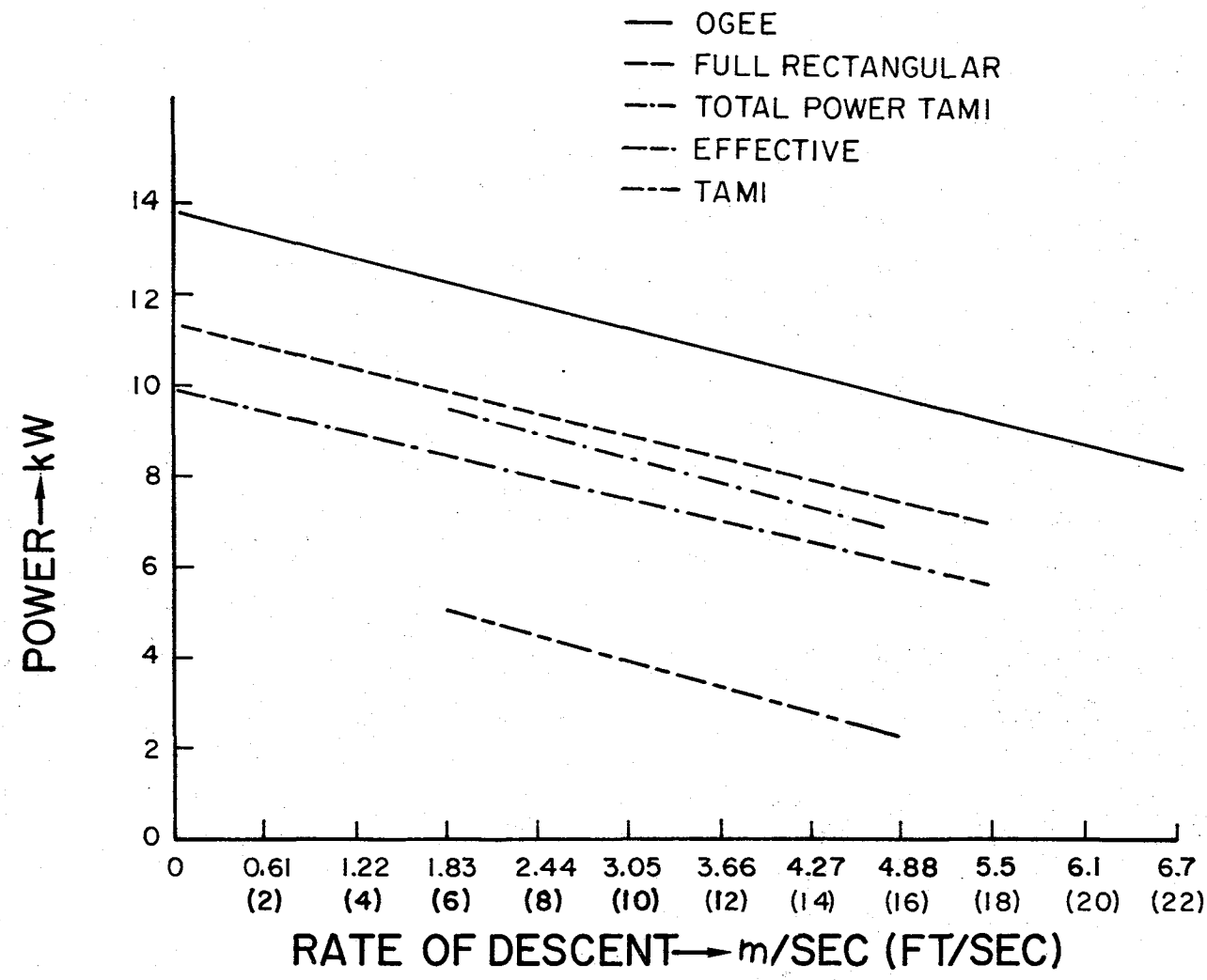


FIGURE 19. Power Absorbed vs. Descent Rate at Advance Ratio of 0.125.

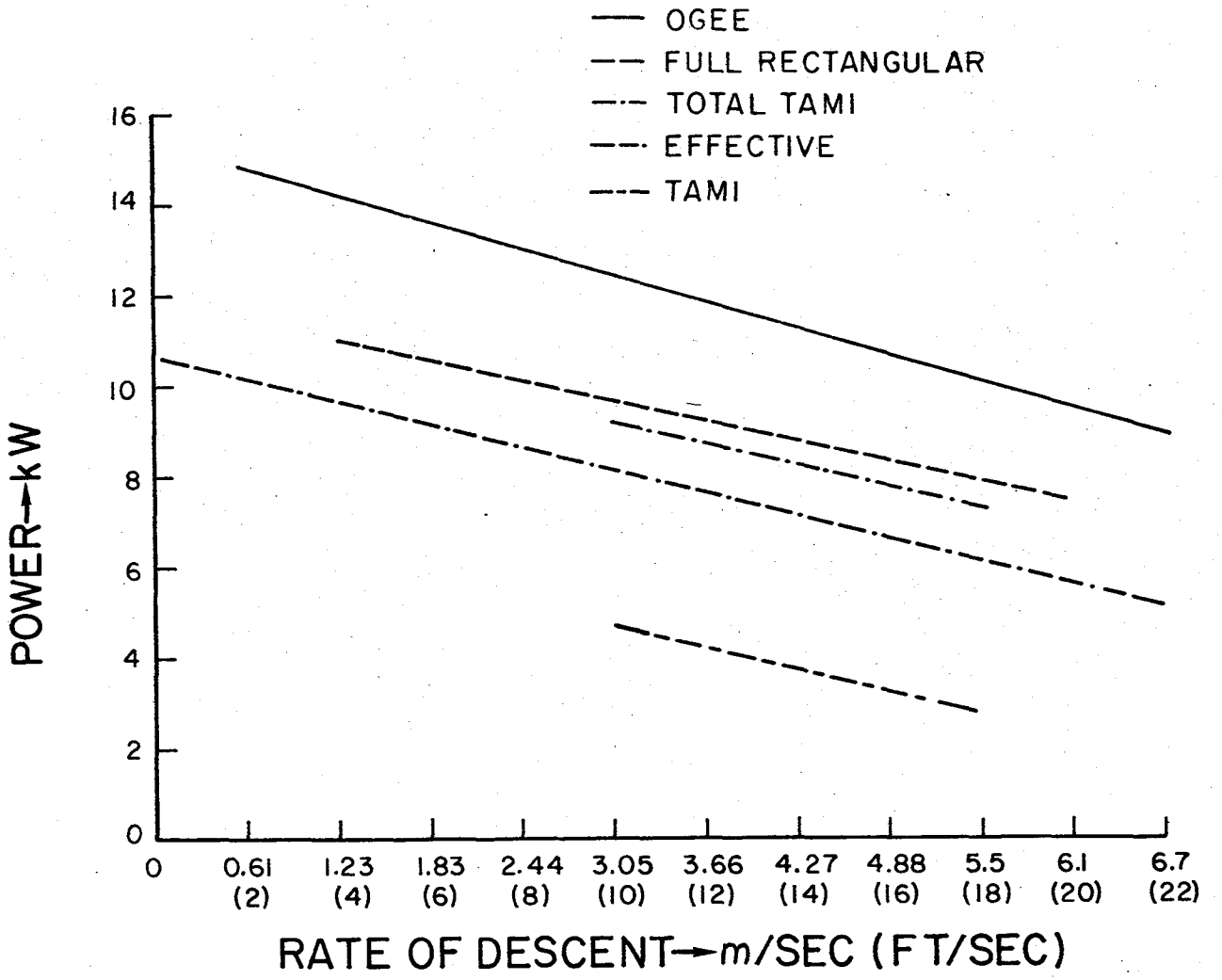


FIGURE 20. Power Absorbed vs. Descent Rate at Advance Ratio of 0.14.